

Matrix representation of the results of Picard–Lefschetz–Pham theory near the real plane in \mathbb{C}^2

A.V.Shanin, A.I.Korolkov, R.C.Assier

December 4, 2024

Abstract

This work is motivated by an attempt to construct a two-dimensional analogue of the Wiener–Hopf method. It is supposed that understanding the branching structure of unknown functions will provide insight into the form in which these functions can be sought. The unknown functions are represented as two-dimensional integrals of analytic functions with parameters, making it natural to study the branching of the integration surface using Picard–Lefschetz theory. A convenient matrix-vector representation of the main result of Picard–Lefschetz theory is introduced, and the following two statements are formulated. First, under certain constraints, the integration surface can be represented as a finite-dimensional vector with coefficients in the group ring over the fundamental group of the space with removed singularities. Second, a bypass in the parameter space around one of the components of the Landau set is described by multiplication by a relatively simple matrix (also composed of elements from the group ring). Successive loops are described by the product of such matrices. As an illustration, it is shown how the matrix formalism yields the Picard-Lefschetz formula and provides nontrivial topological relationships in the parameter space.

1 Introduction

We study the integrals of the form

$$I(t) = \int_{\Gamma} F(z; t) dz_1 \wedge dz_2. \quad (1)$$

Here $z = (z_1, z_2) \in \mathbb{C}^2$, $t = (t_1, t_2, \dots, t_M) \in \mathbb{C}^M$, Γ is some oriented surface of integration.

An example of such an integral is

$$I(t) = \int_{\Gamma} \frac{1}{(z_1 - t_1)(z_2 - t_2)\sqrt{z_1^2 + z_2^2 - 1}} dz_1 \wedge dz_2. \quad (2)$$

We assume that the integration surface Γ belongs to a tubular neighborhood of \mathbb{R}^2 denoted by \mathbb{R}_δ^2 :

$$\mathbb{R}_\delta^2 = \{z \in \mathbb{C}^2 \mid |\operatorname{Im}[z_1]| + |\operatorname{Im}[z_2]| < \delta\} \quad (3)$$

for some small positive δ .

We are particularly interested in the values of t belonging to the neighborhood of the real space $\mathbb{R}^M \subset \mathbb{C}^M$; such a space can be denoted by \mathbb{R}_δ^M .

We assume that $F(z; t)$ is a function holomorphic with respect to all $M + 2$ complex variables almost everywhere. In particular, for some fixed t , F is holomorphic for $z \in \mathbb{R}_\delta^2 \setminus \sigma$. The set $\sigma = \sigma(t)$ is the singularity set:

$$\sigma = \cup_j \sigma_j,$$

where σ_j are irreducible singularity components (analytic sets of complex codimension 1 possibly depending on t).

Each component of singularity is defined by an equation

$$\sigma_j = \{z \in \mathbb{C}^2 \mid g_j(z; t) = 0\}, \quad (4)$$

where g_j is a holomorphic function of all four complex variables everywhere in $\mathbb{R}_\delta^2 \times \mathbb{R}_\delta^M$.

The sets σ_j are assumed to be polar or branch sets of $F(z; t)$ (for fixed t). The branching can be logarithmic. The function F can be continued analytically everywhere in $\mathbb{R}_\delta^2 \times \mathbb{R}_\delta^M$ except the singularities.

Some of the singularity components are *immovable*: for them

$$g_j(z; t) = g_j(z).$$

The other components are *movable*. Our main aim is to study the integral (1) as t varies.

For the example (2) $\sigma = \sigma_1 \cup \sigma_2 \cup \sigma_3$,

$$g_1(z) = z_1^2 + z_2^2 - 1, \quad g_2(z, t) = z_1 - t_1, \quad g_3(z, t) = z_2 - t_2. \quad (5)$$

As it is known, the multidimensional Cauchy's theorem [1] can be applied to the integral (1): one can deform Γ in $\mathbb{R}_\delta^2 \setminus \sigma$ without the integral being changed. Thus, the integral $I(t)$ has singularity only when one cannot deform Γ in such a way that it avoids the singularity. In other words, the contour Γ becomes *pinched* by movable and immovable singularities.

The possible values of t for which such a pinch can happen form a *Landau set* in σ^t . The formal definition of the Landau set is not elementary [2], but we use a simple concept: the Landau set is composed of points where the topological properties of $\mathbb{R}_\delta^2 \setminus \sigma(t)$ differ from the "general case". The topological properties in this case is the homology group $H_2(\mathbb{R}_\delta^2 \setminus \sigma)$. In our examples σ^t is an algebraic set of complex codimension 1, and some elements of H_2 vanish for $t \in L$.

The integration surface Γ can be treated as an element of $H_2(\mathbb{R}_\delta^2 \setminus \sigma)$. The branching of the integral $I(t)$ as the point t bypasses σ^t is caused by branching of $H_2(\mathbb{R}_\delta^2 \setminus \sigma)$, i.e. such a bypass does not put the elements of H_2 to themselves.

The Picard–Lefschetz–Pham theory describes branching of $H_2(\mathbb{R}_\delta^2 \setminus \sigma(t))$ about the Landau set in some terms. Although this is a very powerful and sophisticated theory, it is rather hard to use. Namely, one should compute the intersection numbers of Γ and the so-called *vanishing cycles*. These intersection numbers are not easy to compute. In this paper, we propose a practical approach to the Picard–Lefschetz–Pham theory. Namely, the integration surfaces are represented as “vectors” (more rigorously, elements of module over a group ring), and branching is described as multiplication by certain matrices.

1.1 The real property of the singularities

We assume that the singularity components σ_j do not have any singular points (as a surface with real dimension 2). Such irreducible singularity sets are hence two-dimensional analytic manifolds embedded in \mathbb{C}^2 . Our interest to the singularities having the real property is caused by two reasons:

- Such singularities emerge in a lot practical problems related to wave propagation and diffraction. Namely, such singularities naturally emerge in problem having initially a “real nature” and then complexified.
- It is easy to introduce clear notations for paths and make all computations from the beginning to the end.

Definition 1.1. *We say that an immovable irreducible singularity set σ_j has the real property if its defining holomorphic function g_j is real whenever its arguments are real:*

$$g_j(z) \in \mathbb{R}, \quad \text{if } z \in \mathbb{R}^2. \quad (6)$$

For a movable singularity component, we say that it has the real property if $\sigma(t)$ has the real property for each real t .

Introduce the partial derivatives of g_j :

$$a(z) = \frac{\partial g_j(z)}{\partial z_1}, \quad b(z) = \frac{\partial g_j(z)}{\partial z_2}.$$

The regularity of σ_j is provided by the inequality $a^2 + b^2 \neq 0$, which is assumed to be valid everywhere on σ_j .

As a consequence of the real property, the intersection between \mathbb{R}^2 and an irreducible singularity set σ_j is a one-dimensional curve. Note that this is not normally the case. Indeed, in general (i.e. if the real property is not valid), the intersection of a manifold $g_j(z) = 0$ with the real plane of z is a set of discrete points.

In the case of real property, the one-dimensional curve $\sigma_j \cap \mathbb{R}^2$ is called the *real trace* of σ_j and denoted by σ'_j :

$$\sigma'_j = \sigma_j \cap \mathbb{R}^2.$$

The real trace of a singularity set $\sigma = \cup_j \sigma_j$, denoted σ' , is defined as the union of the real traces of its irreducible components: $\sigma' = \cup_j \sigma'_j$.

Remark. The definition of the real property can be weakened. Namely, instead of (6) one can require that $a(z)$ and $b(z)$ are real if $z \in \sigma_j$ and $z \in \mathbb{R}^2$. However, we prefer to use a simpler and less general definition (6).

2 Riemann domains

2.1 Universal Riemann domain

2.1.1 Definition of the universal Riemann domain

Let \mathcal{X} be the complex space \mathbb{C}^2 or the neighborhood of the real plane \mathbb{R}_δ^2 .

Let there be several holomorphic functions $g_j(z, t)$, and let σ_j be defined by (4). The union of all σ_j is σ . Fix some t that is either real or close to real and use the notation $\sigma_j = \sigma_j(t)$ everywhere. Introduce a concept of the *universal Riemann domain* over $\mathcal{X} \setminus \sigma$.

Note that the universal Riemann domain is not linked to any function F ; it is defined only by the singularity sets. The universal Riemann domain will be defined by \tilde{U} , and it is the widest Riemann domain for a function having the given singular set in \mathcal{X} . What is important, we include the singularities into the universal Riemann domain.

The singularity set σ is a stratified set in the usual sense. The main stratum is σ minus the union of all intersections $\sigma_j \cap \sigma_k$. The real dimension of this stratum is 2. The next stratum is the union of all binary intersections $\sigma_j \cap \sigma_k$. The real dimension of this stratum is 0. We denote these strata by $\sigma^{(1)}$ and $\sigma^{(0)}$, respectively.

Fix a reference point $z^* \in \mathcal{X} \setminus \sigma$. Let $\Pi(z^*, z)$ be the set of continuous paths going from z^* to some point $z \in \mathcal{X}$ (z can belong to σ or not), such that all points of such a path maybe except the end point z belong to $\mathcal{X} \setminus \sigma$. The paths are defined up to a homotopy in $\mathcal{X} \setminus \sigma$, i.e. they are in fact classes of equivalence of paths provided by the homotopy. We will use the notation

$$\gamma_1 = \gamma_2$$

if γ_1 and γ_2 are equivalent in this sense.

The set $\Pi(z^*, z^*)$ can be turned into the fundamental group $\pi_1(\mathcal{X} \setminus \sigma)$ by equipping it with the operations of multiplication and taking the inverse. Indeed, the multiplication is a concatenation. A notation

$$\gamma = \gamma_1 \gamma_2$$

means that the path γ_2 goes after γ_1 . Taking the inverse of γ is passing it in the opposite direction. The trivial bypass is denoted by e .

Any set $\Pi(z^*, z)$, $z \in \mathcal{X} \setminus \sigma$, can be bijectively mapped to $\pi_1(\mathcal{X} \setminus \sigma)$ as follows. Let γ' be some chosen path between z^* and z . Then any path $\gamma \in \Pi(z^*, z)$ can be uniquely represented as $\gamma = \gamma'' \gamma'$ where $\gamma'' \in \Pi(z^*, z^*)$. Note that one generally cannot assign a group structure to $\Pi_1(z^*, z)$ if $z \in \sigma$.

Definition 2.1. The universal Riemann domain \tilde{U} is a set of pairs (z, γ) , where $\gamma \in \Pi(z^*, z)$.

The element z of the pair is the *affix* of the point, γ is the *path-index*. We will say that all points of \tilde{U} having affix z are the *points over* z .

The universal Riemann domain \tilde{U} is a stratified topological space

$$\tilde{U} = \tilde{U}_2 \cup \tilde{U}_1 \cup \tilde{U}_0.$$

The stratum to which the point (z, γ) belongs is defined by the affix z . The main stratum \tilde{U}_2 corresponds to $z \in \mathcal{X} \setminus \sigma$. The next stratum \tilde{U}_{n-1} is built for $z \in \sigma^{(1)}$, the stratum \tilde{U}_0 is built for $z \in \sigma^{(0)}$. Each stratum \tilde{U}_j is a manifold of real dimension $2j$ (moreover, it is a complex manifold of complex dimension j).

Each connectivity component of each stratum of \tilde{U} is by construction a covering over the corresponding subset of \mathcal{X} with a discrete fiber. The main stratum \tilde{U}_2 is a *universal covering* over $\mathcal{X} \setminus \sigma$.

The universal Riemann domain \tilde{U} is a Riemann domain of some function $F(z)$ having logarithmic branching on all σ_j and obeying no additional restrictions (i.e. describing commutation of paths about the branch sets).

Remark. We consider only *finite* singularities here. The infinity requires a separate study.

Example 2.1. Consider the case $z = (z_1, z_2) \in \mathbb{C}^2$. Let be

$$\sigma = \sigma_1 \cup \sigma_2, \quad \sigma_1 : z_1 = 0, \quad \sigma_2 : z_2 = 0.$$

First build the stratum \tilde{U}_2 . Take, say, $z^* = (1, 1)$. Introduce the loops $\gamma_1, \gamma_2 \in \Pi(z^*, z^*)$ bypassing about these singularities. These loops are shown in Fig. 1.

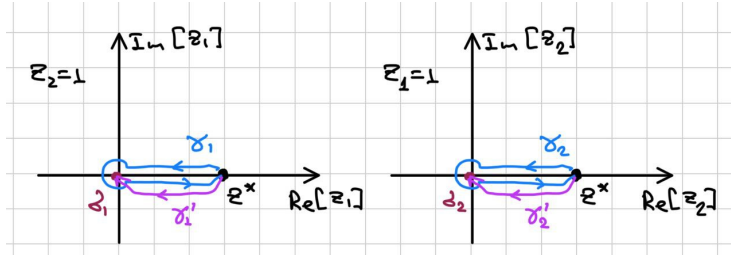


Fig. 1: Contours for Example 2.1

As we demonstrate below, the bypasses along γ_1 and γ_2 commute, i.e. the path $\gamma_1\gamma_2$ can be deformed into $\gamma_2\gamma_1$. Thus,

$$\pi_1(\mathcal{X} \setminus \sigma) = \mathbb{Z}^2,$$

and each element of π_1 is $\gamma_1^{k_1}\gamma_2^{k_2}$ with $k_1, k_2 \in \mathbb{Z}$.

Let us build the stratum \tilde{U}_1 . Take sample points $(0, 1)$ and $(1, 0)$ belonging to σ_1 and σ_2 , respectively. Introduce the paths γ_1' and γ_2' as it is shown in

Fig. 1. The paths from $\Pi(z^*, z')$ can be written as $\gamma_2^k \gamma_1'$, $k \in \mathbb{Z}$, and the paths from $\Pi(z^*, z'')$ can be written as $\gamma_1^k \gamma_2'$.

The stratum \tilde{U}_0 consists of a single point. One can see that all path from z^* to $(0, 0)$ can be deformed one into another.

2.1.2 Universal Riemann domain over the singularities. Locality lemma

Let be $z \in \sigma_j$, moreover, let be $z \in \sigma^{(1)}$, i.e. z does not belong to a crossing of some singularity components. The points of \tilde{U} over z are (z, γ) , where $\gamma \in \Pi(z^*, z)$. It seems useful to describe the singularity using $\Pi(z^*, z^\ddagger)$ for some $z^\ddagger \in \mathbb{R}_\delta^2 \setminus \sigma$ located near z , since such $\Pi(z^*, z^\ddagger)$ is a more regular object (it is linked to the fundamental group).

Introduce a small (open) ball $D \subset \mathbb{R}_\delta^2$ with the center at z . Let the ball be small enough not to cross any other singularity components. In this ball, introduce local coordinates (z'_1, z'_2) instead of (z_1, z_2) such that the singularity described by $z'_1 = 0$, i.e. the singularity component σ_j has a simple structure there. Indeed, one can take

$$z'_1 = g_j(z).$$

Let the coordinate z'_2 for z be equal to 0.

Take a point $z^\ddagger = (z'_1, z'_2)$ in D . Let for this point be $z'_1 \neq 0$, $\text{Arg}[z'_1] = 0$, $z'_2 = 0$ (see Fig. 2). For any $z^s, z^e \in D \setminus \sigma$ introduce a set of *local* paths $\Pi_D(z^s, z^e)$ as the set of paths going from z^s to z^e entirely in $D \setminus \sigma$. Indeed, paths from $\Pi(z^s, z^e)$ that can be deformed homotopically to D also fall into $\Pi_D(z^s, z^e)$.

Introduce also some contour $\gamma_2 \in \Pi(z^\ddagger, z)$, $\gamma_2 \subset D$. Let for simplicity this path be straight segment (in the coordinates (z'_1, z'_2)) connecting z^\ddagger and z .

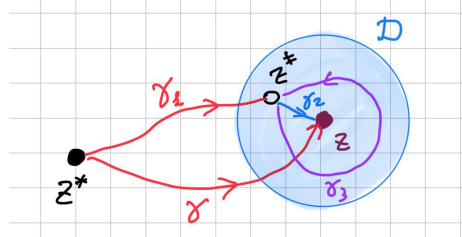


Fig. 2: Local paths near $z \in \sigma$

Lemma 2.1. a) Let there be $\gamma_3 \in \Pi_D(z^\ddagger, z^\ddagger)$. Then $\gamma_3 \gamma_2 = \gamma_2$.

b) Any path $\gamma \in \Pi(z^*, z)$ can be represented as $\gamma = \gamma_1 \gamma_2$ for some $\gamma_1 \in \Pi(z^*, z^\ddagger)$.

c) Let be $\gamma_1, \gamma_1' \in \Pi(z^*, z^\ddagger)$ such that $\gamma_1 \gamma_2 = \gamma_1' \gamma_2$. Then $\gamma_1^{-1} \gamma_1' \in \Pi_D(z^\ddagger, z^\ddagger)$.

See the proof in Appendix A.

The fact that D is small is used only in the proof of point a). Point c) can be proven for *any* neighborhood of z^\ddagger .

It is possible to prove an analog of Lemma 2.1 for a point $z \in \sigma^{(0)}$ provided that the singularities obey an additional condition. We say that $z \in \sigma$ have a *conical property* if, for D small enough centered at z , $D \setminus \sigma$ has a topological structure of a product $p \times (\partial D \setminus \sigma)$, where p is a segment. We require that all samples of p in this product start at z . Thus, any point of $D \setminus \sigma$ is connected with z by a uniquely defined sample of p , and these samples form a continuous family. An illustration of the definition of a conical property is shown in Fig. 3. One can build a proof of point a) for any z having a conical property.

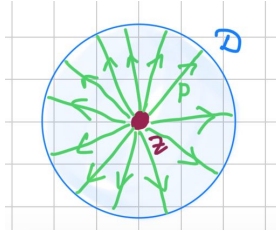


Fig. 3: To the definition of the conical property

The points of $\sigma^{(1)}$ obviously possess the conical property. For a point z^\ddagger the sample of p connecting it with z is a straight segment in the coordinates (z'_1, z'_2) .

A transversal crossing of two branches of singularity (see a definition below) has a conical property. For example, let in \mathbb{C}^2 the singularities be defined by $z_1 = 0$ and $z_2 = 0$. The points $(0, 0) \in \sigma^{(0)}$ has a conical property: one can take straight lines going from the origin as samples of p .

Moreover, a quadratic touch point of two singularity components in \mathbb{C}^2 , say, described by $z_1 = 0$, $z_1 - z_2^2 = 0$, also has a conical properties. The samples of p are straight segments in the coordinates $(\sqrt{z_1}, z_2)$.

Thus, in the practically interesting cases, all singularity points have in fact the conical property, and thus, Lemma 2.1 is valid for them.

Using Lemma 2.1, we can describe the set $\Pi(z^*, z)$, $z \in \sigma$, in the group language. Take the reference point z^* in the small ball D centered at z . Define $\pi_1(\mathcal{X}, \setminus \sigma)$ as $\Pi(z^*, z^*)$. Introduce the subgroup $B \in \pi_1(\mathcal{X}, \setminus \sigma)$ by

$$B = \Pi_D(z^*, z^*). \quad (7)$$

The set $\Pi(z^*, z)$ is the set of all left cosets with respect to the subgroup. Since the local subgroup is not necessarily normal, the set of left cosets is not necessarily a group.

To finish this paragraph, we put here a slight generalization of Lemma 2.1 that will be used a lot below.

Lemma 2.2. *Let $z \in \sigma$ have a conical property. Let D be a small ball centered at z . Let be $z^s, z^e \in D \setminus \sigma$. Let be $\gamma^s \in \Pi_D(z^s, z)$, $\gamma^e \in \Pi_D(z^e, z)$. Let $z^* \in \mathbb{C}^n \setminus \sigma$*

be some reference point, and $\gamma_1 \in \Pi(z^*, z^s)$, $\gamma_2 \in \Pi(z^*, z^e)$. Then

$$\gamma_1 \gamma^s = \gamma_2 \gamma^e$$

if and only if

$$\gamma \equiv \gamma_1^{-1} \gamma_2 \in \Pi_D(z^s, z^e).$$

The proof is similar to that of Lemma 2.1. An illustration to the condition of the lemma is shown in Fig. 4.

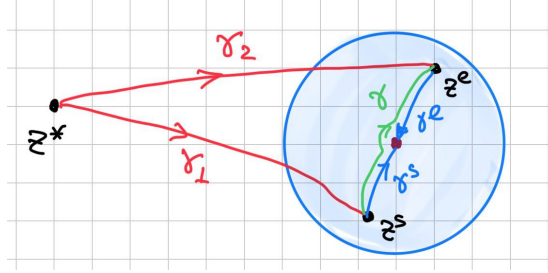


Fig. 4: Paths in the formulation of Lemma 2.2

2.2 Riemann domain of a function

Now consider some possibly multivalued function $F(z)$, $z \in \mathcal{X}$ having singularities at σ . Indeed, $F(z)$ is a single-valued function if z takes values in \tilde{U}_2 .

Fix the reference point $z \in \mathcal{X} \subset \sigma$ and take $\pi_1(\mathcal{X} \setminus \sigma) = \Pi(z^*, z^*)$. Fix some branch of $F(z)$ near z^* . Introduce the subgroup $A \subset \pi_1(\mathcal{X} \setminus \sigma)$ as the set of all path from π_1 leading to the same branch.

Definition 2.2. *The Riemann domain of $F(z)$ in \mathcal{X} is a set of pairs (z, γ') , where $z \in \mathcal{X}$, and γ' is a class of paths $\gamma \in \Pi(z^*, z)$ with respect to the equivalence relation*

$$\gamma_1 \equiv \gamma_2 \quad \text{if} \quad \gamma_1 = \gamma_3 \gamma_2, \quad \gamma_3 \in A.$$

3 Local fundamental groups

Below we will need description of local fundamental groups near points of σ . In the proof of Lemma 2.1 we use the fact that if $z \in \sigma^{(1)}$ then such a group is \mathbb{Z} . Here we compute similar groups for $z' \in \sigma^{(0)}$ for the cases of tangential and quadratic crosses of two singularity components.

3.1 Transversal crossing of two branch lines in \mathbb{C}^2

Let $D \subset \mathbb{C}^2$ be a small open ball centered at some point $z' \in \mathbb{C}^2$. Define the singularities $\sigma = \sigma_1 \cup \sigma_2$,

$$\sigma_1 = \{z \in D \mid g_1(z) = 0\}, \quad \sigma_2 = \{z \in D \mid g_2(z) = 0\}. \quad (8)$$

Let functions $g_1(z)$, $g_2(z)$ have the following properties:

- g_1 and g_2 are holomorphic in D ;
- $g_1(z') = g_2(z') = 0$;
- complex gradients ∇g_1 and ∇g_2 are non-zero in D (a gradient of g is indeed $\nabla g = (\partial_{z_1} g, \partial_{z_2} g)$);
- complex gradients $\nabla g_1(z')$ and $\nabla g_2(z')$ are not proportional to each other, i.e. there exists no complex number c such that $\nabla g_1(z') = c \nabla g_2(z')$.

Such a crossing of singularities σ_1 and σ_2 is referred to as *transversal*.

For simplicity, change the complex coordinates (z_1, z_2) to (s_1, s_2) in D , such that

$$s_1 = g_1(z), \quad s_2 = g_2(z). \quad (9)$$

The singular sets σ_1 and σ_2 are described by $s_1 = 0$ and $s_2 = 0$, respectively.

Let us build the fundamental group $\pi_1(D \setminus \sigma)$. As it is known [3], this group is the same as for any *strict deformation retract* of $D \setminus \sigma$. The deformation retract is the result of continuous “squashing” of the initial space onto some surface. Here we can present such a retraction explicitly. Namely, consider a map

$$(s_1, s_2) \rightarrow (s_1/|s_1|, s_2/|s_2|). \quad (10)$$

One can see that the image of $D \setminus (\sigma_1 \cup \sigma_2)$ under this deformation is a torus. This torus can be described by two real angular variables φ_1, φ_2 taking values in $\mathcal{S}^1 = [0, 2\pi]$, such that

$$s_1/|s_1| = e^{i\varphi_1}, \quad s_2/|s_2| = e^{i\varphi_2}. \quad (11)$$

The values $\varphi_1 = 0$ and 2π are identified. The same is true for φ_2 . Graphically, the torus can be represented as a square in coordinates (φ_1, φ_2) with the opposite sides identified with each other (see Fig. 5, left).

So, the group $\pi_1(D \setminus \sigma)$ is that of a torus. It is well known that this group is \mathbb{Z}^2 . Let us demonstrate this. Take the base point $\varphi_1 = \varphi_2 = 0$. The passes along the sides of the square γ_1 and γ_2 can be used as generators of π_1 , see Fig. 5 (note that just the same paths are shown in a slightly different way in Fig. 1). Indeed, returning to the initial problem, γ_1 corresponds to an elementary bypass about the branch line σ_1 , and γ_2 is an elementary bypass about σ_2 . Say, one can take a reference point (ϵ, ϵ) for some small positive ϵ (in the coordinates (s_1, s_2)), and represent γ_1 parametrically as $(\epsilon e^{i\varphi_1}, \epsilon)$, and γ_2 as $(\epsilon, \epsilon e^{i\varphi_2})$.

The most important property is that these passes commute, i.e.

$$\gamma_1 \gamma_2 = \gamma_2 \gamma_1. \quad (12)$$

In Fig. 5, right we demonstrate a homotopic deformation of $\gamma_1 \gamma_2$ into $\gamma_2 \gamma_1$.

The commutativity of bypasses about σ_1 and σ_2 is a highly non-obvious property of branching in \mathbb{C}^2 . There is no analog of this property in \mathbb{C}^1 .

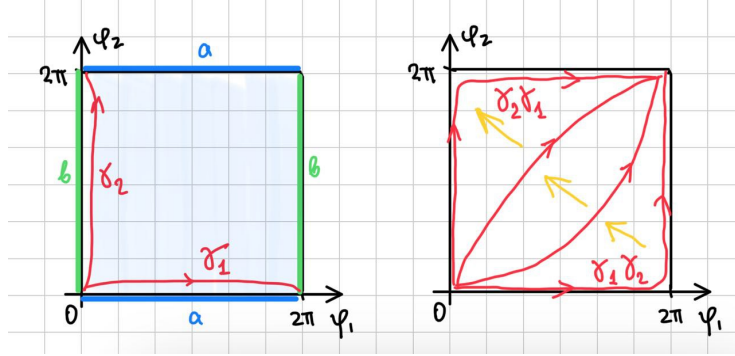


Fig. 5: Computation of π_1 of a torus

3.2 Quadratic tangential touch of two branch lines in \mathbb{C}^2

3.2.1 Standard form of a quadratic tangential touch

Let again the singular set be $\sigma = \sigma_1 \cup \sigma_2$, and σ_j be defined by functions g_j as in (8). Let now the gradient of g_1 and g_2 be non-zero, but let them be proportional at the crossing point $z' = \sigma_1 \cap \sigma_2$:

$$\nabla g_1(z') = c \nabla g_2(z').$$

This makes the crossing tangential. Below we impose the condition making this crossing quadratic. The consideration is held in a small ball D centered at z' .

Let us find a convenient set of local transformed coordinates (s_1, s_2) . Introduce the first transformed coordinate s_1 as

$$s_1(z) = g_1(z).$$

Let w be a linear function of z_1 and z_2 such that the line $w = 0$ is orthogonal to $s_1 = 0$ at the point z' :

$$w = (z_1 - z'_1) \partial_{z_2} g_1(z') - (z_2 - z'_2) \partial_{z_1} g_1(z').$$

this function can be used as a temporary transformed coordinate transversal to s_1 . The crossing of σ_1 and σ_2 is *quadratic* if

$$g_2(s_1 = 0, w) = O(w^2). \quad (13)$$

One can prove the following proposition:

Let σ_1 and σ_2 have tangential quadratic crossing in some small neighborhood $U \subset \mathbb{C}^2$. Then one can introduce a biholomorphic coordinate change $(z_1, z_2) \rightarrow (s_1, s_2)$ such that the surfaces σ_1, σ_2 are defined by the equations

$$\sigma_1 = \{(s_1, s_2) \in U \mid s_1 = 0\}, \quad \sigma_2 = \{(s_1, s_2) \in U \mid s_1 = s_2^2\}. \quad (14)$$

Below we use the coordinates (s_1, s_2) and assume that the singularities have form (14). A computation of the fundamental fundamental group $\pi_1(D \setminus \sigma)$ can be found in [2] in a rather concise form. Here we follow basically the consideration there.

3.2.2 Building a strict deformation retract of $D \setminus \sigma$

Build a deformation retract of $D \setminus \sigma$ in two steps:

Step 1. Represent the variables $s_{1,2}$ in the form

$$s_{1,2} = \rho_{1,2} e^{i\varphi_{1,2}},$$

where $\rho_{1,2}$ are real, and $\varphi_{1,2}$ belong to the real circle $\mathcal{S}^1 = [0, 2\pi]$.

Introduce a map

$$(\rho_1 e^{i\varphi_1}, \rho_2 e^{i\varphi_2}) \longrightarrow \left(e^{i\varphi_1}, \frac{\rho_2}{\sqrt{\rho_1}} e^{i\varphi_2} \right). \quad (15)$$

As the result, $D \setminus \sigma$ becomes mapped onto a bundle, whose base is \mathcal{S}^1 (this corresponds to $s_1 = e^{i\varphi_1}$, $\varphi_1 \in \mathcal{S}^1$), and the fiber is a complex plane s_2 with two points removed: $\mathbb{C} \setminus \{e^{i\varphi_1/2}, -e^{i\varphi_1/2}\}$. Indeed, the two removed points $s_2 = \pm e^{i\varphi_1/2}$ belong to σ_2 .

Step 2. The plane with two removed points removed $\mathbb{C} \setminus \{e^{i\varphi_1/2}, -e^{i\varphi_1/2}\}$ is mapped onto the eight-shaped curve \mathcal{E} :

$$\mathcal{E}_{\varphi_1} : \{\xi \in \mathbb{C} \mid |\xi \pm e^{i\varphi_1/2}| = 1\}.$$

The projection for the case $\varphi_1 = 0$ is shown in Fig. 6. The points outside the eight-shaped curve move along the blue line until they hit the eight-shaped curve, and the points inside the curve move along the red lines.

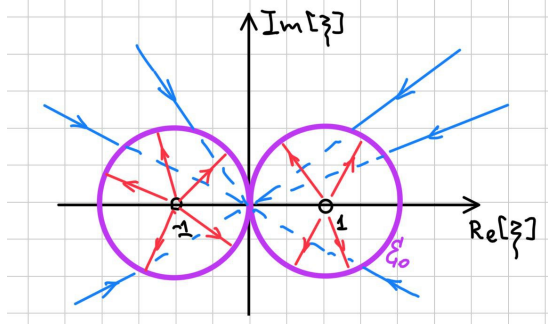


Fig. 6: Projection $\mathcal{E}_0 = \mathbb{C} \setminus \{1, -1\} \longrightarrow \mathcal{E}_0$

As the result, $U \setminus \sigma$ becomes retracted to the bundle with the base \mathcal{S}^1 and the fiber \mathcal{E}_{φ_1} . Note that this bundle is not trivial.

3.2.3 Building the group π_1 of the deformation retract

Let be $\varphi = \varphi_1$. Introduce the angle ψ for the circles forming the eight curve \mathcal{E} as it is shown in Fig. 7, left. Thus, the retract becomes parametrized by two variables: $\psi, \varphi \in \mathcal{S}^1$ (one or two points of the retract correspond to each pair (ψ, φ)). The scheme of the retract is shown in Fig. 7, right. The retract consists

of two rectangles connected in a sophisticated way. The oriented segments marked by the same Latin letters should be attached to each other. Note that there are *three* copies of the segment c . The base point $s^* = (s_1, s_2) = (1, 0)$ corresponds to $\psi = \varphi = 0$ and is shown by six points in Fig. 7, right).

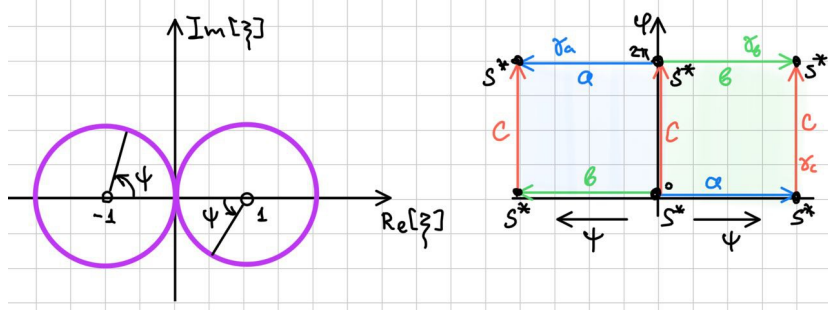


Fig. 7: Coordinate ψ on the \mathcal{E} -loop (left); the scheme of the retract (right)

The generators for our group are the bypasses $\gamma_a, \gamma_b, \gamma_c$, going along the sides a, b, c , respectively (these sides are shown in Fig. 7, right). Note that all these bypasses go from s^* to s^* . An explicit representation of the paths $\gamma_a, \gamma_b, \gamma_c$ is as follows:

$$\begin{aligned}\gamma_a &: (1, 1 - e^{i\psi}), \quad \psi \in [0, 2\pi], \\ \gamma_b &: (1, -1 + e^{i\psi}), \quad \psi \in [0, 2\pi], \\ \gamma_c &: (e^{i\varphi}, 0), \quad \varphi \in [0, 2\pi].\end{aligned}$$

Below we also will need an elementary loop bypassing σ_1 , i.e. a path that comes from s^* to some point s near σ_1 (say along some $\gamma \in \Pi(s^*, s)$), bypassing σ_1 for a single time in a local way and coming back along γ . One can see that a possible choice for such a contour is

$$\tilde{\gamma}_a = \gamma_c \gamma_a^{-1}. \quad (16)$$

The relations defining π_1 are obtained similarly to Fig. 5. Namely, consider the words (group elements) $\gamma_b \gamma_c \gamma_a^{-1} \gamma_c^{-1}$ and $\gamma_a \gamma_c \gamma_b^{-1} \gamma_c^{-1}$. They are bypasses performed along the boundaries of two rectangles shown in Fig. 7, right. Obviously, these bypasses can be shrunk to a point, thus corresponding elements of π_1 are trivial:

$$\gamma_b \gamma_c \gamma_a^{-1} \gamma_c^{-1} = e, \quad \gamma_a \gamma_c \gamma_b^{-1} \gamma_c^{-1} = e. \quad (17)$$

These identities express the topological relations describing $\pi_1(U \setminus \sigma)$.

A corollary of (17) is the pair of commutation relations

$$\gamma_a \gamma_c^2 = \gamma_c^2 \gamma_a, \quad \gamma_b \gamma_c^2 = \gamma_c^2 \gamma_b. \quad (18)$$

3.2.4 Approximation to a quadratic touch

The properties of $\pi_1(\mathbb{C}^2 \setminus \sigma)$ are highly nontrivial. Consider a slightly changed situation, namely let be $\sigma = \sigma_1 \cup \sigma_2(t_1)$, where

$$\sigma_1 : z_1 = 0, \quad \sigma_2(t_1) : z_1 - z_2^2 + t_1 = 0. \quad (19)$$

The real traces of the singularities are shown in Fig. 8. The parameter t_1 is assumed to be real positive.

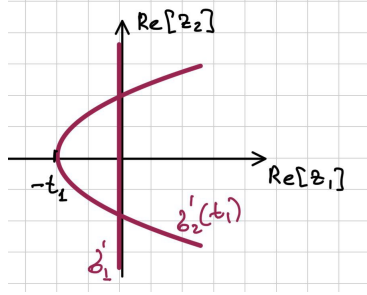


Fig. 8: Singularities σ_1 and $\sigma_2(t_1)$

A naive approach to this configuration may confuse. On the one hand, the singularities have two transversal crossings, thus it seems that the bypasses about the singularities should commute. On the other hand, the quadratic touching is achieved as $t_1 \rightarrow 0$, thus it would be strange if $\pi_1(\mathbb{C}^2 \setminus \sigma)$ is Abelian.

Let us compute $\pi_1(\mathbb{C}^2 \setminus \sigma)$. For this, split \mathbb{C}^2 into two domains:

$$\mathbb{C}^2 = U^+ \cup U^-, \quad U^\pm = \{(z_1, z_2) \in \mathbb{C}^2 \mid \pm \text{Im}[z_2] \geq 0\}.$$

Let us build a strict deformation retract of the sets $U^\pm \setminus \sigma$ as follows. Introduce the variable

$$\zeta = z_1 - z_2^2 - t_1.$$

The deformation is built according to the formulae

$$(z_1, \zeta) \rightarrow (z_1/|z_1|^\alpha, \zeta/|\zeta|^\alpha), \quad \alpha \in [0, 1].$$

One can see that both U^+ and U^- are retracted to a torus $\mathcal{S}^1 \times \mathcal{S}^1$ in the variables

$$\varphi_1 = \text{Arg}[z_1], \quad \varphi_2 = \text{Arg}[\zeta].$$

Thus, we have two copies of a torus. Let both variables take values in $[-\pi, \pi]$.

Now note that the boundary $\mathcal{B} = U^+ \cap U^-$ defined by $\text{Im}[z_2] = 0$ is common for both of domains. One can see that \mathcal{B} is mapped onto the set $|\varphi_2| < |\varphi_1|$. This set is shown by purple in Fig. 9.

One can see that any path on the torus can be deformed into the purple region. Since the purple region is common for both U^+ and U^- . This, $\pi_1(U^+ \cup U^-)$

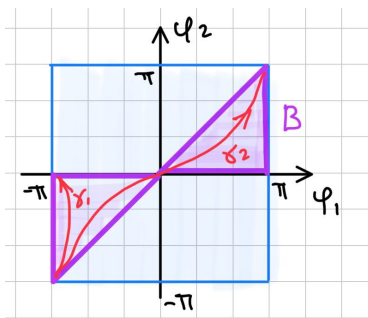


Fig. 9: Image of \mathcal{B} in the coordinates (φ_1, φ_2)

is generated by the paths $\{\gamma_1, \gamma_2\}$ shown in the figure. These paths commute since they belong to the toruses. Finally,

$$\pi_1(\mathbb{C}^2 \setminus \sigma) = \mathbb{Z}^2,$$

so the fundamental group is Abelian. We see that in some sense the case $t_1 = 0$ is more complicated than $t_1 \neq 0$.

4 Representation of surfaces through relative homologies

4.1 Cells, classes, and homologies

Consider the space \mathbb{R}_δ^2 and the singularity set possessing the real property. Define a *cell complex* on \tilde{U} . This cell complex should be matched with the stratification of \tilde{U} : if some element of the cell complex intersects with a stratum \tilde{U}_j , it should fully belong to \tilde{U}_j . Let $\mathcal{G}^0(\tilde{U})$, $\mathcal{G}^1(\tilde{U})$, and $\mathcal{G}^2(\tilde{U})$ be groups of chains of dimension 0, 1, and 2, respectively, related to this cell complex.

We will operate with several types of topological objects associated with \tilde{U} and the cell complex on it. They are:

- Cycles $\mathcal{C}^2(\tilde{U}_2)$. They are boundaryless oriented surfaces in $\mathbb{R}_\delta^2 \setminus \sigma$. These cycles avoid the singular set. Such surfaces may play role of integration surfaces for functions holomorphic in $\mathbb{R}_\delta^2 \setminus \sigma$ and having arbitrary type of branching on σ . Indeed, for integration purposes it makes sense to consider not particular cycles of $\mathcal{C}^2(\tilde{U}_2)$, but homology classes of $H_2(\tilde{U}_2)$ formed by these cycles.
- Relative cycles $\mathcal{C}^2(\tilde{U}, \tilde{U}_1)$. The elements of this group are 2D chains in \tilde{U} that may have boundaries on σ . The elements of $\mathcal{C}^2(\tilde{U}, \tilde{U}_1)$ are needed to describe the “face parts” of integration surfaces (see below). The elements of $\mathcal{C}^2(\tilde{U}, \tilde{U}_1)$ form the homology classes in $H_2(\tilde{U}, \tilde{U}_1)$. As representatives of these classes, one can take polygons in the real plane.

- Cycles $\mathcal{C}^1(\tilde{U}_1)$ and corresponding homologies $H_1(\tilde{U}_1)$. Some of these homologies can be represented as oriented contours of polygons in the real plane.
- Chains (not necessarily cycles) of $\mathcal{G}^2(\tilde{U})$. They are oriented surfaces on \tilde{U} that may have boundaries anywhere including the singular lines.

By definition, the relative cycles of $\mathcal{C}^2(\tilde{U}, \tilde{U}_1)$ are defined up to an arbitrary chain on \tilde{U}_1 , but since \tilde{U}_1 contains no components of dimension 2, there is a single chain in $\mathcal{G}^2(\tilde{U})$ corresponding to an element of $\mathcal{C}^2(\tilde{U}, \tilde{U}_1)$, so there is a natural map

$$\Phi : \mathcal{C}^2(\tilde{U}, \tilde{U}_1) \rightarrow \mathcal{G}^2(\tilde{U}). \quad (20)$$

Let the cycle $W' \in \mathcal{C}^2(\tilde{U}, \tilde{U}_1)$ be a representative of a relative homology class $W \in H_2(\tilde{U}, \tilde{U}_1)$. Take a boundary $\partial(\Phi(W'))$. The result is a cycle from $\mathcal{C}^1(\tilde{U}_1)$. It is well known that one correctly define a homology class $H_1(\tilde{U}_1)$ whose representative is $\partial(\Phi(W'))$. Thus, one can define a boundary operator

$$H_2(\tilde{U}, \tilde{U}_1) \xrightarrow{\partial} H_1(\tilde{U}_1). \quad (21)$$

- Cycles $\mathcal{C}^2(\tilde{U})$. They are boundaryless surfaces defined on the whole \tilde{U} (including the singular set). The corresponding homologies are $H_2(\tilde{U})$.
- In $H_2(\tilde{U}, \tilde{U}_1)$ we study a subgroup $H_2^*(\tilde{U}, \tilde{U}_1)$ whose elements are as follows. The plane \mathbb{R}^2 is split by σ into polygons. These polygons represent some relative homologies in $H_2(\mathbb{R}^2, \sigma')$. The preimages of these homologies in $H_2(\tilde{U}, \tilde{U}_1)$ are generators of $H_2^*(\tilde{U}, \tilde{U}_1)$. In other words, elements of $H_2^*(\tilde{U}, \tilde{U}_1)$ are linear combinations of polygons in \mathbb{R}^2 indexed by path-indexes from $\pi_1(\mathbb{R}_\delta^2 \setminus \sigma)$.

The powerful technique of algebraic topology will be not used in the work. We use the terminology of homology theory, however for us homologies H_2 are just oriented surfaces, H_1 are oriented contours, and the list above describes which surfaces can pass through the singularities, and which can have boundaries. The operator (21) finds a boundary of a sum of polygons that should be a closed contour. We use the homology terminology mainly to combine linear combination of contours and surfaces.

We note that the space \tilde{U} is branched, so for each polygon and segment in it may be represented by an infinite number of samples.

4.2 Elements of $H_2^*(\tilde{U}, \tilde{U}_1)$ and their visual notation

The real traces of singularities σ'_j split the real plane \mathbb{R}^2 into a set of polygons (possibly, curvilinear or infinite). It is quite clear that in our case (in \mathbb{R}_δ^2 and for the singularities having the real property) the elements of $H_2^*(\tilde{U}, \tilde{U}_1)$ can be represented by polygons taken on different sheets. Here we introduce convenient visual notations for these polygons. These notations help us to perform the computations related to the Picard–Lefschetz–Pham theory.

For paths in \mathbb{R}_δ^2 we use the notations described in Appendix B. The notations that we introduce are composed of

- a reference point;
- generators of $\pi_1(\mathbb{R}_\delta^2 \setminus \sigma)$;
- base paths.

As an example, consider the singularity σ composed of three complex straight lines $\sigma_1, \sigma_2, \sigma_3$ in general position. Say, it may be the lines

$$\sigma_1 : z_2 = 0, \quad \sigma_2 : z_1 + z_2 - 1 = 0, \quad \sigma_3 : z_1 - z_2 = 0.$$

Three real traces $\sigma'_1, \sigma'_2, \sigma'_3$ split the plane \mathbb{R}^2 into 7 polygons: A, \dots, G . Take a reference point $x^* = x_A^*$ in the finite triangle A (see Fig. 10, left). This point belongs to $\mathbb{R}^2 \setminus \sigma$.

The generators of $\pi_1(\mathbb{R}_\delta^2 \setminus \sigma)$ are elementary loops $\gamma_1, \gamma_2, \gamma_3$ bypassing the singularities $\sigma_1, \sigma_2, \sigma_3$, respectively, in the positive direction (see the figure). The loops start and end at the base point. According to the commutativity (12) applied to each crossing of the lines, these elementary loops commute:

$$\gamma_1\gamma_2 = \gamma_2\gamma_1, \quad \gamma_1\gamma_3 = \gamma_3\gamma_1, \quad \gamma_2\gamma_3 = \gamma_3\gamma_2.$$

Thus,

$$\pi_1(\mathbb{R}_\delta^2 \setminus \sigma) = \mathbb{Z}^3.$$

and each element of π_1 is thus

$$\gamma = \gamma_1^{m_1} \gamma_2^{m_2} \gamma_3^{m_3}, \quad m_1, m_2, m_3 \in \mathbb{Z}. \quad (22)$$

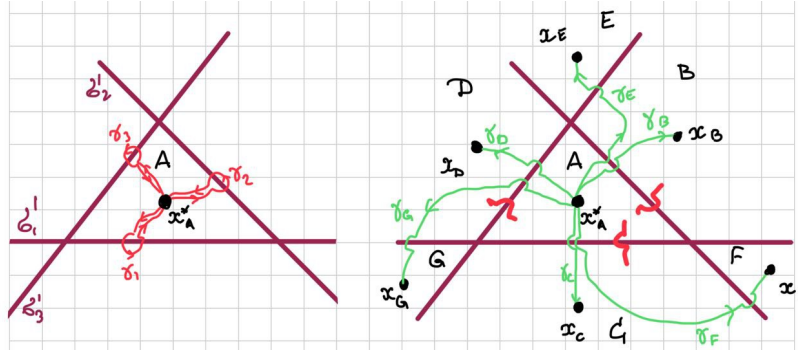


Fig. 10: Reference points and paths connecting them

Now build the *base paths*. For this, in each polygon take its local reference point (let them be x_B, x_C, \dots, x_G). For generality, one may assume that the reference point for A is x_A^* . Introduce some paths going from x_A^* to the local

reference point (assume that the path for A is trivial). Denote these paths by $\gamma_A, \gamma_B, \gamma_C, \dots, \gamma_G$. They are shown in Fig. 10, right, and referred to as the base paths.

The choice of the base paths is arbitrary, but there is a convenient way to choose them, such that the display and some computations become more convenient. Namely, choose some surface Γ that is a real plane indented near the singularities. This surface can be shown by the bridge symbols (red in Fig. 10, right). Assume that all base path belong to Γ . One can see that the green base paths and the red bridge notations match.

Now one can introduce notations for the polygons located on different sheets of \tilde{U} . Namely, let Q stands for the polygon name, i.e. $Q \in \{A, \dots, G\}$. Any path going from x^* to x_Q can be written as

$$\gamma\gamma_Q = \gamma_1^{m_1} \gamma_2^{m_2} \gamma_3^{m_3} \gamma_Q, \quad \gamma \in \pi_1(\mathbb{R}_\delta^2 \setminus \sigma)$$

We introduce the notation Q_γ corresponding to the polygon Q and the path-index $\gamma\gamma_Q$.

The change of the reference points and the base paths is described as follows.

Lemma 4.1. *Let x^* be some reference point and $\gamma_A, \dots, \gamma_G$ be some base paths. Introduce a new reference point \tilde{x}^* and the new base paths for the initial configuration: $\tilde{\gamma}_A, \dots, \tilde{\gamma}_G$. Let the path connecting x^* with \tilde{x}^* be γ_* .*

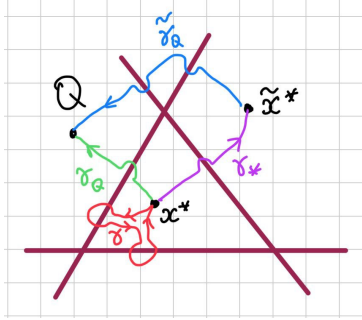


Fig. 11: To the change of contours

Let some element of $H_2^*(\tilde{U}, \tilde{U}_1)$ have notation Q_γ for the “old” reference point and base paths ($Q \in \{A, \dots, G\}$). Then, for the “new” reference point and the base paths the notation of the same element is $Q_{\gamma_*^{-1}\gamma\gamma_Q\tilde{\gamma}_Q^{-1}}$

The lemma is trivial.

in Lemma 4.1, the fundamental group $\pi_1(\mathbb{R}_\delta^2 \setminus \sigma)$ has two realizations: with the reference point x^* and \tilde{x}^* . Denote these realizations by π_1 and $\tilde{\pi}_1$. Indeed, $\gamma \in \pi_1$ and $\gamma_*^{-1}\gamma\gamma_Q\tilde{\gamma}_Q^{-1} \in \tilde{\pi}_1$.

Let π_1 be Abelian. Then the isomorphism

$$\pi_1 \rightarrow \tilde{\pi}_1 : \quad \gamma \rightarrow \gamma_*^{-1}\gamma\gamma_*$$

is *unique*, i.e. does not depend on γ_* . This isomorphism can be established, say, by representing γ in the form (22) where $\gamma_1, \gamma_2, \gamma_3$ are *some* elementary bypasses about the singularity components taken in the positive direction. The triplets (m_1, m_2, m_3) are common for both realizations. Thus, one can use the same notations for the fundamental group for the “old” reference point and paths, and for the “new” ones.

Using this isomorphism, one can formulate an important corollary of Lemma 4.1.

Let $\pi_1(\mathbb{R}_\delta^2 \setminus \sigma)$ be Abelian. Let Γ be a deformed plane \mathbb{R}^2 indented near σ in an arbitrary way. Let all basic paths $\gamma_A, \dots, \gamma_G, \tilde{\gamma}_A, \dots, \tilde{\gamma}_G$ (old and new ones), and γ_ belong to Γ (i.e. the paths are matched with the bridge symbols of Γ). Then the change of the base point and basic paths maps Q_γ to Q_γ .*

In other words, the position of the base point is not important.

4.3 Map $H_2^*(\tilde{U}, \tilde{U}_1) \rightarrow H_2(\tilde{U}_2)$

4.3.1 Formulation of the theorem of inflation

As we show below, the main tool for description of the integration surfaces are the elements of $H_2^*(\tilde{U}, \tilde{U}_1)$. Take some $W \in H_2^*(\tilde{U}, \tilde{U}_1)$. Let this cycle be represented as

$$W = \sum_j a_j Q_{\gamma_j}^{(m_j)}, \quad (23)$$

where $Q^{(j)}$ is a polygon in $\mathbb{R}^2 \setminus \sigma'$ (we may take $Q^{(1)} = A$, $Q^{(2)} = B$, etc), $a_j \in \mathbb{Z}$ are some coefficients, γ_j are paths describing the reference points of polygons in \tilde{U}_2 . We assume that all polygons are oriented in a natural way.

The following theorem plays an important role in description of integration surfaces.

Theorem 4.1 (Inflation). *Let all crossings of σ_j be transversal. Let $W \in H_2(\tilde{U}, \tilde{U}_2)$ be defined by (23). If*

$$\partial W = 0 \quad (24)$$

then any representative of W in $\mathcal{C}^2(\tilde{U}, \tilde{U}_1)$ admits a small deformation into some representative of a certain element $W'' \in H_2(\tilde{U}_2)$.

The boundary operator of (24) is understood in the sense of (21). The theorem states that if the relative cycle of the form (23) is a cycle (its boundary is zero), it corresponds to some boundaryless oriented surface W'' not passing through the singularity. In other words, a system of polygons with boundaries on the singularities can be slightly “inflated” and removed from the singularity.

We can illustrate the statement of the theorem by an elementary example. Let $\sigma = \sigma_1$,]

$$\sigma_1 : z_1 = 0$$

(see Fig. 12). There are two polygons denoted A and B . The group $\pi_1(\mathbb{R}_\delta^2 \setminus \sigma)$ is \mathbb{Z} ; its generator is γ . The reference point x^* is taken in A , and the base path γ_B is shown in the figure.

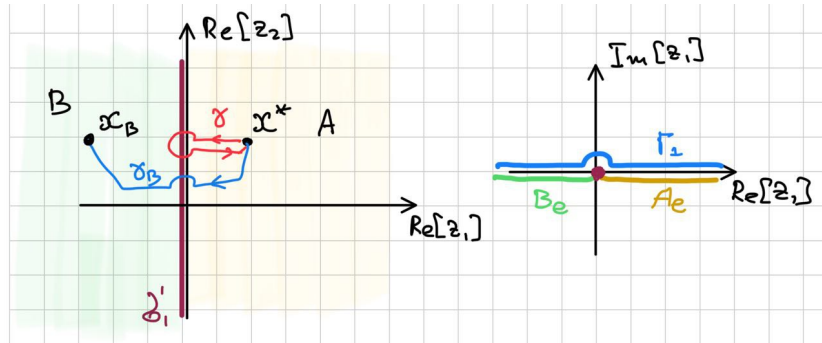


Fig. 12: An elementary example for Theorem 4.1

Take

$$W = A_e + B_e.$$

One can see that the boundary of this chain is zero (the boundary of A_e is $-\sigma'_1$, and the boundary of B_e is σ'_1), thus W obeys the conditions of the theorem. The inflation of W is the surface $W'' = \Gamma_1 \times \mathbb{R}$, where contour Γ_1 is shown in the right part of the figure. One can see that $A_e + B_e$ passes through σ , while Γ is shifted from σ .

The proof of the theorem is constructive. Namely, we build a surface S out of W , and deform it into W'' . For this, we draw narrow strips along the real traces σ'_j (see Fig. 13). The surface S is split into the parts lying outside these strips (they are face zones), the edge zones surrounding σ'_j but not including the neighborhoods of the vertices, and the vertex zones.

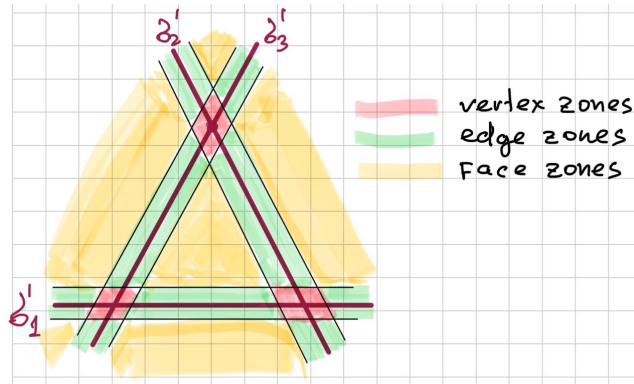


Fig. 13: Vertex, edge, and face zones

We leave the face parts of W as is, and deform this surface in the edge zones and in the vertex zones. The deformation of the edge zones is simple, while the deformation in the vertex zones is a bit more complicated.

A detailed proof can be found in Appendix C.

It is important to note that condition (24) can be checked directly. Namely, one can introduce notations for the elements of $\mathcal{C}^1(\tilde{U}_1, \tilde{U}_0)$ (i.e. for the edges of polygons) similar to the notations for polygons introduced above. For this one can take a reference point x on each polygon edge and index the edge by the path from $\Pi(x^*, x)$. Then one can compute the boundary for each term of (23) and check whether it equals zero.

4.3.2 Some remarks to the theorem of inflation

The condition of transversality of the crossings is not necessary. We can generalize the theorem to the case of quadratic tangential crossing. It should be handled as follows. For each vertex we build a contour γ (see Fig. 54 and 55). This contour can be put onto a deformation retract described in Subsection 3.2. This path should be contractible. The procedure of contraction of this loop into a point produces a surface over the deformation retract of a small part of \mathbb{C}^2 near the vertex. This surface may be used as a vertex patch for $\mathcal{E}(W)$.

Define $H_2^*(\tilde{U})$ by

$$H_2^*(\tilde{U}) = \{W \in H_2^*(\tilde{U}, \tilde{U}_1) \mid \partial W = 0\}.$$

The theorem can be reformulated as follows: *Under certain simplifying conditions there is a map*

$$\mathcal{E} : H_2^*(\tilde{U}) \rightarrow H_2(\tilde{U}_2). \quad (25)$$

We will use notations like $W'' = \mathcal{E}(W)$ below. The map \mathcal{E} makes an “inflation” of edge and vertex parts of W .

One should prove correctness of the definition of \mathcal{E} . Namely, the surface S is built from W not in a unique way, thus, formally, there is ambiguity in building of W'' . However, the resulting homology \mathcal{E} is the same.

To prove this, construct two different cycles W_1'' and W_2'' starting from the same W . Consider the cycle

$$W_d'' = W_2'' - W_1''.$$

Let us show that this cycle corresponds to a zero homology in $H_2(\tilde{U}_2)$. One can see that this cycle contains no face parts, so it can contain only edge and vertex parts. Moreover, this cycle is “finite”, namely, it does not contain infinite number of points with the same affix. By considering a single edge, one can easily see that there can exist no edge part of the cycle that is finite. Thus, W_d'' cannot contain edge parts. Similarly, one can prove that it cannot contain vertex parts.

4.3.3 Examples of application of the theorem of inflation

Example 4.1. Let the singularity be a circle

$$\sigma : z_1^2 + z_2^2 = 1.$$

The trace σ' splits the real plane into the parts A and $\mathbb{R}^2 \setminus A$, where A is the internal part of the real circle (see Fig. 14, left). Introduce the contour γ starting and ending at some reference point x^* and encircling σ in the positive direction.

The universal covering \tilde{U} is constructed as follows. The stratum \tilde{U}_2 is composed of $\mathbb{R}_\delta^2 \setminus \sigma$ indexed by the contours $\gamma^m \in \pi_1$. The stratum \tilde{U}_1 consists of a single sample of $\sigma \cap \mathbb{R}_\delta^2$. The stratum \tilde{U}_0 is empty.

Let be

$$W = A_e - A_\gamma.$$

Note that

$$\partial W = 0,$$

since $\partial A_e = \partial A_\gamma = \sigma'$. Thus, according to Theorem 4.1 it can be deformed into $\mathcal{E}(W) \in H_2(\tilde{U}_2)$. Let us describe the result of this deformation.

There is a single edge σ' and no vertexes. According to the proof of Theorem 4.1, the cycle $\mathcal{E}(W)$ consists of three parts: two face parts A_e and A_γ , and the edge part. The face parts are circles of radius $1 - \epsilon$, where ϵ is the width of the narrow strip drawn near the singularity. The edge part is the product of σ' and the arc belonging to γ , i.e. it is a torus cut along a circle. The radii of the torus are ϵ and $1 - \epsilon$. The scheme of $\mathcal{E}(W)$ is shown in Fig. 14, right. The edges labeled by the same numbers should be attached to each other.

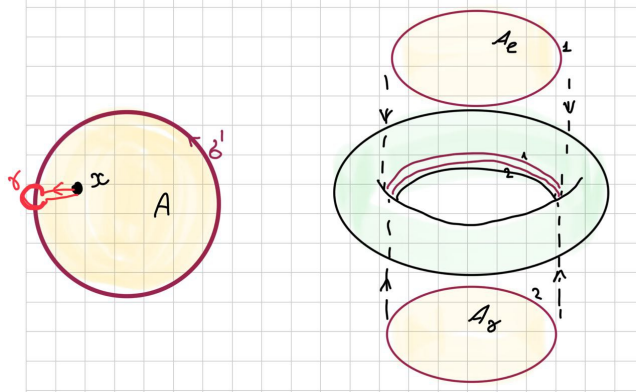


Fig. 14: The case $W = A_e - A_\gamma$

Example 4.2. Let the singular set be $\sigma = \sigma_1 \cup \sigma_2$,

$$\sigma_1 : z_1 = 0, \quad \sigma_2 : z_2 = 0. \quad (26)$$

The real traces σ'_1, σ'_2 split the plane into four quarters: A, B, C, D (see Fig. 15, left). Take the reference point x_A^* in A , and the reference points x_B, x_C, x_D in the sectors B, C, D . Draw some contour γ from x_A^* to x_A^* homotopical to zero in $\mathbb{R}_\delta^2 \setminus \sigma$ and passing through the points x_B, x_C, x_D (see the figure).

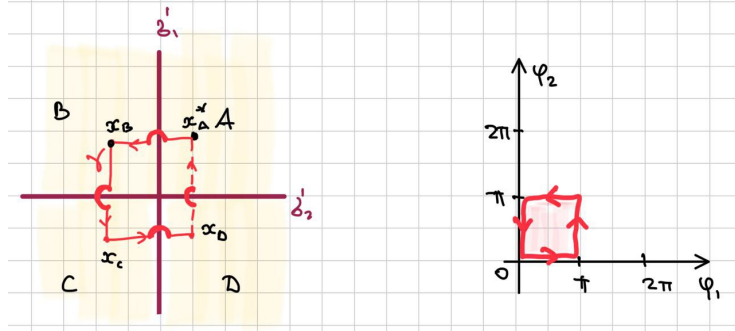


Fig. 15: The case $W = A_e + B_{\gamma_{AB}} + C_{\gamma_{AC}} + D_{\gamma_{AD}}$

Denote corresponding parts of γ by γ_{AB} , γ_{AC} , γ_{AD} (say, AC starts at x_A^* and ends at x_C). As usual, e is a trivial contour going from x_A^* to x_A^* . Take γ_{AB} , γ_{AC} , and γ_{AD} as the base contours for B, C, D .

Consider the chain

$$W = A_e + B_e + C_e + D_e. \quad (27)$$

Let us prove that $\partial W = 0$. Note that the contours γ_{AB} , γ_{BC} , γ_{CD} are local (they can be localized near corresponding parts of σ'_1 and σ'_2). Thus, the boundaries between A_e and B_e , B_e and C_e , C_e and D_e are common for these polygons, and thus, these parts of the boundary vanish in ∂W . Finally, consider the boundary between D_e and A_e . Since γ is homotopical to zero the contour γ_{AD} is homotopical to a local contour γ_{DA}^{-1} . So finally, this part of the boundary also vanishes.

The contour γ is exactly the contour that is the boundary of the vertex part of $\mathcal{E}(W)$ (see Fig. 54). Let us plot this contour in the coordinates (φ_1, φ_2) . The corresponding graph is shown in Fig. 15. Note that this contour is indeed closed.

The surface $\mathcal{E}(W)$ is built is four face parts, four edge parts, and one vertex part (see Fig. 16, left). The edge parts are half-cylinders of a small radius, and the vertex part is a quarter of a torus (a product of two arcs of angle π).

Indeed, building of $\mathcal{E}(W)$ is rather trivial in this case. The surface $\mathcal{E}(W)$ is a product of contours γ_1 and γ_2 in the planes ν_1 and ν_2 shown in Fig. 16, right.

Example 4.3. Let again the singularity have form (26). Let A be one of the quarter-planes of \mathbb{R}^2 split by σ'_1 and σ'_2 . Take a reference point x^* in A (see Fig. 17, left). Introduce the paths γ_1 , γ_2 starting and ending at x^* and bypassing σ_1 and σ_2 , respectively. Let be

$$W = A_e - A_{\gamma_1} - A_{\gamma_2} + A_{\gamma_1\gamma_2}. \quad (28)$$

One can connect the reference points on the corresponding sheets by local paths in the following order:

$$A_e \rightarrow A_{\gamma_1} \rightarrow A_{\gamma_1\gamma_2} \rightarrow A_{\gamma_2} \rightarrow A_e.$$

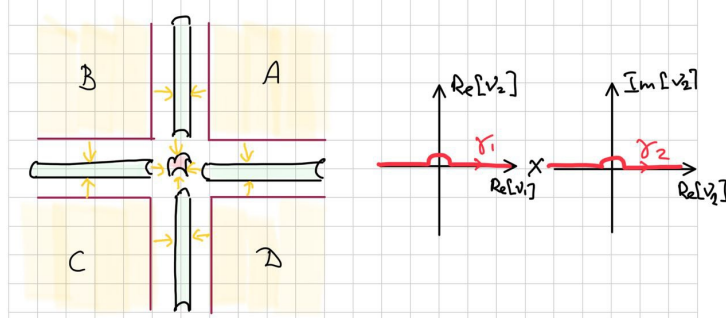


Fig. 16: The cycle $\mathcal{E}(W)$ for $W = A_e + B_e + C_e + D_e$

(The corresponding path in the (φ_1, φ_2) coordinates is shown in Fig. 17, left). This, together with the signs of the polygons, yields $\partial W = 0$. According to Theorem 4.1, W can be transformed into $\mathcal{E}(W) \in H_2(\tilde{U}_2)$.

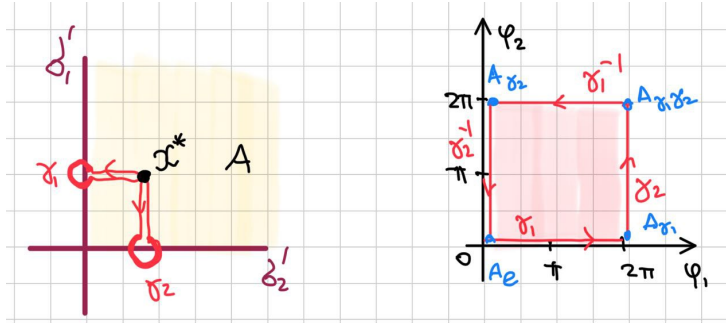


Fig. 17: The case $W = A_e - A_{\gamma_1} - A_{\gamma_2} + A_{\gamma_1 \gamma_2}$

The deformed surface $\mathcal{E}(W)$ consists of four face parts (sectors), four edge parts (cut half-infinite cylinders), and a single vertex part. The vertex part follows from the right part of Fig. 17, and it is a torus cut along to two circles (see Fig. 18, left).

Indeed, the surface is a product $\gamma_1 \times \gamma_2$ shown in Fig. 18, right.

Remark. Note that contour $\gamma = \gamma_1 \gamma_2 \gamma_1^{-1} \gamma_2^{-1}$ is the Pochhammer's contour in a certain sense.

Example 4.4. The following example develops Example 4.3 further. Consider the singular set

$$\sigma = \sigma_1 \cup \sigma_2, \quad \sigma_1 : z_1 = 0, \quad \sigma_2 : z_1 = z_2^2 - 1.$$

The traces of singularities split the plane \mathbb{R}^2 into five polygons. Let A be the finite biangle (see Fig. 19, left). Introduce the reference point $x^* \in A$ and

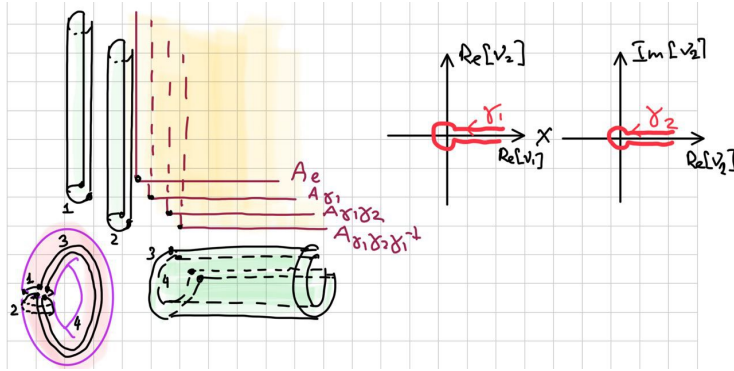


Fig. 18: The cycle $\mathcal{E}(W)$ for $W = A_e - A_{\gamma_1} - A_{\gamma_2} + A_{\gamma_1\gamma_2}$

elementary loops γ_1, γ_2 about the singularities. Let again be

$$W = A_e - A_{\gamma_1} - A_{\gamma_2} + A_{\gamma_1\gamma_2}.$$

Using the same logic as above, one can prove that $\partial W = 0$. Moreover, locally near the vertexes the structure of W is similar to that of Example 4.3. The structure of $\mathcal{E}(W)$ can be easily built as before. It is shown in Fig. 19, right.

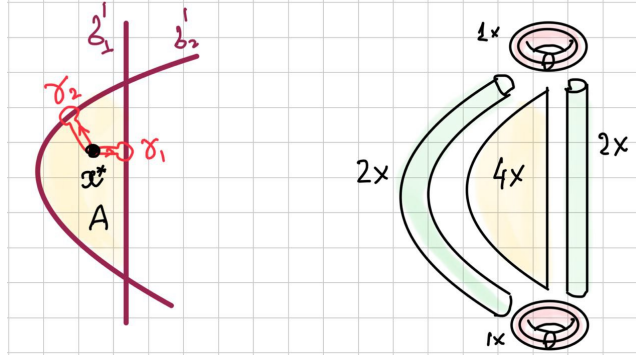


Fig. 19: The homology $\mathcal{E}(W)$ for $W = A_e - A_{\gamma_1} - A_{\gamma_2} + A_{\gamma_1\gamma_2}$

Note that the surface $\mathcal{E}(W)$ cannot be presented as a product of two contours. Note also that topologically $\mathcal{E}(W)$ is a sphere.

Example 4.5. Let the singularities be

$$\sigma = \sigma_1 \cup \sigma_2 \cup \sigma_3,$$

$$\sigma_1 : z_1 = 0, \quad \sigma_2 : z_2 = 0, \quad \sigma_3 : z_1 + z_2 = 1.$$

The traces of the singularities form a triangle. We denote the triangle by A and take the reference point x^* in it. Introduce the elementary loops $\gamma_1, \gamma_2, \gamma_3$

as it is shown in Fig. 20, left. Our aim is to build a surface $\mathcal{E}(W)$ composed of several copies of A (with some edge and vertex parts). For this, we should construct a corresponding $W \in H_2(\tilde{U}, \tilde{U}_1)$ such that $\partial W = 0$.

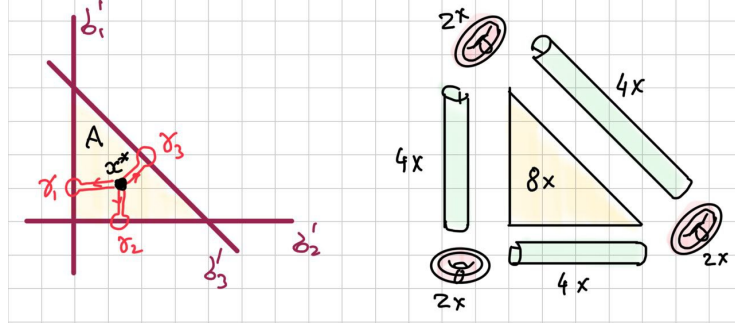


Fig. 20: The cycle $\mathcal{E}(W)$ for $W = A_e - A_{\gamma_1} - A_{\gamma_2} - A_{\gamma_3} + A_{\gamma_1\gamma_2} + A_{\gamma_2\gamma_3} + A_{\gamma_1\gamma_3} - A_{\gamma_1\gamma_2\gamma_3}$

Let us start with

$$W = A_e + \dots$$

The boundary of A_e (3 sides) should be annihilated by something. Thus, we should take

$$W = A_e - A_{\gamma_1^m} - A_{\gamma_2^k} - A_{\gamma_3^l} + \dots$$

for arbitrary $m, k, l \in \mathbb{Z}$. As a result, we have totally 12 segments of boundary, 6 of which compensate each other. A good idea is to cancel, say, boundaries of $-A_{\gamma_1^m} - A_{\gamma_2^k}$ by adding $+A_{\gamma_1^m\gamma_2^k}$, which has common boundaries with both of them. So, we have

$$W = A_e - A_{\gamma_1^m} - A_{\gamma_2^k} - A_{\gamma_3^l} + A_{\gamma_1^m\gamma_2^k} + A_{\gamma_1^m\gamma_3^l} + A_{\gamma_2^k\gamma_3^l} + \dots$$

Finally, we add the last term that cancels the remaining three sides:

$$W = A_e - A_{\gamma_1^m} - A_{\gamma_2^k} - A_{\gamma_3^l} + A_{\gamma_1^m\gamma_2^k} + A_{\gamma_1^m\gamma_3^l} + A_{\gamma_2^k\gamma_3^l} - A_{\gamma_1^m\gamma_2^k\gamma_3^l}. \quad (29)$$

This chain has the property $\partial W = 0$.

Let us take $m = k = l = 1$ for simplicity of display and deform W' into $\mathcal{E}(W)$. The face and edge parts are constructed in a simple way as before, so let us focus on the vertex parts. Consider the vertex that is the crossing of σ_1 and σ_2 . The cycle W can be transformed into two terms:

$$W = W_1 + W_2,$$

$$W_1 = A_e - A_{\gamma_1} - A_{\gamma_2} + A_{\gamma_1\gamma_2},$$

$$W_2 = -A_{\gamma_3} + A_{\gamma_1\gamma_3} + A_{\gamma_2\gamma_3} - A_{\gamma_1\gamma_2\gamma_3}.$$

One can see that each of the terms corresponds to Example 4.3, so each of these terms produce a cut torus.

Finally, the scheme of $\mathcal{E}(W)$ is shown in Fig. 20, right. It consists of 8 triangles, 12 cut cylinders, and 6 cut toruses.

Topologically, $\mathcal{E}(W)$ is a sphere. What is interesting, one can imagine $\mathcal{E}(W)$ as an octahedron (see Fig. 21).

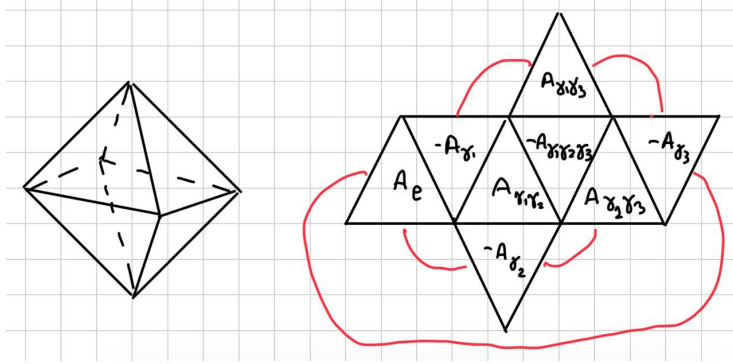


Fig. 21: The cycle W' as an octahedron

The Examples 4.1, 4.4, 4.5 are very important, since they provide typical structures of compact homologies from $H_2(\mathbb{U}_2)$. The singularities under consideration (a circle/oval, a biangle, and a triangle) are the main types of vanishing cycles from [2] (page 91, middle column there).

4.4 Group ring and vector notations

According to [4], we should introduce a *group ring* for $\pi_1(\mathbb{R}_\delta^2 \setminus \sigma)$ and a *module* over this group ring. Here we explain these basic objects in brief.

Let there be some fixed singularity set σ , some fixed reference point x^* , and the corresponding group $\pi_1(\mathbb{R}_\delta^2 \setminus \sigma)$ whose elements are denoted by γ_m (generally, there is an infinite number of elements, and the group can be non-Abelian). The unit element is denoted by e . Note that now the notation γ_m is related not necessary to the generators of the group.

First, introduce the *free group ring* Ω for $\pi_1(\mathbb{R}_\delta^2 \setminus \sigma)$ over \mathbb{Z} . The elements of Ω are finite formal sums

$$a = \alpha_{m_1} \gamma_{m_1} + \cdots + \alpha_{m_k} \gamma_{m_k}, \quad \alpha_m \in \mathbb{Z}, \quad (30)$$

i.e. they are formal linear combinations of γ_m with integer coefficients. We assume that if some γ_j does not participate in the sum, this is equivalent to $\alpha_j = 0$. The zero element of the ring is the empty sum (all coefficients are zero). The operation “+” is commutative.

One can define a sum of such elements. If, in addition to (30),

$$b = \beta_{m_1} \gamma_{m_1} + \cdots + \beta_{m_k} \gamma_{m_k}$$

then

$$a + b = (\alpha_{m_1} + \beta_{m_1})\gamma_{m_1} + \cdots + (\alpha_{m_k} + \beta_{m_k})\gamma_{m_k}$$

One can define also a product of two elements in a formal way. Say,

$$(\alpha_1\gamma_1 + \alpha_2\gamma_2 + \alpha_3\gamma_3)(\beta_4\gamma_4 + \beta_5\gamma_5) =$$

$$\alpha_1\beta_4\gamma_1\gamma_4 + \alpha_2\beta_4\gamma_2\gamma_4 + \alpha_3\beta_4\gamma_3\gamma_4 + \alpha_1\beta_5\gamma_1\gamma_5 + \alpha_2\beta_5\gamma_2\gamma_5 + \alpha_3\beta_5\gamma_3\gamma_5$$

($\gamma_j\gamma_k$ is a product of group element, i.e. a concatenation). The unit element of Ω is $1e = e$. Note that the multiplication is generally not commutative, so the order of factors is important.

Let us explain why we need the ring Ω . Introduce the polygons into which the real traces σ'_j split the plane \mathbb{R}^2 . For example, in Fig. 10 these polygons are A, B, \dots, G . The elements of $H_2(\tilde{U}, \tilde{U}_1)$ are sums of samples of these polygons taken on different sheets of \tilde{U}_2 .

Introduce a reference point and the base contours for all polygons. Consider a particular polygon of this set, say A . Construct some element of $H_2(\tilde{U}, \tilde{U}_1)$ that contains only samples of A (in which the reference point is taken). Such an element can be written as

$$W = \alpha_{m_1}A_{\gamma_{m_1}} + \alpha_{m_2}A_{\gamma_{m_2}} + \cdots + \alpha_{m_k}A_{\gamma_{m_k}}.$$

Let us associate an element $a = \alpha_{m_1}\gamma_{m_1} + \cdots + \alpha_{m_k}\gamma_{m_k} \in \Omega$ and introduce a notation

$$W = Aa.$$

The last notation is purely formal, we just state that

$$A(\alpha_{m_1}\gamma_{m_1} + \cdots + \alpha_{m_k}\gamma_{m_k}) \equiv \alpha_{m_1}A_{\gamma_{m_1}} + \cdots + \alpha_{m_k}A_{\gamma_{m_k}}. \quad (31)$$

An arbitrary element of $H_2^*(\tilde{U}, \tilde{U}_1)$ is a sum of all A -polygons, B -polygons, C -polygons, etc. By applying the notation (31), this element can be written in the form

$$W = Aa_A + Ba_B + Ca_C + \dots, \quad (32)$$

where $a_A, a_B, a_C, \dots \in \Omega$.

One can see that $H_2^*(\tilde{U}, \tilde{U}_1)$ is a vector space with the basis $\{A, B, C, \dots\}$ and the coefficients $a_A, a_B, a_C, \dots \in \Omega$. Below everywhere we write W as a vector-row

$$\mathbf{w} = (a_A, a_B, \dots).$$

Remark. A vector space with coefficients in Ω is a *module* (right or left, depending on how we are going multiply the elements). Such modules are used, say, in [4]. Here we prefer not to introduce these concepts since we don't use deep algebraic results related to them.

4.5 Reduction of homologies for non-logarithmic singularities

In all examples above, homologies $\mathcal{E}(W)$ are built in the universal covering \tilde{U}_2 . The structure of this covering assumes that all components of the singularity set are logarithmic branch lines. Typically, however, we use these cycles to integrate a function $F(z_1, z_2)$ having the same singularity set, but typically a simpler structure.

One may wonder, whether one can use the the Riemann domain \hat{U} instead of the universal Riemann domain \tilde{U} from the very beginning. However, it is not possible to prove an analog of Theorem 4.1 in this case. Namely, the edge parts of $\mathcal{E}(W)$ are chosen not uniquely, and therefore it is not possible to prove that the vertex parts always exist.

Example 4.6. Consider the Riemann domain of the function

$$f(z_1, z_2) = \sqrt{z_1 z_2 (1 - z_1 - z_2)}.$$

One can introduce the Riemann domain \hat{U} of this function. It has two sheets over the regular points, and a single set of the singularity set. One can introduce a cell complex over \hat{U} . Then, one can define relative homologies $H_2(\hat{U}, \hat{U}_1)$ chains $\mathcal{G}^2(\hat{U})$, and map Φ . Let $A_e \in \mathcal{G}^2(\hat{U})$ be a triangle. One can see that

$$\partial\Phi(A_e - A_{\gamma_1}) = 0.$$

However, there exists no element $W'' \in H_2(\hat{U}_2)$ corresponding to $W = A_e - A_{\gamma_1}$.

However, if we succeeded to build a surface $\mathcal{E}(W) \in H_2(\tilde{U}_2)$, we can state that the function $F(z_1, z_2)$ with the same singularities is single-valued on this surface, i.e. that W'' can be used as an integration surface for F . Moreover, since the Riemann domain of F can have “smaller amount of sheets” comparatively to \tilde{U} , the surface $\mathcal{E}(W)$ possibly can be reduced. This reduction is made by canceling all parts of W'' that bear the same function F but bearing opposite signs in the sum (22). Some examples of this reduction are given here.

Mathematically, in each case there is a map

$$\Psi : \tilde{U} \rightarrow \mathcal{R},$$

where \mathcal{R} is the Riemann domain of F .

Example 4.7. Consider the case of Example 4.3. Let a function $F(z)$ have simple poles at σ_1 and σ_2 (and no branching). Then the cycle W'' whose structure is shown in Fig. 18, left, is simplified significantly. First, note that the face parts A_e and $-A_{\gamma_1}$ cancel each other due to the sign. So do $-A_{\gamma_2}$ and $A_{\gamma_1\gamma_2}$. The edge parts for σ_1 (cut cylinders) cancel each other (they also participate with opposite orientations). So do the edge parts for σ_2 . Finally, $\Psi(\mathcal{E}(W))$ is the small torus near the vertex. The torus is no longer cut, and it produces the composed residue for the crossing of the singularities.

Example 4.8. Consider the singularities and cycle $\mathcal{E}(W)$ of Example 4.4. Let σ_2 be a branch line for function $F(z)$, and σ_1 be a simple polar set. Here we describe the reduction of $\mathcal{E}(W)$ shown in Fig. 19.

The face part A_e and $-A_{\gamma_1}$ cancel each other. So do $-A_{\gamma_2}$ and $A_{\gamma_1\gamma_2}$. The edge parts related to σ_2 cancel each other as well. The remaining parts are two cylinders (they are not cut anymore), and two toruses cut along a single circle. These components are shown in Fig. 22, left.

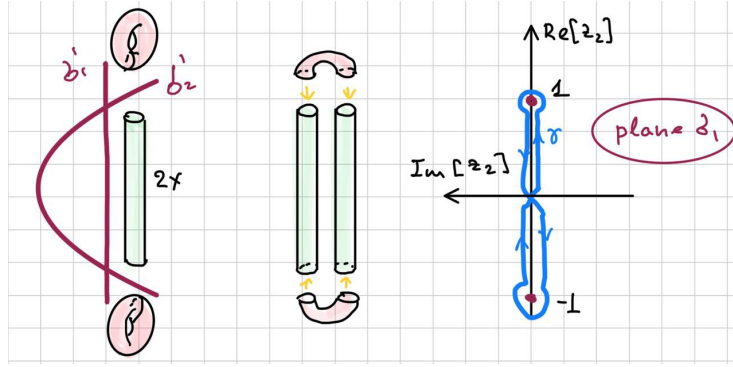


Fig. 22: The reduced homology for the biangle

The remaining edge and vertex parts are attached to each other as it is shown in the middle part of the figure. The resulting topology is a torus. Indeed, this torus is one of the realizations the Leray coboundary (see [2]) of some contour $\gamma \subset \sigma_1$. The set σ_1 can be parametrized by the variable z_2 ; the intersection $\sigma_1 \cap \sigma_2$ corresponds to $z_2 = \pm 1$. The contour γ is shown in the right part of the figure. The resulting integral can be computed using the Leary residue.

Example 4.9. Consider the structure of singularities from Example 4.5. Let function $F(z)$ have branching at σ_3 and simple poles at σ_1, σ_2 .

One can easily see that the reduced cycle $\Psi(\mathcal{E}(W))$ consists of two toruses located near $\sigma_1 \cap \sigma_2$ (see Fig. 23, left).

Example 4.10. Consider again the singularities from Example 4.5. Let σ_1 be a polar set, and σ_2, σ_3 be branch lines. Then the reduced cycle consists of 4 cut toruses, and 4 edge cylinders going along σ'_1 (see Fig. 23, center).

The resulting cycle is a Leray coboundary of the contour γ shown in the right part of the figure. The contour lies in the plane σ_1 parametrized by the variable z_2 .

5 Transformation of relative homologies

5.1 Landau set in the space of parameters

Consider the space $z \in \mathbb{R}_\delta^2 \setminus \sigma$, where $\sigma(t) = \sigma_1(t) \cup \sigma_2(t) \cup \dots$. The singularity components $\sigma_j(t)$ depend on complex parameters t . The parameter

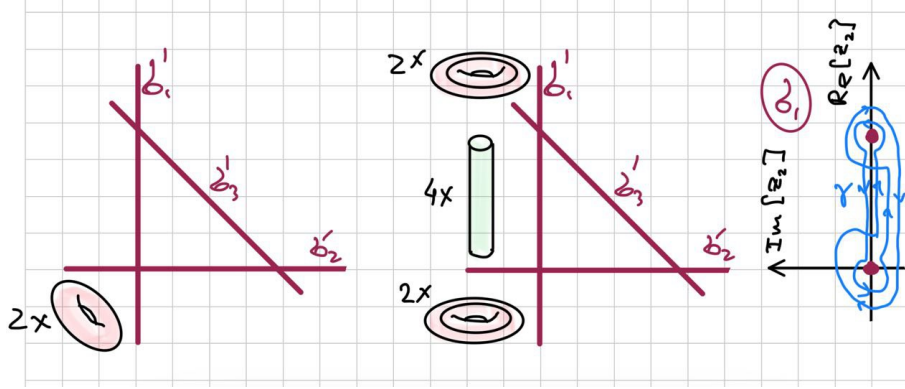


Fig. 23: The reduced cycle for a triangle

t may be a complex scalar belonging to \mathbb{R}_δ , or it may be multidimensional, i.e. $t = (t_1, t_2, \dots, t_M) \in \mathbb{R}_\delta^M$. We assume for clarity that $\sigma(t)$ obeys the real property for real t .

Construct the universal Riemann domain \tilde{U} for the space $\mathbb{R}_\delta^2 \setminus \sigma(t)$. Indeed, this universal Riemann domain depends on t . Our main object of study is the set of homologies $H_2(\tilde{U}_2)$, which also depends on t (we can denote this by $H_2(\tilde{U}_2(t))$).

The whole domain of t is split into two set: the regular points and the singular points. The set of singular points in the t -space (denoted σ^t) is an object different from the set in the z -space ($\sigma(t)$). It is usually referred to as the *Landau set*. The formal definition of the Landau set is quite complicated (see [2, 5]), and we do not use it here. Instead, we use a rather vague “definition”:

Definition 5.1. *The singular set σ^t is the set for which $\sigma(t)$ degenerates. This means that some elements of $H_2(\mathbb{R}_\delta^2, \sigma(t))$ vanish.*

The definition means that some polygon formed by the traces of the singularities σ_j^t turns into a point. Indeed, at this moment, the polygons on all sheets of the universal Riemann domain also disappear, they are elements of $H_2^*(\tilde{U}, \tilde{U}_1)$.

We assume (and this is shown below by construction in examples) that σ^t is an analytic set whose main stratum has complex codimension 1, i.e. it has real dimension $2M - 2$.

Let be

$$B = \mathbb{R}_\delta^M \setminus \sigma^t.$$

We assume that $H_2(\tilde{U}_2(t))$ is the same for all $t \in B$, and the representatives of the classes can be chosen varying continuously with t . Thus, a map

$$H_2(\tilde{U}_2(t)) \rightarrow t, \quad t \in B$$

produces a fiber bundle over B with a fiber $H_2(\tilde{U}_2)$.

The relation (34) defines a set σ^t of complex codimension 1 (this is a straight line).

The space $B = \mathbb{C}^3 \setminus \sigma^t$ is not simple-connected. Its fundamental group is \mathbb{Z} . Its generator is an elementary bypass about the line σ^t .

One can imagine the bypass about σ^t as follows. Fix the variables t_1 and t_2 , i.e. consider the cross-section of the whole domain of t . There is a selected point $t_3^* = t_1 + t_2$ in this cross-section. This point corresponds to the special position of the singularity σ_3 with respect to σ_1 and σ_2 . This special position is shown in the left part of Fig. 24, left. Perform a bypass λ shown in the right part of the figure. One can see that σ_3 bypasses about the position of σ_3^* as it is shown in the left.

One can also fix the position of σ_1 and σ_3 , and carry σ_2 about its critical position (see Fig. 25, left). Alternatively, one can fix the position of σ_2 and σ_3 , and carry σ_1 (see Fig. 25, right). What is important, the result will always be the same, since the value $t_1 + t_2 - t_3$ makes a single bypass about zero in the positive direction. All such variants of realization of λ are homotopical in B .

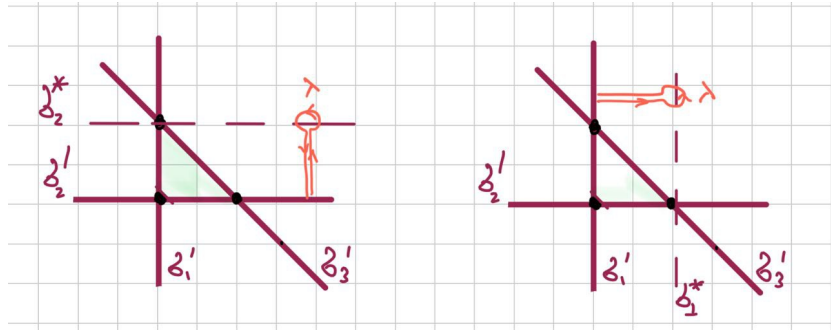


Fig. 25: Variants of realization of bypass λ

Example 5.2. Consider the singularities

$$\sigma_1(t) : z_1 = t_1, \quad \sigma_2(t) : z_1 - z_2^2 = t_2. \quad (35)$$

The space of parameters is \mathbb{C}^2 . These singularities form a biangle AB (see Fig. 26, left). This biangle vanishes if

$$t_1 - t_2 = 0. \quad (36)$$

This equation forms the set σ^t , which is again a straight line, i.e. a set of complex codimension 1.

The elementary bypass about σ^t can be made in two ways shown in Fig. 26, right and left. The result of both bypasses is the same.

Example 5.3. Finally, there one can define a circle

$$z_1^2 + z_2^2 = t. \quad (37)$$

The space of parameters is \mathbb{C} . The circle vanishes at a single point $\sigma^t : t = 0$.

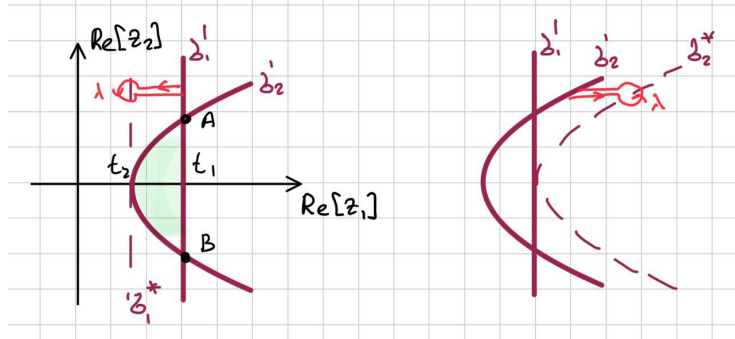


Fig. 26: Vanishing of a biangle

A key statement of the Picard–Lefschetz–Pham theory is that a surface $\Gamma \in H_2(\tilde{U}_2)$ changes as a result of bypass λ_j if and only if the corresponding vanishing relative homology *pinches* it. “Pinches” means that Γ has a non-zero intersection index with the corresponding relative homology. The intersection index is a topological invariant, so one cannot deform Γ in such a way that it passes far enough from the vanishing homologies. So, a sort of a catastrophe happens with Γ when the relative homology vanishes.

Below we study the cases described in these examples one-by-one. We use a slightly different method comparatively to what is used in a standard exposition of the Picard–Lefschetz–Pham theory. Namely, instead of finding ramification of the absolute homologies from $H_2(\tilde{U}_2)$, we find the ramification of relative homologies from $H_2^*(\tilde{U}, \tilde{U}_1)$. As we have shown in Theorem 4.1, each element of $H_2^*(\tilde{U}, \tilde{U}_1)$ corresponds to an element of $H_2^*(\tilde{U}_2)$. Thus, we have a description of ramification of the elements of $H_2^*(\tilde{U}_2)$. In other words, we assume that the diagram

$$\begin{array}{ccc}
 W & \xrightarrow{\varepsilon} & W'' \\
 \lambda \downarrow & & \downarrow \lambda \\
 W_\lambda & \xrightarrow{\varepsilon} & W''_\lambda
 \end{array} \tag{38}$$

is commutative (the horizontal arrows stand for application of Theorem 4.1). The symbols W and W''_λ stand for the elements of $H_2^*(\tilde{U}, \tilde{U}_1)$ and $H_2^*(\tilde{U})$ after the bypass λ .

The commutativity of this diagram follows from continuity.

5.3 Branching of the fundamental group

Before we start with the branching of the relative homologies $H_2^*(\tilde{U}, \tilde{U}_1)$ as the singularity set $\sigma(t)$ is deformed, let us study branching of the fundamental group $\pi_1(\mathbb{R}_\delta^2 \setminus \sigma(t))$. The branching should occur about the same Landau set σ^t .

The branching of $\pi_1(\mathbb{R}_\delta^2 \setminus \sigma(t))$ can be described as follows. Each bypass λ

in the t -space bypassing σ^t corresponds to a map

$$\psi_\lambda : \pi_1(\mathbb{R}_\delta^2 \setminus \sigma(t)) \rightarrow \pi_1(\mathbb{R}_\delta^2 \setminus \sigma(t))$$

that is an isomorphism.

There is a seemingly surprising property of branching of $\pi_1(\mathbb{R}_\delta^2 \setminus \sigma(t))$ following from the consideration of dimensions:

Lemma 5.1. *If a vanishing homology is local, the elements of π_1 are not ramified.*

The explanation is as follows: generally, one can deform a path $\gamma \in \pi_1(\mathbb{R}_\delta^2 \setminus \sigma(t))$ and make it pass far from the vanishing homology. Thus, in this case

$$\psi_\lambda(\gamma) = \gamma.$$

More formal reason of this is that one cannot correctly define an intersection index an 1D object (contour) and a 2D object (a vanishing relative homology from $H_2(\mathbb{R}_\delta^2, \sigma(t))$).

The statement of Lemma 5.1 is quite important for the consideration below, since the map ψ_λ formally participates in the notations of the relative homology transformations. According to the lemma, we replace $\psi_\lambda(\gamma)$ by γ .

We should note, however, that there is an important particular case, for which the fundamental group branches. Let there exist elements of $H_3(\mathbb{R}_\delta^2 \setminus \sigma)$ that vanish. Then, if the intersection index of γ and such elements is non zero, the branching may occur.

Consider an example. Let be

$$\sigma_1 : z_1 = 0, \quad \sigma_2(t) : z_1 = t.$$

Let t bypass zero. Then, the contours γ_1 and γ_2 bypassing σ_1 and σ_2 are ramified as it is shown in Fig. 27. Indeed, the vanishing element of $H_3(\mathbb{R}_\delta^2 \setminus \sigma)$ is the product of the segment $[0, t]$ in the z_1 -plane and the whole z_2 -plane, i.e. formally it is not local.

Below, however, we consider only the cases, for which the fundamental group is not branching.

5.4 Elementary transformations

5.4.1 Triangle

Consider three singularity components $\sigma = \sigma_1 \cup \sigma_2 \cup \sigma_3$ having the real property. Introduce the notations and contours enabling us to study the situation algebraically. Namely, denote the polygons of $\mathbb{R}^2 \setminus \sigma$ by the letters A, \dots, F as it is shown in Fig. 28, left. Choose the orientation of the polygons in the natural way. The triangle A will be a vanishing cell. Take a reference point x^* in any of non-vanishing polygons, say in B . Introduce the base paths γ_A, γ_F (the path γ_B is trivial). as it is shown Fig. 28, left. The paths are shown by green. One

Represent W as a vector-row of elements of Ω :

$$W \leftrightarrow \mathbf{w} = (a_A, a_B, \dots, a_G). \quad (40)$$

Below we use widely the vector notations instead of sums like (39). We use also left and right multiplication of W by $b \in \Omega$:

$$bW \leftrightarrow (ba_A, ba_B, \dots, ba_G),$$

$$Wb \leftrightarrow (a_Ab, a_Bb, \dots, a_Gb),$$

and multiplication of vectors by matrices whose elements belong to Ω .

Theorem 5.1. *Let one of the singularity components bypass the crossing of two other lines in the positive direction as it is shown in Fig. 29. The bypass is denoted by λ .*

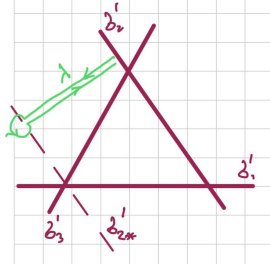


Fig. 29: A basic bypass for triangle

Any relative homology W of the form (39) is transformed according to the matrix-vector formula

$$\mathbf{w} \xrightarrow{\lambda} \mathbf{w} \mathbf{T}_3, \quad \mathbf{T}_3 = \begin{pmatrix} \gamma_1 \gamma_2 \gamma_3 & 0 & 0 & 0 & 0 & 0 & 0 \\ \gamma_2 - \gamma_1 \gamma_2 \gamma_3 & e & 0 & 0 & 0 & 0 & 0 \\ \gamma_1 - \gamma_1 \gamma_2 \gamma_3 & 0 & e & 0 & 0 & 0 & 0 \\ \gamma_3 - \gamma_1 \gamma_2 \gamma_3 & 0 & 0 & e & 0 & 0 & 0 \\ -\gamma_2 \gamma_3 + \gamma_1 \gamma_2 \gamma_3 & 0 & 0 & 0 & e & 0 & 0 \\ -\gamma_1 \gamma_2 + \gamma_1 \gamma_2 \gamma_3 & 0 & 0 & 0 & 0 & e & 0 \\ -\gamma_1 \gamma_3 + \gamma_1 \gamma_2 \gamma_3 & 0 & 0 & 0 & 0 & 0 & e \end{pmatrix}. \quad (41)$$

The elements of the matrix \mathbf{T}_3 belong to Ω , the addition and multiplication are understood in the sense of the ring Ω .

The proof of the theorem can be found in Appendix D.

Remark. For the bypass λ^{-1} one can use the formulae (172)–(178) after the change $\gamma_1 \rightarrow \gamma_1^{-1}$, $\gamma_2 \rightarrow \gamma_2^{-1}$, $\gamma_3 \rightarrow \gamma_3^{-1}$.

5.4.2 Biangle

Let be $\sigma = \sigma_1 \cup \sigma_2$, and the traces of the singularities form a biangle in \mathbb{R}^2 (see Fig. 30). The basic contours are shown in the same figure. The crossings of the singularities are transversal. Consider the bypass λ of σ_1 about the tangent σ_{1*} to σ_2 (see Fig. 31).

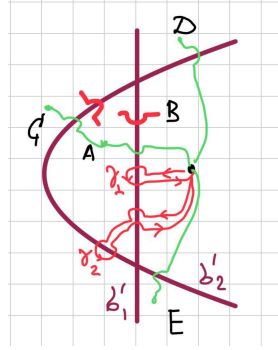


Fig. 30: Notations for biangle

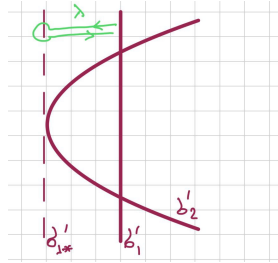


Fig. 31: Bypass λ for biangle

The group $\pi_1(\mathbb{R}_\delta^2 \setminus \sigma)$ is a commutative group with generators $\{\gamma_1, \gamma_2\}$ shown in Fig. 30.

Let be

$$W = A a_A + B a_B + C a_C + D a_D + E a_E. \quad (42)$$

The polygons A, \dots, E are shown in Fig. 30, right. Associate the vector

$$w = (a_A, a_B, a_C, a_D, a_E)$$

with W .

Theorem 5.2. *As the result of the bypass λ , the vector w transforms as follows:*

$$w \xrightarrow{\lambda} w \mathbf{T}_2, \quad \mathbf{T}_2 = \begin{pmatrix} -\gamma_1\gamma_2 & 0 & 0 & 0 & 0 \\ \gamma_1 + \gamma_1\gamma_2 & e & 0 & 0 & 0 \\ \gamma_2 + \gamma_1\gamma_2 & 0 & e & 0 & 0 \\ -\gamma_1\gamma_2 & 0 & 0 & e & 0 \\ -\gamma_1\gamma_2 & 0 & 0 & 0 & e \end{pmatrix}. \quad (43)$$

5.4.3 Circle

Finally, consider a circle. Namely, σ be defined by

$$\sigma : z_1^2 + z_2^2 = t, \quad (44)$$

and t moves along a contour bypassing zero in the positive direction (see Fig. 32). We denote this bypass by λ .

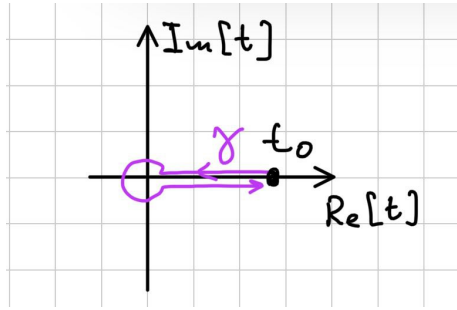


Fig. 32: A loop γ for variable t

The real trace σ' splits \mathbb{R}^2 into the parts A and B as it is shown in Fig. 33.

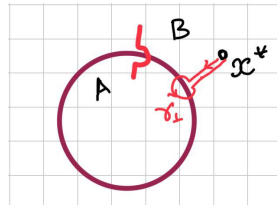


Fig. 33: Notations for a circle

The elements of $H_2(\tilde{U}, \tilde{U}_1)$ are described as

$$W = A a_A + B a_B,$$

with which we associate the vector

$$w = (a_A, a_B).$$

Theorem 5.3. *Vector w is transformed as follows:*

$$w \xrightarrow{\lambda} w \mathbf{T}_1, \quad \mathbf{T}_1 = \begin{pmatrix} \gamma_1 & 0 \\ 0 & e \end{pmatrix}. \quad (45)$$

6 Branching of homologies from $H_2^*(U_2)$

6.1 Classical formulation of the Pham's result

Above, we considered only changes of the relative homologies from $H_2^*(\tilde{U}, \tilde{U}_1)$ under some bypasses λ . Here we consider the changes of absolute homologies from $H_2^*(\tilde{U}_2)$. This description follows from the the diagram (38), i.e. one can use the formulae for the relative homologies.

Here and below we formulate the classical results without proofs. Some details can be found in [4]

Let be $W \in H_2^*(\tilde{U}, \tilde{U}_1)$, and $w \in \Omega^J$ is a corresponding vector introduced above. Here J is the number of polygons in $\mathbb{R}^2 \setminus \sigma$.

Proposition 6.1. *The set of W obeying the condition (24) is a left module over Ω , i.e. for any two such W , namely W_1 and W_2 , and any element $a \in \Omega$, then $W_1 + W_2$ and aW_1 belong to the same set.*

This statement is obvious.

Remark. Surprisingly, the condition (24) cannot be written in the matrix form in Ω in an easy way.

Remark. The module is *left* because the path-indices for the elements of $H_1(\tilde{U}_1)$ are *left* cosets with respect to local subgroups (7).

Denote the set of $w \in \Omega^M$ such that corresponding W obeys (24) by $h_2(\tilde{U}_2)$. Denote also the subset of compact elements of $h_2(\tilde{U}_2)$ by $h_2^c(\tilde{U}_2)$. Indeed, $h_2^c(\tilde{U}_2)$ is also a left module over Ω .

The set $h_2(\tilde{U}_2)$ taken as a group is isomorphic to $H_2(\tilde{U}_2)$. The same is true for compact homologies and $h_2^c(\tilde{U}_2)$.

Proposition 6.2. *Let Q be a compact element of $H_2^*(\tilde{U}, \tilde{U}_1)$, and W'' be an element of $H_2(\tilde{U}_2)$. Then one can define correctly the intersection index of Q and W'' denoted $\ll Q, W'' \gg$.*

This statement is non-trivial, and it implies three important facts. 1) Due to the dimension analysis, the intersection index exists. 2) The intersection index is a topological invariant. 3) The intersection index depends not only on a polygon of Q , but also on its path-index.

Let us illustrate the second statement by a 1D example. Let be $\sigma = \{0, 1\} \in \mathbb{C}$. A fragment of the universal Riemann domain is shown in Fig. 34. We take $W'' = \mathcal{E}(A_e + B_e + C_e)$ and $Q = A_e$. One can see that the intersection index $\ll Q, W'' \gg$ is non-zero: W'' crosses Q . At the same time, take Q' on another sheet of the universal Riemann domain, say $Q' = A_{\gamma_1}$. One can see that the intersection index $\ll Q', W'' \gg$ is zero (W'' does not cross Q').

Let us formulate the main result of Picard–Lefschetz–Pham theory.

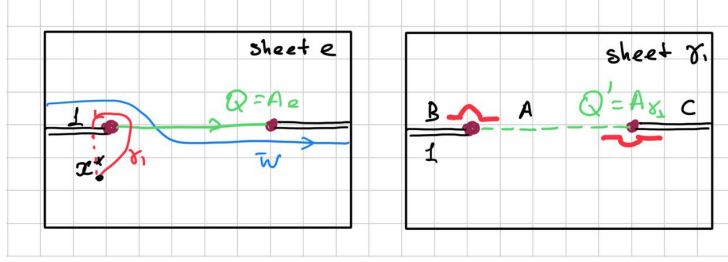


Fig. 34: Illustration of dependence of the intersection index on the path-index of Q

Theorem 6.1 (Pham). *Let λ be an elementary bypass (single, in the positive direction) about a component of σ^t corresponding to a vanishing polygon K , which may be a circle, a biangle, or a triangle formed by singularity components σ_1 , $\{\sigma_1, \sigma_2\}$, or $\{\sigma_1, \sigma_2, \sigma_3\}$, respectively. Let $\gamma_1, \gamma_2, \gamma_3$ be elementary bypasses about $\sigma_1, \sigma_2, \sigma_3$. Let $W'' \in H_2(\tilde{U}_2)$. Then*

$$W'' \xrightarrow{\lambda} W''_{\lambda}, \quad (46)$$

$$W''_{\lambda} = W'' + \sum_{\gamma} \langle\langle W'', K_{\gamma} \rangle\rangle \mathcal{E}(K_{\gamma} a), \quad (47)$$

where

$$a = \begin{cases} e - \gamma_1 & \text{for a circle} \\ (e - \gamma_1)(e - \gamma_2) & \text{for a biangle} \\ (e - \gamma_1)(e - \gamma_2)(e - \gamma_3) & \text{for a triangle} \end{cases} \quad (48)$$

The summation is held over all $\gamma \in \pi_1$.

Remark. Indeed, only a finite number of terms in (47) have non-zero intersection indexes.

This theorem enables one (in principle) to describe a change of W'' under λ in all cases.

We introduce the notation for the variation of a homology from $H_2(\tilde{U}_2)$:

$$\text{var}_{\lambda}(W'') = W''_{\lambda} - W''. \quad (49)$$

6.2 Illustration of Theorem 6.1 obtained by applying the matrix formalism

We demonstrate the statement of the theorem by several examples. Namely, we take homologies W that are pinched and not pinched by the vanishing cycle. In all

Example 6.1. Consider the triangle, i.e. the conditions of Theorem 5.1. Let be

$$W = A_e + B_e + C_e + D_e + E_e + F_e + G_e, \quad (50)$$

i.e.

$$w = (e, e, e, e, e, e, e).$$

The bridge notations for surface $\mathcal{E}(W)$ are shown in Fig. 35, left. Note that according to the standard definition [3]

$$\langle\langle W, A_e \rangle\rangle = -1.$$

One can easily demonstrate that $\langle\langle W, A_\gamma \rangle\rangle = 0$ for all $\gamma \neq e$.

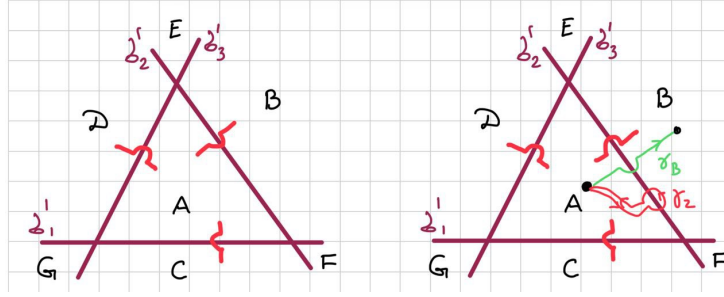


Fig. 35: Bridge notations for W for triangle

Apply the bypass λ described in the condition of Theorem 5.1. Indeed,

$$\text{var}_\lambda(w) \equiv w_\lambda - w = w\mathbf{T}_3 - w, \quad (51)$$

Performing a simple matrix computations, obtain

$$\text{var}_\lambda(w) = (b, 0, 0, 0, 0, 0, 0), \quad (52)$$

$$b = -e + \gamma_1 + \gamma_2 + \gamma_3 - \gamma_1\gamma_2 - \gamma_2\gamma_3 - \gamma_1\gamma_3 + \gamma_1\gamma_2\gamma_3 = \\ -(1 - \gamma_1)(1 - \gamma_2)(1 - \gamma_3). \quad (53)$$

This means that the bypass λ changes W by adding a homology A_b . According to the scheme (38),

$$\mathcal{E}(W) \xrightarrow{\lambda} \mathcal{E}(W) + \mathcal{E}(A_b).$$

The additional homology is built in details in Example 4.5.

Example 6.2. Let the singularity σ and the bypass λ again correspond to the conditions of Theorem 5.1. Let be

$$W = A_e + B_{\gamma_2^{-1}} + C_e + D_e + E_{\gamma_2^{-1}} + F_{\gamma_2^{-1}} + G_e. \quad (54)$$

This notation corresponds to the integration surface having the bridge notations shown in Fig. 35, right. The element (54) corresponds to the vector

$$w = (e, \gamma_2^{-1}, e, e, \gamma_2^{-1}, \gamma_2^{-1}, e). \quad (55)$$

This homology has zero intersection index with any A_γ .

Apply formula (51). The result is

$$\text{var}_\lambda(w) = (0, 0, 0, 0, 0, 0), \quad (56)$$

i.e. corresponding integration surface does not change.

Example 6.3. Let σ and λ correspond to the conditions of Theorem 5.2. Let be

$$W = A_e + B_e + C_e + D_e + E_e. \quad (57)$$

The bridge notations for this surface are shown in Fig. 36, left. W has a non-zero intersection index with A . The vector describing W is

$$w = (e, e, e, e, e). \quad (58)$$

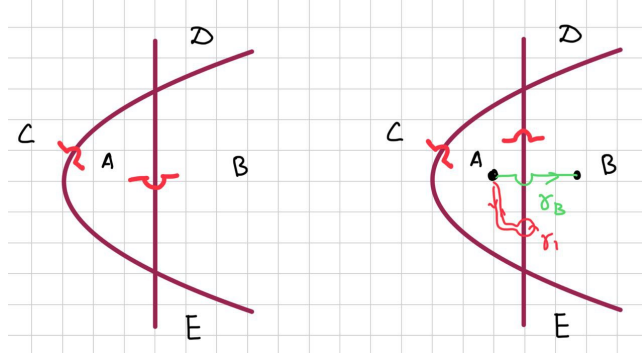


Fig. 36: Bridge notations for W for biangle

Apply the formula

$$\text{var}_\lambda(w) = w\mathbf{T}_2 - w, \quad (59)$$

The result is

$$\text{var}_\lambda(w) = (a, 0, 0, 0, 0), \quad (60)$$

$$a = -e + \gamma_1 + \gamma_2 - \gamma_1\gamma_2. \quad (61)$$

Thus, $\mathcal{E}(\text{var}_\lambda(W))$ is the surface shown in Example 4.4.

Example 6.4. Let σ and λ again correspond to the conditions of Theorem 5.2.

Let be

$$W = A_e + B_{\gamma_1^{-1}} + C_e + D_{\gamma_1^{-1}} + E_{\gamma_1^{-1}}. \quad (62)$$

The resulting surface has bridge notations shown in Fig. 36, right. Applying formula (59), obtain

$$\text{var}_\lambda(w) = (0, 0, 0, 0, 0), \quad (63)$$

Example 6.5. Let σ and λ correspond to the conditions of Theorem 5.3. Let be

$$W = A_e + B_e, \quad (64)$$

and thus

$$w = (e, e). \quad (65)$$

One can see that

$$\text{var}_\lambda(w) \equiv w\mathbf{T}_1 - w = (\gamma_1 - e, 0). \quad (66)$$

$\mathcal{E}(\text{var}_\lambda(w))$ is the surface described in Example 4.1.

One can see that all examples above are in agreement with (47). One can see also that these examples can be used to prove Theorem 6.1, not only to illustrate it.

6.3 Matrix/vector description of branching of $H_2^*(\tilde{U}_2)$

6.3.1 A basis in $H_2^*(\tilde{U}_2)$ and its transformation by matrices M_λ

Assume that the *left* module $h_2^c(\tilde{U}_2)$ has a finite basis, i.e. there exists a set

$$\{w_1^c, \dots, w_s^c\} \subset h_2^c(\tilde{U}_2),$$

such that for any $w^c \in h_2^c(\tilde{U}_2)$ there exists a representation

$$w^c = a_1 w_1^c + \dots + a_s w_s^c, \quad a_1, \dots, a_s \in \Omega \quad (67)$$

Example 6.6. Consider the configuration from Theorem 5.1. The basis of $h_2^c(\tilde{U}_2)$ is composed of a single element

$$w_1^c = (1 - \gamma_1)(1 - \gamma_2)(1 - \gamma_3)(e, 0, 0, 0, 0, 0).$$

This statement is non-trivial. A sketch of the proof is as follows. Let be $w \in h_2^c(\tilde{U}_2)$. Indeed,

$$w = A_e a, \quad a \in \Omega.$$

Our aim is to show that

$$a = b(e - \gamma_1)(e - \gamma_2)(e - \gamma_3).$$

The element a can be written as

$$a = \sum_{m_1, m_2, m_3} \alpha_{m_1, m_2, m_3} \gamma_1^{m_1} \gamma_2^{m_2} \gamma_3^{m_3}.$$

First, make all m'_1, m'_2, m'_3 non-negative by

$$a = \gamma_1^{M_1} \gamma_2^{M_2} \gamma_3^{M_3} \sum_{m'_1, m'_2, m'_3} \alpha'_{m'_1, m'_2, m'_3} \gamma_1^{m'_1} \gamma_2^{m'_2} \gamma_3^{m'_3},$$

where $M_j = \min(m_j)$. Split the sum into the terms, for which $m'_1 = 0$, $m'_2 = 0$, $m'_3 = 0$ and all the rest:

$$a = \gamma_1^{M_1} \gamma_2^{M_2} \gamma_3^{M_3} (c\gamma_1\gamma_2\gamma_3 + d).$$

Consider the expression

$$r = c\gamma_1\gamma_2\gamma_3 + d + c(e - \gamma_1)(e - \gamma_2)(e - \gamma_3)$$

By construction, $r \in h_2^c(\tilde{U}_2)$, and it is a linear combination of expressions $\gamma_1^{m'_1} \gamma_2^{m'_2} \gamma_3^{m'_3}$, for which at least one exponent m'_1, m'_2, m'_3 is zero. One can see that each element $A_{\gamma_1^{m'_1} \gamma_2^{m'_2} \gamma_3^{m'_3}}$ should have an uncompensated boundary in the linear combination. Thus, $r = 0$.

Introduce the matrix \mathbf{Y}^c composed of the elements (vector-rows) of the basis of h^c . Namely, in the block form

$$\mathbf{Y}^c = \begin{pmatrix} w_1^c \\ \vdots \\ w_s^c \end{pmatrix}. \quad (68)$$

Due to (67), any homology $w^c \in h_2^c(\tilde{U}_2)$ can be written in the matrix-vector form:

$$w^c = (a_1, \dots, a_s) \mathbf{Y}^c. \quad (69)$$

Besides, let be $w \in h_2(\tilde{U}_2)$, i.e. w is not necessarily compact. Compose an extended matrix

$$\mathbf{Y} = \begin{pmatrix} w \\ w_1^c \\ \vdots \\ w_s^c \end{pmatrix}. \quad (70)$$

Let σ depend on parameters t and there be a bypass λ about some component (branch line) of the Landau set. This bypass changes the homologies $H_2(\tilde{U}, \tilde{U}_1)$ and $H_2(\tilde{U}_2)$. First, one can use the formulae of the type (41), (43), (45).

$$w \xrightarrow{\lambda} \psi_\lambda(w) \mathbf{T}_\lambda = w \mathbf{T}_\lambda \quad (71)$$

for some square matrix \mathbf{T}_λ . Here ψ_λ is a map from Section 5.1. We assume that ψ_λ is the identity map.

This formula can be applied to each row of \mathbf{Y} :

$$\mathbf{Y} \xrightarrow{\lambda} \mathbf{Y} \mathbf{T}_\lambda. \quad (72)$$

According to Theorem 6.1, any bypass λ in the space of parameters changes any homology from $h_2(\tilde{U}_2)$ by adding linear combinations of some compact homologies. Thus, there exists a square matrix \mathbf{M}_λ of elements of Ω such that

$$\mathbf{Y} \xrightarrow{\lambda} \mathbf{M}_\lambda \mathbf{Y}. \quad (73)$$

A composition of several bypasses λ_j is described by a product of matrices:

$$w \xrightarrow{\lambda_1 \lambda_2} w \mathbf{T}_{\lambda_1} \mathbf{T}_{\lambda_2}. \quad (74)$$

Note that

$$w = \mathbf{a} \mathbf{Y}, \quad \mathbf{a} = (e, 0, \dots, 0).$$

Therefore

$$w \xrightarrow{\lambda_1 \lambda_2} \mathbf{a} \mathbf{Y} \mathbf{T}_{\lambda_1} \mathbf{T}_{\lambda_2}. \quad (75)$$

Similarly,

$$w \xrightarrow{\lambda_1 \lambda_2} \mathbf{a} \mathbf{M}_{\lambda_1} \mathbf{M}_{\lambda_2} \mathbf{Y}. \quad (76)$$

Thus, one can have \mathbf{Y} fixed and study the change of \mathbf{a} , and write down that

$$\mathbf{a} \xrightarrow{\lambda} \mathbf{a} \mathbf{M}_\lambda. \quad (77)$$

This change will describe the the change of $w = \mathbf{a} \mathbf{Y}$ purely in terms of the elements of $\mathfrak{h}_2(\tilde{U}_2)$.

In the proposed approach based on the relative homologies, the matrices \mathbf{T}_λ can be computed from the elementary matrices (41), (43), (45). Then, matrices \mathbf{M}_λ can be found as some matrices obeying the identities

$$\mathbf{M}_\lambda \mathbf{Y} = \mathbf{Y} \mathbf{T}_\lambda. \quad (78)$$

A standard approach is more straightforward: Theorem 6.1 enables one to compute \mathbf{M}_λ directly. We, instead, will construct \mathbf{M}_λ from \mathbf{T}_λ . Knowledge of the basis \mathbf{Y}^c and the matrices \mathbf{M}_λ is the main aim of the study of the branching of homologies. This is the maximum of what we can get from topology. Namely, consider the integral (1). Let Γ be represented as $\mathcal{E}(W)$, and W is described by $w \in \mathfrak{h}(\tilde{U}_2)$. Let t is carried along some loop λ , and let \mathbf{Y}_λ be known, and

$$w \xrightarrow{\lambda} w + \sum_j a_j w_j^c. \quad (79)$$

Expand each a_j according to (30):

$$a_j = \sum_l \alpha_{jl} \gamma_l. \quad (80)$$

Rewrite (79) as

$$w \xrightarrow{\lambda} w + \sum_{jl} \alpha_{jl} \gamma w_j^c. \quad (81)$$

The integral (1) is analytically continued along λ is as follows:

$$I(t) \xrightarrow{\lambda} I(t) + \sum_{jl} \alpha_{jl} \int_{\mathcal{E}(w_j^c)} F_{\gamma_l}(z, t) dz_1 \wedge dz_2, \quad (82)$$

where $F_{\gamma_l}(z, t)$ is the function F continued along the path γ_l in the domain of variables z .

6.3.2 Block form of \mathbf{M}_λ

Let us make one more simplification. Let $w \in \mathfrak{h}_2(\tilde{U}_2)$ be non-compact. By construction, matrix \mathbf{M}_λ has a block form: it consists of a first row depending on w and the last s rows depending only on the basis elements w_1^c, \dots, w_s^c . The last s rows can be grouped into a matrix \mathbf{M}_λ^c obeying the relation

$$\mathbf{M}_\lambda^c \mathbf{Y}^c = \mathbf{Y}^c \mathbf{T}_\lambda. \quad (83)$$

Indeed, the matrix \mathbf{M}_λ^c describes the transformation of \mathbf{Y}^c :

$$\mathbf{Y}^c \xrightarrow{\lambda} \mathbf{M}_\lambda^c \mathbf{Y}^c. \quad (84)$$

According to Pham's theorem,

$$w \xrightarrow{\lambda} w + a_1 w_1^c + \dots + a_s w_s^c. \quad (85)$$

Group the values $a_1, \dots, a_s \in \Omega$ into a row-vector m_λ :

$$m_\lambda = (a_1, \dots, a_s), \quad w \xrightarrow{\lambda} w + m_\lambda \mathbf{Y}^c. \quad (86)$$

Thus, in the block form

$$\mathbf{M}_\lambda = \left(\begin{array}{c|c} e & m_\lambda \\ \hline 0 & \mathbf{M}_\lambda^c \end{array} \right) \quad (87)$$

According to (86) and (78), vector m_λ can be found from equation

$$m_\lambda \mathbf{Y}^c = w \mathbf{T}_\lambda - w. \quad (88)$$

7 Examples

7.1 Two lines and a parabola

7.1.1 Geometry of the problem

Consider an example. Consider the space $(z_1, z_2) \in \mathbb{R}_\delta^2$. Let the singularities have form

$$\sigma = \sigma_a \cup \sigma_b \cup \sigma_c, \quad \sigma_a : z_1 = t_1, \quad \sigma_b : z_2 = t_2, \quad \sigma_c : z_1 - z_2^2 = 0, \quad (89)$$

where t_1 and t_2 are complex parameters. We assume that $t = (t_1, t_2)$ belongs to \mathbb{R}_δ^2 . The objects \tilde{U} , $\pi_1(\mathbb{R}_\delta^2 \setminus \sigma)$, $H_2^*(\tilde{U}, \tilde{U}_1)$, etc are first built for the (z_1, z_2) -space. Later on, we build some objects in the (t_1, t_2) -space.

The singularities in the (z_1, z_2) -space are shown in Fig. 37, left. As above, we introduce the polygons A, \dots, M , the reference point in A , the generators

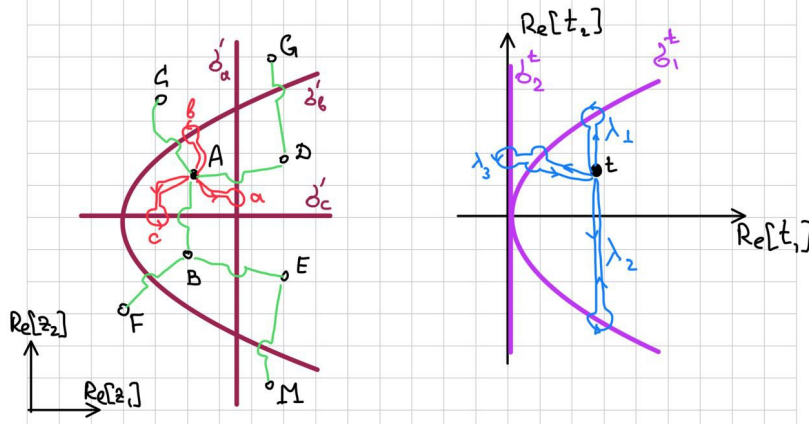


Fig. 37: Singularities in the (z_1, z_2) -space (left) and in the (t_1, t_2) -space (right)

of π_1 that are $\gamma_a, \gamma_b, \gamma_c$, and the basic paths between the polygons (shown by green).

The structure of $H_2(\mathbb{R}_\delta^2 \setminus \sigma)$ degenerates when $t_1 - t_2^2 = 0$ or $\zeta_1 = 0$. Introduce the following singularities in the t -space:

$$\sigma_1^t : t_1 - t_2^2 = 0, \quad \sigma_2^t : t_1 = 0. \quad (90)$$

We also use the notation

$$\sigma^t = \sigma_1^t \cup \sigma_2^t.$$

The singularities (branch lines) in the t -space are shown in Fig. 37, right. Our aim is to describe branching of $H_2^*(\tilde{U}_2)$ as the point t bypasses along the contours $\lambda_1, \lambda_2, \lambda_3$ shown in the figure.

This study is related, say, to the properties of the integral

$$I(t) = \int_{\Gamma} (z_1 - t_1)^{\mu_a} (z_2 - t_2)^{\mu_b} (z_1 - z_2^2)^{\mu_c} dz_1 \wedge dz_2 \quad (91)$$

for some μ_a, μ_b, μ_c not necessary rational and for some integration surface Γ . This integral is branching over σ_1^t and σ_2^t . Branching of the value of I is connected with branching (ramification) of $H_2(\tilde{U}_2)$.

7.1.2 Finding the matrices \mathbf{T}_j

We describe the elements of $H_2^*(\tilde{U}, \tilde{U}_1)$ as the elements of corresponding module over the group ring Ω . Each element can be written as

$$W = A a_A + B a_B + C a_C + D a_D + E a_E + F a_F + G a_G + M a_M. \quad (92)$$

For $t \notin \sigma^t$ the intersections of $\sigma_a, \sigma_b, \sigma_c$ are transversal, thus the paths a, b, c commute. Therefore $\pi_1(\mathbb{R}_\delta^2 \setminus \sigma)$ is Abelian, and Ω is Abelian.

We associate a vector w with (92):

$$w = (a_A, a_B, a_C, a_D, a_E, a_F, a_G, a_M). \quad (93)$$

Each of the bypasses λ_j corresponds to a matrix \mathbf{T}_j :

$$w \xrightarrow{\lambda_j} w\mathbf{T}_j. \quad (94)$$

Let us build the matrices $\mathbf{T}_1, \mathbf{T}_2, \mathbf{T}_3$. Matrices \mathbf{T}_1 and \mathbf{T}_2 can be obtained by direct application of the triangle formula (41). The matrix \mathbf{T}_1 is obtained by applying (41) to the vanishing triangle A and to six polygons surrounding it:

$$\mathbf{T}_1 = \begin{pmatrix} abc & 0 & 0 & 0 & 0 & 0 & 0 & 0 \\ c - abc & e & 0 & 0 & 0 & 0 & 0 & 0 \\ b - abc & 0 & e & 0 & 0 & 0 & 0 & 0 \\ a - abc & 0 & 0 & e & 0 & 0 & 0 & 0 \\ -ac + abc & 0 & 0 & 0 & e & 0 & 0 & 0 \\ -bc + abc & 0 & 0 & 0 & 0 & e & 0 & 0 \\ -ab + abc & 0 & 0 & 0 & 0 & 0 & e & 0 \\ 0 & 0 & 0 & 0 & 0 & 0 & 0 & e \end{pmatrix} \quad (95)$$

Similarly, \mathbf{T}_2 is the transform (41) applied to the vanishing triangle B and six polygons surrounding it:

$$\mathbf{T}_2 = \begin{pmatrix} e & e - ab & 0 & 0 & 0 & 0 & 0 & 0 \\ 0 & abc & 0 & 0 & 0 & 0 & 0 & 0 \\ 0 & -b + ab & e & 0 & 0 & 0 & 0 & 0 \\ 0 & -a + ab & 0 & e & 0 & 0 & 0 & 0 \\ 0 & a - abc & 0 & 0 & e & 0 & 0 & 0 \\ 0 & b - abc & 0 & 0 & 0 & e & 0 & 0 \\ 0 & 0 & 0 & 0 & 0 & 0 & e & 0 \\ 0 & -ab + abc & 0 & 0 & 0 & 0 & 0 & e \end{pmatrix} \quad (96)$$

(Note that Lemma 4.1 is used to take into account the base contours correctly).

Computation of \mathbf{T}_3 is more complicated. We show the derivation of it in Appendix E. The result is as follows:

$$\mathbf{T}_3 = \begin{pmatrix} 0 & -ab & 0 & 0 & 0 & 0 & 0 & 0 \\ -abc & 0 & 0 & 0 & 0 & 0 & 0 & 0 \\ b & ab & e & 0 & 0 & 0 & 0 & 0 \\ a & ab & 0 & e & 0 & 0 & 0 & 0 \\ abc & a & 0 & 0 & e & 0 & 0 & 0 \\ abc & b & 0 & 0 & 0 & e & 0 & 0 \\ -ab & -ab & 0 & 0 & 0 & 0 & e & 0 \\ -abc & -ab & 0 & 0 & 0 & 0 & 0 & e \end{pmatrix} \quad (97)$$

7.1.3 Branching in the space of parameters

Now consider the domain \mathbb{R}_δ^2 of the parameters (t_1, t_2) (not of variables (z_1, z_2)). As we noted, there are singularities σ_1^t and σ_2^t in this space. The function $I(t)$ defined, say, by (91) can be analytically continued to the whole $\mathbb{R}_\delta^2 \setminus \sigma^t$, and this analytical continuation may have branching on σ_1^t, σ_2^t . Let us describe this branching.

We described branching of the integration surfaces by (94). The integral surfaces depend on t continuously, thus branching of the integration contours should reflect the topological properties of $\mathbb{R}_\delta^2 \setminus \sigma^t$. Namely, if some bypasses in $\mathbb{R}_\delta^2 \setminus \sigma^t$ can be deformed into one another, these bypasses should lead to the same change of the surfaces.

Namely, the formulae (18) derived above for the quadratic touch of singularities should be valid for the homologies. This is equivalent to the matrix identities

$$\mathbf{T}_3^2 \mathbf{T}_1 = \mathbf{T}_1 \mathbf{T}_3^2, \quad \mathbf{T}_3^2 \mathbf{T}_2 = \mathbf{T}_2 \mathbf{T}_3^2, \quad (98)$$

One can *check directly* that these identities are true. Another check that can be made is that the resulting group is non-commutative:

$$\mathbf{T}_3 \mathbf{T}_1 \neq \mathbf{T}_1 \mathbf{T}_3. \quad (99)$$

Thus, matrices (95)–(97) provide a linear (in Ω) representation of the group $\pi_1(\mathbb{R}_\delta^2 \setminus \sigma^t)$.

7.2 Sokhotsky-type integrals in 2D

7.2.1 Sokhotsky integrals as integrals with parameters

Let $f(z)$, $z \in \mathbb{C}^2$ be a function having some singular set σ_f having the real property. Assume that $f(z)$ is holomorphic but not necessarily single-valued in $\mathbb{R}_\delta^2 \setminus \sigma_f$. The singularity σ_f is the *fixed singularity*. Define the universal covering \tilde{U}_2^f of $\mathbb{R}_\delta^2 \setminus \sigma_f$.

Let Γ be an integration surface, $\Gamma \in H_2(\tilde{U}_2^f)$ that is an indented plane \mathbb{R}^2 . We fix the indentation of σ_f by setting bridge symbols as it is described above.

Let us introduce the *movable singularities* in addition to σ_f :

$$\sigma_1 : z_1 = t_1, \quad \sigma_2 : z_2 = t_2, \quad (100)$$

where $t = (t_1, t_2) \in \mathbb{R}_\delta^2$ are some parameters. Let us introduce Let be

$$\sigma = \sigma(t) = \sigma_f \cup \sigma_1 \cup \sigma_2.$$

Define \tilde{U} for \mathbb{R}_δ^2 and $\sigma(t)$. Introduce four surfaces $\Gamma_{++}, \Gamma_{+-}, \Gamma_{-+}, \Gamma_{--}$ as follows. They are all versions of indented \mathbb{R}^2 . The singularity σ_f is bypassed in the same way as Γ , and the singularities σ_1, σ_2 are bypassed as it is shown in Fig. 38, right, i.e. each pair of indexes corresponds to its pair of bridge symbols.

The orientation of all $\Gamma_{\mu\nu}$, $\mu, \nu = \pm$ is natural. Define also the universal Riemann domain for σ denoted \tilde{U} . Choose the base contours, say, in accordance

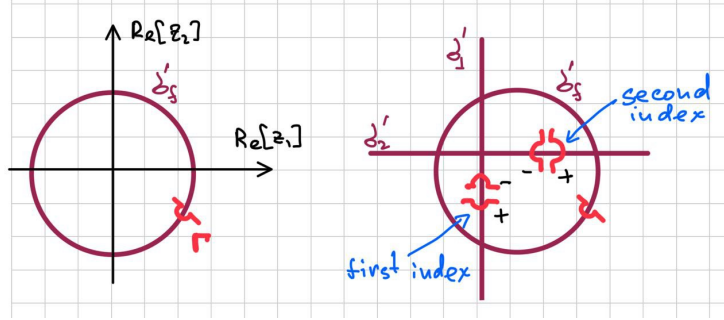


Fig. 38: Surfaces for integration for the additional singularities

with Γ_{++} . Choose the reference point x^* say somewhere in the far top-right of the real plane.

Introduce the Sokhotsky-type integrals

$$f_{\mu\nu}(t_1, t_2) = \frac{1}{(2\pi i)^2} \int_{\Gamma_{\mu\nu}} \frac{f(z_1, z_2)}{(z_1 - t_1)(z_2 - t_2)} dz_1 \wedge dz_2. \quad (101)$$

We assume that the integrals are convergent or regularized if necessary (see below).

It is clear that

$$f(t_1, t_2) = f_{++}(t_1, t_2) - f_{+-}(t_1, t_2) - f_{-+}(t_1, t_2) + f_{--}(t_1, t_2), \quad (102)$$

and thus (102) is an additive decomposition of $f(t_1, t_2)$. Namely, $f_{\mu,\nu}$ is holomorphic in the quarter-space $\mu\text{Im}[t_1] > 0$, $\nu\text{Im}[t_2] > 0$.

Moreover, one can say that one can say that $f_{\mu,\nu}$ is holomorphic in the quarter-space $\mu\text{Im}[t_1] \geq 0$, $\nu\text{Im}[t_2] \geq 0$, provided that the fragments of σ belong to the corresponding quarter-spaces.

The expression (102) can be called a *four-part additive decomposition*. Besides, one can define *two-part additive decompositions*:

$$f = f_{+0} - f_{-0}, \quad f_{+0} \equiv f_{++} - f_{+-}, \quad f_{-0} \equiv f_{-+} - f_{--}, \quad (103)$$

$$f = f_{0+} - f_{0-}, \quad f_{0+} \equiv f_{++} - f_{-+}, \quad f_{0-} \equiv f_{+-} - f_{--}. \quad (104)$$

7.2.2 Radlow's integral

Hereafter we consider the following example:

$$\sigma_f : \quad z_1^2 + z_2^2 = 1, \quad (105)$$

$$f(z) = \frac{1}{2} \log(1 - z_1^2 - z_2^2). \quad (106)$$

Note that this corresponds to multiplicative factorization of the function

$$h(z_1, z_2) = (1 - z_1^2 - z_2^2)^{1/2}.$$

Introduce the reference point x^* , the polygons A, \dots, M , the base paths and the generators a, b, c of $\pi_1(\mathbb{R}_\delta^2 \setminus \sigma)$ as it is shown in Fig. 39. Note that $\pi_1(\mathbb{R}_\delta^2 \setminus \sigma) = \mathbb{Z}^3$, i.e. it is Abelian. Let Ω be the group ring of π_1 over \mathbb{Z} .

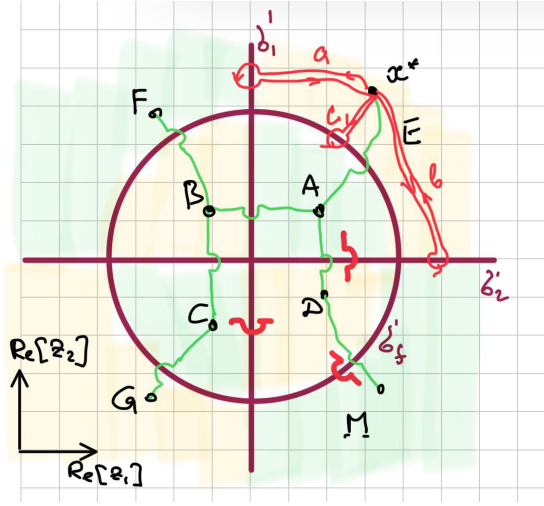


Fig. 39: Polygons and base contours for the example

The integration surfaces $\Gamma_{\mu\nu}$ correspond to vectors $w_{\mu\nu}$, namely

$$w_{++} = (e, e, e, e, e, e, e, e), \quad (107)$$

$$w_{-+} = (e, a, a, e, e, e, a, a, e), \quad (108)$$

$$w_{+-} = (e, e, b, b, e, e, b, b), \quad (109)$$

$$w_{--} = (e, a, ab, b, e, a, ab, b). \quad (110)$$

For the decompositions (103) and (104) introduce also the integration surfaces defined by

$$w_{0+} = w_{++} - w_{-+} = (e - a)(0, e, e, 0, 0, e, e, 0), \quad (111)$$

$$w_{-0} = w_{-+} - w_{--}, \quad w_{+0} = w_{++} - w_{+-}, \quad w_{0-} = w_{+-} - w_{--}. \quad (112)$$

In particular, we are interested in the integration surfaces w_{++} and w_{0+} . Corresponding functions

$$h_{++}(t) = \exp \left\{ -\frac{1}{8\pi^2} \int_{\Gamma_{++}} \frac{\log(1 - z_1^2 - z_2^2)}{(z_1 - t_1)(z_2 - t_2)} dz_1 \wedge dz_2 \right\}, \quad (113)$$

$$h_{0+}(t) = \exp \left\{ -\frac{1}{8\pi^2} \int_{\Gamma_{0+}} \frac{\log(1 - z_1^2 - z_2^2)}{(z_1 - t_1)(z_2 - t_2)} dz_1 \wedge dz_2 \right\} \quad (114)$$

play an important role in conical diffraction problems. The first of them is the Radlow's coefficient [7], and the second one is the half-plane coefficient.

The second function can be found without taking the integral. One can see that it provides a factorization of the function $\sqrt{1 - t_1^2 - t_2^2}$ for a fixed t_1 into factors regular in the upper and lower half-planes of t_2 . Thus, after an appropriate regularization,

$$h_{0+}(t) = \sqrt{t_2 + \sqrt{1 - t_1^2}}. \quad (115)$$

The first function has a more complicated structure that should be revealed below.

7.2.3 Branching of the relative homologies

Let t vary in $\mathbb{R}_\delta^2 \setminus \sigma$. Carrying t along some loops can lead to branching of the relative and absolute homologies. As it is stated in Subsection 5, branching sets are those at which the space $\mathbb{R}_\delta^2 \setminus \sigma$ degenerates comparatively to the general position. This happens when:

- The crossing $\sigma_1 \cap \sigma_2$ belongs to σ_f , i.e. for

$$t_1^2 + t_2^2 = 1. \quad (116)$$

This set is denoted by σ_c^t .

- The line σ_1 is tangential to σ_f , i.e. for

$$t_1 = \pm 1. \quad (117)$$

These sets are denoted by $\sigma_{1\pm}^t$.

- The line σ_2 is tangential to σ_f , i.e. for

$$t_2 = \pm 1. \quad (118)$$

These sets are denoted by $\sigma_{2\pm}^t$.

The corresponding branching sets in the t -space are shown in Fig. 40. Introduce also the paths λ_{1+} , λ_{1-} , λ_{2+} , λ_{2-} , λ_A , λ_B , λ_C , λ_D as it is shown in the figure.

We denote

$$\sigma^t = \sigma_c^t \cup \sigma_{1+}^t \cup \sigma_{1-}^t \cup \sigma_{2+}^t \cup \sigma_{2-}^t$$

and introduce a fundamental group $\pi_1^t = \pi_1(\mathbb{R}_\delta^2 \setminus \sigma^t)$. Note that π_1^t is pretty different from $\pi_1(\mathbb{R}_\delta^2 \setminus \sigma)$. For example, $\pi_1(\mathbb{R}_\delta^2 \setminus \sigma)$ is Abelian, while π_1^t is not.

Our next aim is to describe branching of the relative homologies from $H_2^*(\tilde{U}, \tilde{U}_1)$ as t is carried along the paths λ_j . Each such homology is described with a vector

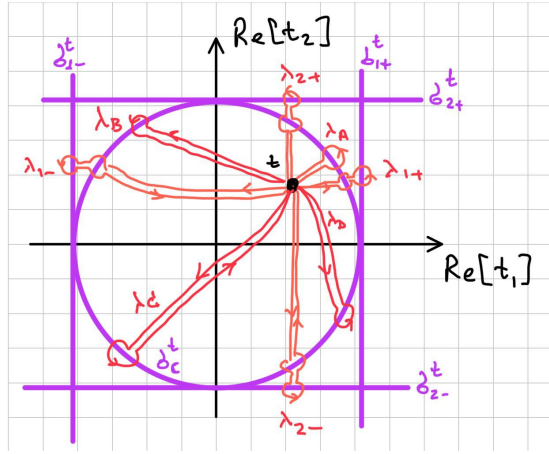


Fig. 40: Branching lines and paths in t -space

w of dimension 1×8 with elements in Ω . Each bypass corresponds to a linear transform:

$$w \xrightarrow{\lambda_j} w \mathbf{T}_j.$$

The matrices \mathbf{T}_j are constructed in the way similar to the one described in Subsection 7.1. Some rather lengthy but elementary computations yield:

$$\mathbf{T}_A = \begin{pmatrix} abc & 0 & 0 & 0 & 0 & 0 & 0 & 0 \\ e - bc & e & 0 & 0 & 0 & 0 & 0 & 0 \\ -e + c & 0 & e & 0 & 0 & 0 & 0 & 0 \\ e - ac & 0 & 0 & e & 0 & 0 & 0 & 0 \\ c - abc & 0 & 0 & 0 & e & 0 & 0 & 0 \\ -c + bc & 0 & 0 & 0 & 0 & e & 0 & 0 \\ 0 & 0 & 0 & 0 & 0 & 0 & e & 0 \\ -c + ac & 0 & 0 & 0 & 0 & 0 & 0 & 0 \end{pmatrix} \quad (119)$$

$$\mathbf{T}_{1+} = \begin{pmatrix} 0 & 0 & 0 & -abc & 0 & 0 & 0 & 0 \\ e & e & 0 & bc & 0 & 0 & 0 & 0 \\ c & 0 & e & e & 0 & 0 & 0 & 0 \\ -ac & 0 & 0 & 0 & 0 & 0 & 0 & 0 \\ c & 0 & 0 & abc & e & 0 & 0 & 0 \\ -c & 0 & 0 & -bc & 0 & e & 0 & 0 \\ -c & 0 & 0 & -c & 0 & 0 & e & 0 \\ ac & 0 & 0 & c & 0 & 0 & 0 & e \end{pmatrix} \quad (120)$$

$$\mathbf{T}_{2+} = \begin{pmatrix} 0 & -abc & 0 & 0 & 0 & 0 & 0 & 0 \\ -bc & 0 & 0 & 0 & 0 & 0 & 0 & 0 \\ c & e & e & 0 & 0 & 0 & 0 & 0 \\ e & ac & 0 & e & 0 & 0 & 0 & 0 \\ c & abc & 0 & 0 & e & 0 & 0 & 0 \\ bc & c & 0 & 0 & 0 & e & 0 & 0 \\ -c & -c & 0 & 0 & 0 & 0 & e & 0 \\ -c & -ac & 0 & 0 & 0 & 0 & 0 & e \end{pmatrix} \quad (121)$$

$$\mathbf{T}_{1-} = \begin{pmatrix} e & a & abc & 0 & 0 & 0 & 0 & 0 \\ 0 & 0 & -abc & 0 & 0 & 0 & 0 & 0 \\ 0 & -ac & 0 & 0 & 0 & 0 & 0 & 0 \\ 0 & ac & a & e & 0 & 0 & 0 & 0 \\ 0 & -ac & -abc & 0 & e & 0 & 0 & 0 \\ 0 & c & abc & 0 & 0 & e & 0 & 0 \\ 0 & ac & c & 0 & 0 & 0 & e & 0 \\ 0 & -ac & -ac & 0 & 0 & 0 & 0 & e \end{pmatrix} \quad (122)$$

$$\mathbf{T}_{2-} = \begin{pmatrix} e & 0 & abc & b & 0 & 0 & 0 & 0 \\ 0 & e & b & bc & 0 & 0 & 0 & 0 \\ 0 & 0 & 0 & -bc & 0 & 0 & 0 & 0 \\ 0 & 0 & -abc & 0 & 0 & 0 & 0 & 0 \\ 0 & 0 & -abc & -bc & e & 0 & 0 & 0 \\ 0 & 0 & -bc & -bc & 0 & e & 0 & 0 \\ 0 & 0 & c & bc & 0 & 0 & e & 0 \\ 0 & 0 & abc & c & 0 & 0 & 0 & e \end{pmatrix} \quad (123)$$

Besides, according to (82),

$$\mathbf{T}_B = \mathbf{T}_{2+} \mathbf{T}_A \mathbf{T}_{2+}^{-1}, \quad \mathbf{T}_C = \mathbf{T}_{1-} \mathbf{T}_B \mathbf{T}_{1-}^{-1}, \quad \mathbf{T}_D = \mathbf{T}_{1+} \mathbf{T}_A \mathbf{T}_{1+}^{-1}. \quad (124)$$

These matrices can be computed easily.

We can directly check that, for example,

$$\mathbf{T}_A \mathbf{T}_{1+}^2 = \mathbf{T}_{1+}^2 \mathbf{T}_A \quad (125)$$

(see (98)).

Moreover, we can find the matrices

$$\tilde{\mathbf{T}}_{1+} \equiv \mathbf{T}_{1+} \mathbf{T}_A^{-1}, \quad \tilde{\mathbf{T}}_{2+} \equiv \mathbf{T}_{2+} \mathbf{T}_A^{-1}, \quad (126)$$

corresponding to elementary bypasses about σ_{1+}^t and σ_{2+}^t . One can check directly that

$$\tilde{\mathbf{T}}_{1+} \tilde{\mathbf{T}}_{2+} = \tilde{\mathbf{T}}_{2+} \tilde{\mathbf{T}}_{1+} \quad (127)$$

This identity reflects the fact that that corresponding elementary bypasses commute in π_1^t (see Subsection 3.1).

Moreover, one can check that

$$\mathbf{I} + \tilde{\mathbf{T}}_{1+}\tilde{\mathbf{T}}_{2+} = \tilde{\mathbf{T}}_{1+} + \tilde{\mathbf{T}}_{2+}. \quad (128)$$

This identity is related to the additive crossing concept. Namely, this proves that the point $t = (1, 1)$ is an *additive* crossing of the singularities σ_{1+}^t and σ_{2+}^t for any of the functions $f_{\mu\nu}$.

7.2.4 Branching of compact absolute homologies

Let us “guess” the basis of absolute compact homologies¹ from $H_2^*(\tilde{U}_2)$:

$$w_A^c = (e - a)(e - b)(e - c)(e, 0, 0, 0, 0, 0, 0, 0), \quad (129)$$

$$w_{AB}^c = (e - b)(e - c)(e, e, 0, 0, 0, 0, 0, 0), \quad (130)$$

$$w_{AD}^c = (e - a)(e - c)(e, 0, 0, e, 0, 0, 0, 0), \quad (131)$$

$$w_{ABCD}^c = (e - c)(e, e, e, e, 0, 0, 0, 0), \quad (132)$$

Compose the block matrix

$$\mathbf{Y}^c = \begin{pmatrix} w_A^c \\ w_{AB}^c \\ w_{AD}^c \\ w_{ABCD}^c \end{pmatrix}. \quad (133)$$

This is a matrix 4×8 , whose elements take values in Ω .

The matrix \mathbf{Y}^c is transformed as (84), and the matrices \mathbf{M}_λ are found from equation (83), which can be easily solved.

$$\mathbf{M}_A = \begin{pmatrix} abc & 0 & 0 & 0 \\ -bc & e & 0 & 0 \\ -ac & 0 & e & 0 \\ c & 0 & 0 & e \end{pmatrix}, \quad (134)$$

$$\mathbf{M}_{1+} = \begin{pmatrix} abc & 0 & -abc + ab^2c & 0 \\ -bc & e & bc - b^2c & 0 \\ -ac & 0 & -abc & 0 \\ c & 0 & bc & e \end{pmatrix}, \quad (135)$$

$$\mathbf{M}_{1-} = \begin{pmatrix} e - a + abc & a(a - e)(bc - e) & abc(b - e) & abc(a - e)(b - e) \\ e & a & 0 & 0 \\ -ac & ac(e - a) & e - a - abc & a(e - a)(e + bc) \\ 0 & 0 & e & a \end{pmatrix}, \quad (136)$$

¹We do not need to prove that this is a basis. As we see below, the elements of this basis are transformed in terms of it, and the elements of non-compact homologies are transformed only in terms of it. This is sufficient for us.

$$\mathbf{M}_{2+} = \begin{pmatrix} abc & (a-e)abc & 0 & 0 \\ -bc & -abc & 0 & 0 \\ -ac & ac(e-a) & e & 0 \\ c & ac & 0 & e \end{pmatrix}, \quad (137)$$

$$\mathbf{M}_{2-} = \begin{pmatrix} e-b+abc & abc(a-e) & b(b-e)(ac-e) & abc(a-e)(b-e) \\ -bc & 1-b-abc & bc(e-b) & b(e-b)(e+ac) \\ e & 0 & b & 0 \\ 0 & e & 0 & b \end{pmatrix}, \quad (138)$$

and, besides,

$$\mathbf{M}_B = \mathbf{M}_{2+}^{-1} \mathbf{M}_A \mathbf{M}_{2+}, \quad \mathbf{M}_C = \mathbf{M}_{1-}^{-1} \mathbf{M}_B \mathbf{M}_{1-}, \quad \mathbf{M}_D = \mathbf{M}_{1+}^{-1} \mathbf{M}_A \mathbf{M}_{1+}. \quad (139)$$

7.2.5 Ramification of non-compact absolute homologies

First let be

$$\mathbf{w}_{++} = (e, e, e, e, e, e, e).$$

According to (87), ramification of non-compact homologies can be described by vectors \mathbf{m}_c that can be found from (88). The equations can be easily solved. The result is

$$\mathbf{m}_A = \mathbf{m}_B = \mathbf{m}_D = \mathbf{m}_{1p} = \mathbf{m}_{2p} = (0, 0, 0, 0), \quad (140)$$

$$\mathbf{m}_{1-} = (0, 0, e, a - e), \quad (141)$$

$$\mathbf{m}_{2-} = (0, e, 0, b - e), \quad (142)$$

$$\mathbf{m}_C = (-e, e - a, e - b, -(e - a)(e - b)), \quad (143)$$

Second, let be

$$\mathbf{w}_{0+} = (e - a)(0, e, e, 0, 0, e, e, 0).$$

Then

$$\mathbf{m}_A = \mathbf{m}_B = \mathbf{m}_{2+} = (0, 0, 0, 0), \quad (144)$$

$$\mathbf{m}_C = \mathbf{m}_{2-} = (-e, e - a, e - b, -(e - a)(e - b)), \quad (145)$$

$$\mathbf{m}_D = (-e, 0, e - b, 0), \quad (146)$$

$$\mathbf{m}_{1+} = (0, 0, e, 0), \quad (147)$$

$$\mathbf{m}_{1-} = (0, 0, e, a - e), \quad (148)$$

7.2.6 Study of the function $h_{0+}(t)$ and $h_{++}(t)$

Let us study the integrals

$$I_j(t) = -\frac{1}{8\pi^2} \int_{\mathcal{E}(w_j)} \frac{\log(1 - z_1^2 - z_2^2)}{(z_1 - t_1)(z_2 - t_2)} dz_1 \wedge dz_2, \quad (149)$$

where w_j are compact homologies from the set (129)–(132). These integrals can be simplified and, some of them, computed explicitly.

First, note that since the integrand contains a logarithm and rational functions, one can easily deduce that a multiplication of w_j by any $\gamma \in \pi_1(\mathbb{R}_\delta^2 \setminus \sigma)$:

$$-\frac{1}{8\pi^2} \int_{\mathcal{E}(w_j\gamma)} \frac{\log(1 - z_1^2 - z_2^2)}{(z_1 - t_1)(z_2 - t_2)} dz_1 \wedge dz_2 = I_j. \quad (150)$$

Consider the inflated triangles corresponding to w_A, w_B, w_C, w_D . These integrals can be reduced according to Subsection 4.5. Namely, the homology is reduced to the pair of toruses shown in Fig. 23, left. Taking the double pole, we obtain

$$I_A = -\pi i. \quad (151)$$

Introduce the values

$$h_{AB}(t) = \exp\{I_{AB}\}. \quad (152)$$

$$h_{AD}(t) = \exp\{I_{AD}\} \quad (153)$$

(indeed, we can compute this function in terms of square roots). Using the relations (134)–(139) and (151), obtain

$$h_{AB} \xrightarrow{\lambda_A} -h_{AB}, \quad h_{AB} \xrightarrow{\lambda_B} -h_{AB}, \quad (154)$$

$$h_{AB} \xrightarrow{\lambda_C} -h_{AB}, \quad h_{AB} \xrightarrow{\lambda_D} -h_{AB}, \quad (155)$$

$$h_{AB} \xrightarrow{\lambda_{1+}} -h_{AB}, \quad h_{AB} \xrightarrow{\lambda_{1-}} -h_{AB}, \quad (156)$$

$$h_{AB} \xrightarrow{\lambda_{2+}} -h_{AB}^{-1}, \quad h_{AB} \xrightarrow{\lambda_{2-}} -h_{AB}^{-1}, \quad (157)$$

$$h_{AD} \xrightarrow{\lambda_A} -h_{AD}, \quad h_{AD} \xrightarrow{\lambda_B} -h_{AD}, \quad (158)$$

$$h_{AD} \xrightarrow{\lambda_C} -h_{AD}, \quad h_{AD} \xrightarrow{\lambda_D} -h_{AD}, \quad (159)$$

$$h_{AD} \xrightarrow{\lambda_{1+}} -h_{AD}^{-1}, \quad h_{AD} \xrightarrow{\lambda_{1-}} -h_{AD}^{-1}, \quad (160)$$

$$h_{AD} \xrightarrow{\lambda_{2+}} -h_{AD}, \quad h_{AD} \xrightarrow{\lambda_{2-}} -h_{AD}, \quad (161)$$

Consider the transformation of w_{0+} . Using (144)–(147), obtain

$$h_{0+} \xrightarrow{\lambda_A} h_{0+}, \quad h_{0+} \xrightarrow{\lambda_B} h_{0+}, \quad (162)$$

$$h_{0+} \xrightarrow{\lambda_C} -h_{0+}, \quad h_{0+} \xrightarrow{\lambda_D} -h_{0+}, \quad (163)$$

$$h_{0+} \xrightarrow{\lambda_{1+}} h_{0+} h_{AD}, \quad h_{0+} \xrightarrow{\lambda_{1-}} h_{0+} h_{AD}, \quad (164)$$

$$h_{0+} \xrightarrow{\lambda_{2+}} h_{0+}, \quad h_{0+} \xrightarrow{\lambda_{2-}} -h_{0+}, \quad (165)$$

One can see that the function has four values over each t . They are

$$h_{+0}(t), \quad -h_{+0}(t), \quad h_{+0}(t)h_{AD}(t), \quad -h_{+0}(t)h_{AD}(t).$$

Now consider the properties of h_{++} . Using (140)–(143), obtain

$$h_{++} \xrightarrow{\lambda_A} h_{++}, \quad h_{++} \xrightarrow{\lambda_B} h_{++}, \quad (166)$$

$$h_{++} \xrightarrow{\lambda_C} -h_{++}, \quad h_{++} \xrightarrow{\lambda_D} h_{++}, \quad (167)$$

$$h_{++} \xrightarrow{\lambda_{1+}} h_{++}, \quad h_{++} \xrightarrow{\lambda_{2+}} h_{++}, \quad (168)$$

$$h_{++} \xrightarrow{\lambda_{1-}} h_{++} h_{AD}, \quad h_{++} \xrightarrow{\lambda_{2-}} h_{++} h_{AB}, \quad (169)$$

One can see that h_{++} has an infinite number of sheets, and the values on these sheets are

$$\pm h_{++}(t) h_{AB}^{m_1}(t) h_{AD}^{m_2}(t), \quad m_1, m_2 \in \mathbb{Z}.$$

8 Conclusion

We developed a matrix-vector representation of the Picard–Lefschetz theory, that offers a concise and practical framework for describing the topology of the surface of integration. Under specific constraints, the surface of integration can be presented as a finite-dimensional vector with coefficients in the group ring of the fundamental group of the space with removed singularities. The matrix formalism reproduces the Picard–Lefschetz formula and unveils nontrivial topological relationships in the parameter space, demonstrating its utility in analysing of branching integrals in complex space.

References

- [1] Shabat, B.V., Introduction to complex analysis. Part II, functions of several variables, AMS, 1992.
- [2] Pham, F., Singularities of integrals. Homology, hyperfunctions and microlocal analysis. Springer, 2011.
- [3] Vassiliev, V.A., Applied Picard–Lefschetz Theory, AMS, 2002.
- [4] Pham, F., Formules de Picard–Lefschetz généralisées et ramification des intégrales // Bull. Soc. Math. France, 93 (1965), 333–367.

- [5] Hwa, R.C., Teplitz, V.L., Homology and Feynman integrals, W.A.Benjamin, Inc., 1966.
- [6] Assier R.C., Shanin, A.V., Korolkov A.I., A contribution to the mathematical theory of diffraction: a note on double Fourier integrals // QJMAM V.76, PP.1–47, 2022.
- [7] Radlow, J. Diffraction by a quarter-plane. Arch. Rational Mech. Anal. 8, 139–158 1961.

Appendix A. Proof of Lemma 2.1

a) Represent the path $\gamma_3\gamma_2$ as a function $(z'_1(\tau), z'_2(\tau))$, $\tau = [0, 1]$. The homotopy $\gamma_3\gamma_2 \rightarrow \gamma_2$ is given by the formulae

$$|z'_1(\tau)| \rightarrow |z'_1(\tau)|, \quad \text{Arg}[z'_1(\tau)] \rightarrow \alpha \text{Arg}[z'_1(\tau)], \quad z'_2(\tau) \rightarrow \alpha z'_2(\tau).$$

Here α is a parameter describing the homotopy as α changes from 1 to 0.

Point b) follows from a) in a straightforward way.

Point c) is the most complicated. Parametrize paths $\gamma = \gamma_1\gamma_2$ and $\gamma' = \gamma'_1\gamma_2$ by variables τ and τ' taking values in $[0, 1]$. By condition of point c), there should exist a homotopy ψ of $(\gamma_1\gamma_2)^{-1}\gamma'_1\gamma_2$ into the point z . Let the homotopy be described by parameter $\alpha \in [0, 1]$. Thus, we defined the points $\gamma(\tau, \alpha)$ and $\gamma'(\tau, \alpha)$ belonging to the corresponding paths in the course of the homotopy.

Due to continuity, there should be values τ_* and τ'_* , such that the parts of the contour γ for $\tau_* \leq \tau \leq 1$ and γ' for $\tau'_* \leq \tau' \leq 1$ do not leave D during the homotopy. Assume that $\gamma(\tau_*, 0) \in \gamma_2$ and $\gamma'(\tau'_*, 0) \in \gamma_2$.

Add to the homotopy a stretching in τ in the beginning to make

$$\gamma(\tau_*, 0) = \gamma'(\tau'_*, 0) = z^\ddagger.$$

Connect the points $\gamma(\tau_*, \alpha)$ and z^\ddagger with a path $\gamma_D(\alpha) \in \Pi_D(\gamma(\tau_*, \alpha), z^\ddagger)$. Similarly, connect the points $\gamma'(\tau'_*, \alpha)$ and z^\ddagger with a path $\gamma'_D(\alpha) \in \Pi_D(\gamma'(\tau'_*, \alpha), z^\ddagger)$.

Introduce the paths

$$\tilde{\gamma}(\alpha) = \gamma(\tau, \alpha), \quad 0 \leq \tau \leq \tau_*, \quad \tilde{\gamma}'(\alpha) = \gamma'(\tau, \alpha), \quad 0 \leq \tau \leq \tau'_*,$$

see Fig. 41.

One can see that, first,

$$\gamma_1(\alpha = 0) = \tilde{\gamma}(0)\gamma_D(0), \quad \gamma'_1(\alpha = 0) = \tilde{\gamma}'(0)\gamma'_D(0).$$

Second,

$$(\tilde{\gamma}(1)\gamma_D(1))^{-1}\tilde{\gamma}'(1)\gamma'_D(1) \in \Pi_D(z^\ddagger, z^\ddagger).$$

These statements yield the point c).

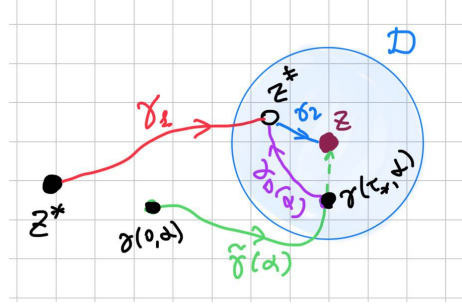


Fig. 41: To the proof of point c) of Lemma 2.1

Appendix B. Visual notations for paths and loops

Bridges notations for paths

Consider the domain $\mathbb{R}_\delta^2 \setminus \sigma(t)$ of variable z for some fixed real t . We assume that the singularities have the real properties. Here we introduce convenient notations to describe graphically paths in $\mathbb{R}_\delta^2 \setminus \sigma(t)$. We are particularly interested in paths connecting real points of $\mathbb{R}_\delta^2 \setminus \sigma(t)$; such points will be denoted by symbol $x = (x_1, x_2)$ rather than $z = (z_1, z_2)$.

Let the beginning and the end of some path are some points x^b and x^e belonging to $\mathbb{R}^2 \setminus \sigma'$. Our aim is to describe a path γ going from x^b to x^e in $\mathbb{R}_\delta^2 \setminus \sigma$.

Project the path γ onto the plane \mathbb{R}^2 . The result is the contour γ' . This contour can cross some traces σ'_j . We assume that each such crossing is simple, i.e. γ' does not pass through crossings $\sigma'_j \cap \sigma'_k$.

At each crossing point $\gamma' \cap \sigma'_j$ we should show how the contour γ bypasses σ_j . Consider a point $z^* = (z_1^*, z_2^*) \in \sigma'_j$. Introduce local variables (ν, τ) near z^* by the formulae

$$\begin{aligned} \nu &= g(z_1, z_2), \\ \tau &= -(z_1 - z_1^*) \sin \phi + (z_2 - z_2^*) \cos \phi, \end{aligned}$$

where ϕ is an angle between normal vector to σ'_j and the real axis z_1 (see Fig. 42, top left). Note that ϕ is a real angle, and g has real values for real z . We say that ν is the *transversal variable*.

Consider (locally) the contour γ in the complex plane ν (see Fig. 42, right). The singularity σ_j is depicted in the figure by the point $\nu = 0$. The contour γ projected onto the ν -plane coincides with the real axis almost everywhere, and it should bypass the origin either above or below. Consider the right part of the figure as an “icon” in the transversal variable.

Finally, take the red “bridge” from the icon and put it atop the main figure (see Fig. 42, bottom left). This bridge shows how γ bypasses the singularity.

Another example of bridges is shown in Fig. 43. For display purposes, we integrate the bridge notations in the contour γ' and obtain contour γ'' (see

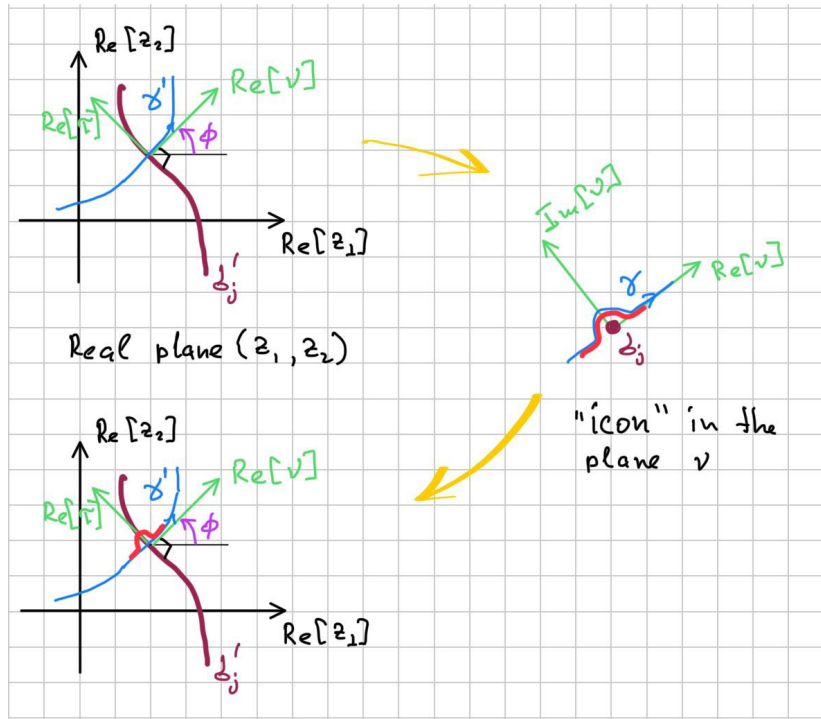


Fig. 42: Icon in the plane ν

Fig. 44).

The bridge notations for integration surfaces are introduced in [6].

An addition to bridges: small loops

Beside the bridge notations, there can be *small loops*. Namely, a projection of γ onto the plane of the transversal variable ν can make a full circle about $\nu = 0$, i.e. about the singularity. A corresponding icon is put on γ (see Fig. 45), left.

Indeed, a small loop is not something totally new. In Fig. 45, right, a loop is represented as a combination of two bridges.

Finally, introduce an *elementary loop*. These loops are important since they can be used as generators for the fundamental group of $\mathbb{R}_\delta^2 \setminus \sigma$. An elementary loop is a concatenation of three parts

$$\gamma = \gamma_1 \gamma_2 \gamma_1^{-1},$$

where γ_2 is a small loop, γ_1 is a path with bridges, and γ_1^{-1} is the same path passed in the inverse direction. An example of an elementary loop is shown in Fig. 46.

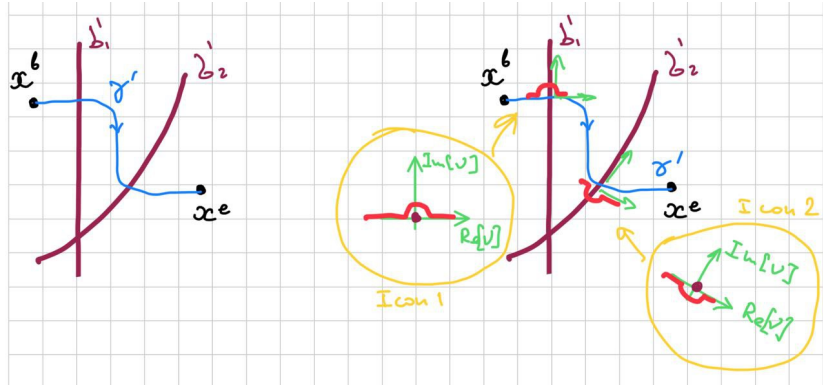


Fig. 43: Projection γ' (left); icons at the crossings (right)

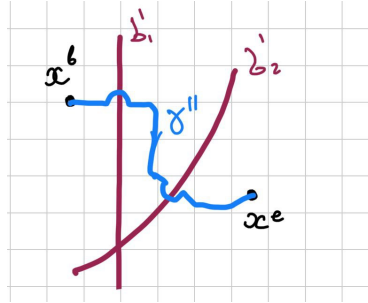


Fig. 44: The resulting contour γ''

Example: notations for a quadratic touch

As an example of application of new notations, consider the tangential touch described in Subsection 3.2. The contours $\gamma_a, \gamma_b, \gamma_c$ can be deformed into $\mathbb{R}_\delta^2 \setminus \sigma$ and they can be drawn as it is shown in Fig. 47. Note that the contour γ_c can be drawn in two equivalent ways.

According to (17),

$$\gamma_b = \gamma_c \gamma_a \gamma_c^{-1}, \quad \gamma_a = \gamma_c \gamma_b \gamma_c^{-1}. \quad (170)$$

These formulae can be used to transform γ_a into γ_b and vice versa.

Notations for paths in the domain of variable t

We will study paths of variable t in the space $\mathbb{R}_\delta^2 \setminus \sigma^t$, since passes along these paths lead to branching of the integration surfaces, and the integral itself. As we will see, in the interesting cases σ^t will also possess the real property, and the visual path notation developed above can be used for t .

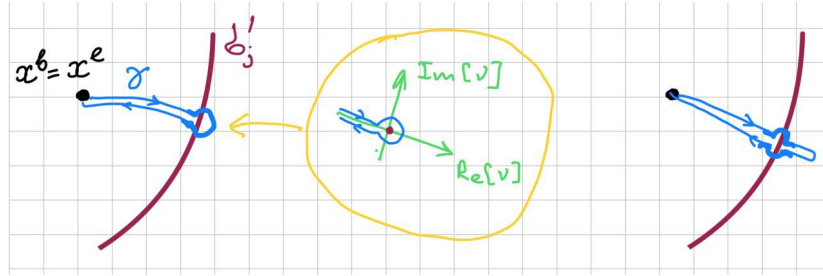


Fig. 45: A small loop on γ

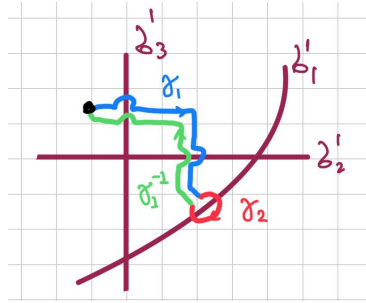


Fig. 46: An elementary loop

Bridge notations for surfaces

Let Γ be a surface coinciding with the real plane of variables (z_1, z_2) almost everywhere and slightly deformed (indented) to avoid singularity components σ_j having the real property. The bridge notation can be used to indicate the indentation of the surface. Namely, consider Γ near some point z^* belonging to σ_j' and not belonging to other singularity components. Take some contour $\gamma \subset \Gamma$, such that the projection of γ onto the real plane denoted γ' passes through z^* (see Fig. 48). The same is done for all other components of singularity.

In [6], we formulate some rules of usage of the bridge symbol for surfaces. The rules are needed, since the choice of contour $\gamma \subset \Gamma$ is arbitrary. These rules can be formulated here as follows:

- The bridge symbol does not depend on the choice of contour γ at a particular point z^* .
- The bridge symbol can be carried continuously along a component σ_j' . Thus, it is enough to define the bridge symbol at a single point of σ_j' , then one can carry the bridge it along σ_j' (see Fig. 49, left). Note that, in particular, the bridge symbol can be carried through a crossing point of two singularity components; it cannot change even there.
- Let z^* be a point of *transversal* crossing of two singularity components σ_j'

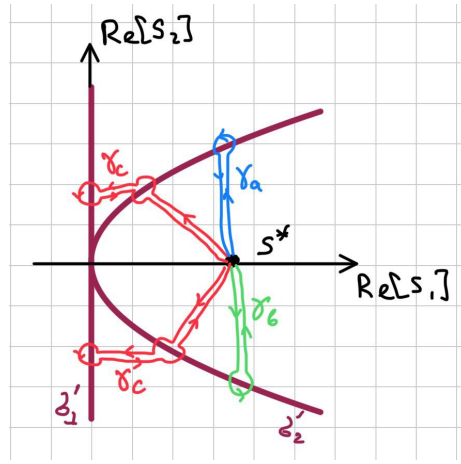


Fig. 47: Notations for generators of π_1

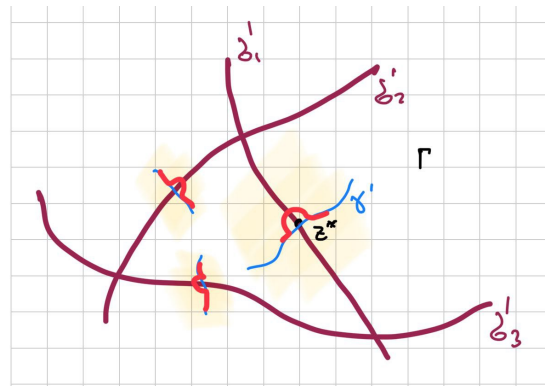


Fig. 48: Indentation of a surface

and σ'_k . The bridge symbols corresponding to these components can be chosen independently.

- Let z^* be a point of *tangential* crossing of two singularity components σ'_j and σ'_k . The bridge symbols corresponding to these components should match (see Fig. 49, right).

Appendix C. Proof of the theorem of inflation

The proof is made in several steps

Step 1. Introducing the “local adjacency”.

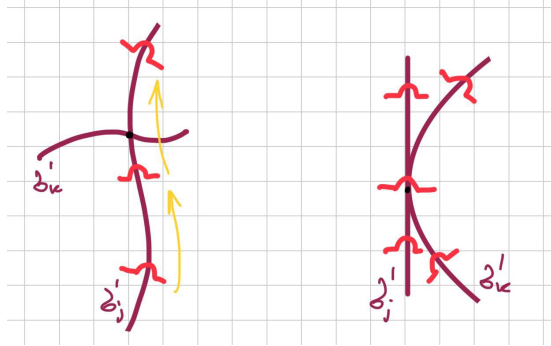


Fig. 49: Rules for bridges indicating indentation of a surface

Definition 8.1. Let $Q^{(j)}, Q^{(k)} \in H_2(\tilde{U}, \tilde{U}_1)$ be elements having a common side $a \in \mathcal{G}^1(\tilde{U}_1)$ (it is allowed that $Q^{(j)} = Q^{(k)}$).

Consider the representatives of these homologies in $\mathcal{C}^2(\tilde{U}, \tilde{U}_1)$ that are polygons in \mathbb{R}^2 . The side a belongs to some singularity trace σ'_l . The representatives of $Q^{(j)}, Q^{(k)}$ are also denoted by $Q^{(j)}, Q^{(k)}$.

The polygons $Q_{\gamma_j}^{(m_j)}, Q_{\gamma_k}^{(m_k)} \in H_2(\tilde{U}, \tilde{U}_1)$ are referred to as locally adjacent along a if there exists a small ball D with the center on a , not intersecting any singularity components other than σ_l , such that one can take the some points on $Q_{\gamma_j}^{(m_j)}$ and $Q_{\gamma_k}^{(m_k)}$ in $D \setminus \sigma_l$ and connect these points with a contour fully belonging to $D \setminus \sigma_l$.

An illustration of this definition is shown in Fig. 50. The contour γ connects the corresponding reference points. Note that the fundamental group of $D \setminus \sigma$ is \mathbb{Z} due to logarithmic type of branching.

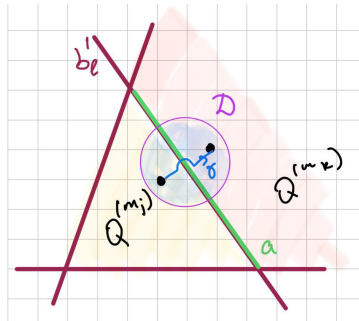


Fig. 50: To the definition of local adjacency

The key lemma for our consideration is as follows.

Lemma 8.1. $Q_{\gamma_j}^{(m_j)}$ and $Q_{\gamma_k}^{(m_k)}$ are locally adjacent along a if and only if $\partial Q_{\gamma_j}^{(m_j)}$ and $\partial Q_{\gamma_k}^{(m_k)}$ have a common part corresponding to a . This boundary part have

the same sign if $Q^{(m_j)} = Q^{(m_k)}$ and the opposite signs otherwise.

Let us prove the lemma. Let be $Q^{(m_j)} \neq Q^{(m_k)}$ (the case $Q^{(m_j)} = Q^{(m_k)}$ is considered the same way). Introduce the reference points and the paths as it is shown in Fig. 51. The common boundary is a , the reference point on it is x^a , the reference points $x^{(m_j)}$ and $x^{(m_k)}$ belong to a small ball D centered at x^a .

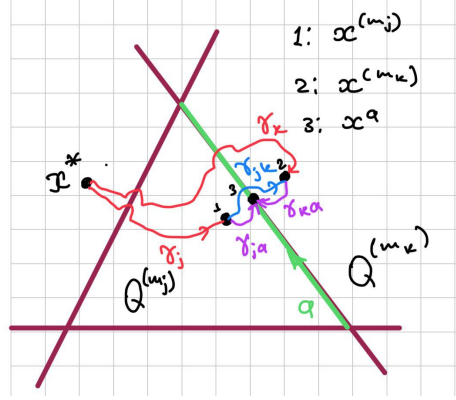


Fig. 51: Local paths near the boundary

The fact that a is a common part of $\partial Q_{\gamma_j}^{(m_j)}$ and $\partial Q_{\gamma_k}^{(m_k)}$ is expressed as

$$\gamma_j \gamma_{ja} = \gamma_k \gamma_{ka}.$$

According to Lemma 2.2, this is equivalent to the fact that

$$\gamma_{jk} = \gamma_j^{-1} \gamma_k$$

is a local path in $D \setminus \sigma$.

The signs are considered in an elementary way.

Step 2. Building a “surface” in \tilde{U}

Rewrite W as a sum of terms with coefficients equal ± 1 , i.e. split each term $\pm a_j Q_{\gamma_j}^{(m_j)}$ into a_j terms $\pm Q_{\gamma_j}^{(m_j)}$. The result is the the new sum

$$W = \sum_j \pm Q_{\gamma_j}^{(m_j)}. \quad (171)$$

Let the condition of the theorem be valid: $\partial W = 0$.

Consider some side a of some of a polygon $Q^{(m_j)}$. It is easy to prove by induction that all polygons $Q_{\gamma_k}^{(m_k)}$ from (171) having a as a boundary can be split into pairs, in which the samples of a compensate each other.

According to Lemma 8.1, the terms of (171) having a side a can be split into pairs of locally adjacent terms. If two terms correspond to the same polygon $Q^{(m_j)} = Q^{(m_k)}$, the signs in (171) should be different. Otherwise the signs should be the same.

One can, thus, consider the sum (171) as a “surface” in the combinatorial sense. It has faces (the polygons), edges (sides), and vertices (crossing points $\sigma_j \cap \sigma_k$). Each edge belongs to exactly two faces, and these faces are locally adjacent along this edge. Denote this surface by S .

The surface S is something more than a sum (171) obeying $\partial W = 0$. Beside this sum, this is a rule of attaching the edges of the polygons to each other pairwise. The surface S is defined in not a unique way by (171), moreover, S may be not connected. The faces, edges, and vertexes of S are elements of $\mathcal{G}^2(\tilde{U})$, $\mathcal{G}^1(\tilde{U})$, and $\mathcal{G}^0(\tilde{U})$, respectively.

Step 3. Deformation of W' in the edge zones

Consider an edge of the surface S built on the previous step. Let this edge connect the polygons $Q_{\gamma_j}^{(m_j)}$ and $Q_{\gamma_k}^{(m_k)}$. There are two cases: in case 1 the polygons $Q^{(m_j)}$ and $Q^{(m_k)}$ are different (but neighboring), in case 2 this is the same polygon.

Consider case 1 (shown in Fig. 52, left). Take some reference points $x^{(m_j)}$ and $x^{(m_k)}$ in the polygons $Q^{(m_j)}$ and $Q^{(m_k)}$, respectively. Let these points be close to each other.

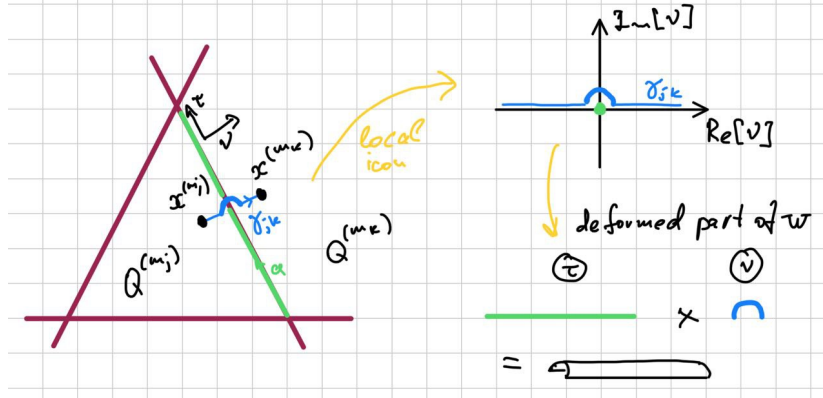


Fig. 52: Local paths near the boundary, case 1

The boundary fragment a , being oriented as it is shown in the figure, participates in $\partial Q^{(m_j)}$ with the $+$, and in $\partial Q^{(m_k)}$ with sign $-$. Thus, if this boundary participates with the same path index, the pieces of boundary compensate each other.

Introduce the local coordinate ν transversal to the singularity and the longitudinal coordinate τ along the singularities (see Fig. 52). Draw the local path γ_{jk} connecting $x^{(m_j)}$ and $x^{(m_k)}$. This path is shown in Fig. 51. This path can be represented as two stems and an arc. The arc is not necessarily of angle π (as it is shown in the figure). In more general situation, the arc may be of angle $\pi + 2\pi h$, $h \in \mathbb{Z}$.

We can build now a desired deformation of W in the edge zone. The deformed surface is a product of a real segment in the plane of longitudinal variable

τ , and the aforementioned arc in the plane of transversal variable ν . Thus, the corresponding fragment of W'' in the edge zone is a half of cylinder (if the arc angle is π). The straight parts of the boundary of this half-cylinder are attached to the polygons in the face zones. The “round” part of boundary of the half-cylinder are attached to the vertex parts built below.

Consider case 2 (see Fig. 53). The same reasoning as above shows that the path γ_{jk} , connecting the reference points taken in $Q_{\gamma_j}^{m_j}$ and in $Q_{\gamma_k}^{m_k}$, can be represented as a local path (see Fig. 53, right). Each such local path is composed of two stems and an arc. The arc now has the angle $2\pi h$, $h \in \mathbb{Z}$. The deformed surface W'' in the corresponding edge zone is a product of a straight segment and a cut circle, thus it is a cut cylinder.

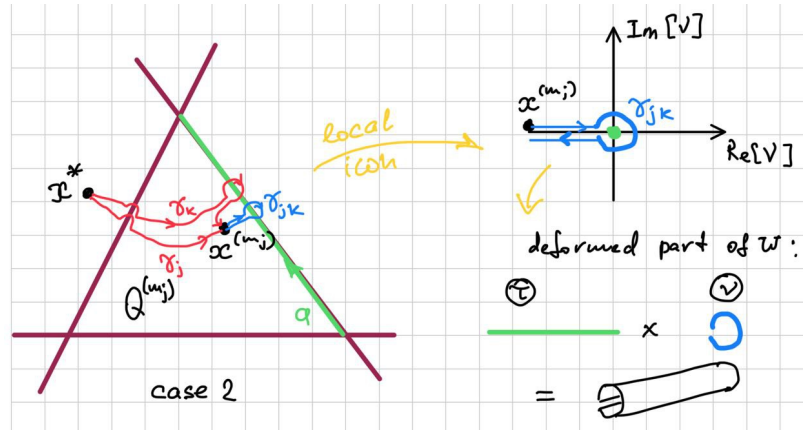


Fig. 53: Local paths near the boundary, case 2

Taking the face parts of W and attaching the edge parts as shown above, we build the surface W'' everywhere except the neighborhoods of the vertices. Below we finish this procedure and build patches near the vertices.

Step 3. Building W'' near the vertices

For each vertex of S , build a sequence of faces and edges incident to this vertex. For this, take the some face, say S , incident to the selected vertex. There are two edges of this face, say a and b , meeting at the vertex. Take one of these edges, say a . Find another face attached to b , let this face be B . Find the next edge of B incident to the vertex and incident to the vertex, etc. Thus, get the sequence

$$A \rightarrow b \rightarrow B \rightarrow \dots$$

After a finite number of steps, this sequence should come back to A . As the result, get a cyclical sequence.

Two examples of such a sequence are shown in Fig. 54. In the left part of the figure, W' is composed of four different sectors, and in the right part there are four copies of one sector, taken for different paths. In both cases, the sequence

consists of four faces and four edges. For the left part, the sequence is

$$A \rightarrow b \rightarrow B \rightarrow c \rightarrow C \rightarrow d \rightarrow D \rightarrow a \rightarrow A.$$

For the right part, the sequence is

$$A_e \rightarrow b \rightarrow A_{\gamma_1} \rightarrow c \rightarrow A_{\gamma_1\gamma_2} \rightarrow d \rightarrow A_{\gamma_2} \rightarrow a \rightarrow A_e.$$

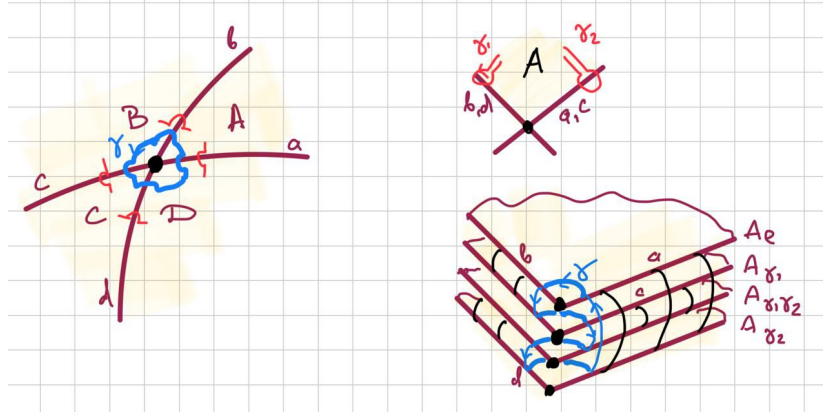


Fig. 54: A sequence of faces and edges at a vertex

Such a sequence can be depicted as a contour γ encircling the vertex of S . This contour is drawn in both parts of the figure. Assume that this contour lies in a small ball D with the center located at the vertex. The contour γ can be drawn in the bridge/loop style, as above (see Fig. 53, left, and Fig. 55, right). Note that the bridge/loop parts of γ coincide with the local paths for the edges. The contour γ can be considered as a boundary of a “hole” in S that should be patched by the corresponding vertex part.

Let the vertex be a crossing of the singularities σ_1 and σ_2 having defining functions g_1 and g_2 . Introduce the local variables

$$\nu_1 = g_1(z), \quad \nu_2 = g_2(z).$$

Introduce also the angles

$$\varphi_1 = \text{atan} \left(\frac{\text{Im}[\nu_1]}{\text{Re}[\nu_1]} \right), \quad \varphi_2 = \text{atan} \left(\frac{\text{Im}[\nu_2]}{\text{Re}[\nu_2]} \right).$$

Draw the contour γ in the coordinates (φ_1, φ_2) (Fig. 55, right). The result is always a closed polygon since γ is closed.

The vertex patch of W'' is built as follows. Let it be parametrised by the variables (φ_1, φ_2) and real strictly positive continuous functions ρ_1, ρ_2 :

$$\nu_1 = \rho_1(\varphi_1, \varphi_2)e^{i\varphi_1}, \quad \nu_2 = \rho_2(\varphi_1, \varphi_2)e^{i\varphi_2}.$$

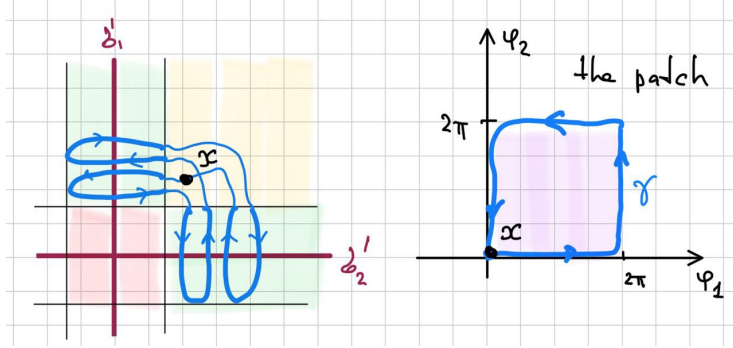


Fig. 55: Contour $\gamma \in W''$ drawn near a vertex

Take the variables φ_1, φ_2 belonging to the polygon shown in Fig. 55, right. Take the functions ρ_1, ρ_2 in any appropriate way (their values on γ are prescribed by the edge and the face parts of W''). The resulting patch does not cross σ and closes the hole in W'' .

Building the patches for all such holes near the vertexes finishes the proof.

Appendix D. The proof of theorems about matrix representation of branching of relative homologies

Proof of Theorem 5.1

Let us prove a set of formulae.

$$A_e \xrightarrow{\lambda} A_{\gamma_1 \gamma_2 \gamma_3}, \quad (172)$$

$$B_e \xrightarrow{\lambda} B_e + A_{\gamma_2} - A_{\gamma_1 \gamma_2 \gamma_3}, \quad (173)$$

$$C_e \xrightarrow{\lambda} C_e + A_{\gamma_1} - A_{\gamma_1 \gamma_2 \gamma_3}, \quad (174)$$

$$D_e \xrightarrow{\lambda} D_e + A_e - A_{\gamma_1 \gamma_2 \gamma_3}, \quad (175)$$

$$E_e \xrightarrow{\lambda} E_e - A_{\gamma_2 \gamma_3} + A_{\gamma_1 \gamma_2 \gamma_3}, \quad (176)$$

$$F_e \xrightarrow{\lambda} F_e - A_{\gamma_1 \gamma_2} + A_{\gamma_1 \gamma_2 \gamma_3}, \quad (177)$$

$$G_e \xrightarrow{\lambda} G_e - A_{\gamma_1 \gamma_3} + A_{\gamma_1 \gamma_2 \gamma_3}. \quad (178)$$

Indeed, these formulae are particular cases of (41). Say, (172) is the transformation of the vector

$$w = (e, 0, 0, 0, 0, 0, 0).$$

As we show below, these particular cases are enough to prove the general formula (41).

We need two lemmas.

Lemma 8.2. *Let σ_{2*} be a line parallel to σ_2 and passing through $\sigma_1 \cap \sigma_3$. Let us consider the deformation of σ such that σ_2 bypasses σ_{2*} as it is shown in Fig. 56, left. The new position of the singularity σ_2 is $\sigma_{2\#}$. The deformation of the singularity is denoted by λ_+ . (Note that in the same figure we introduce also the bypass λ_- that will be used below. The bypass λ is obviously a composition $\lambda = \lambda_+ \lambda_-$).*

For the deformed configuration of the singularities $\sigma_1, \sigma_{2\#}, \sigma_3$ introduce the polygons A', \dots, G' as shown in Fig. 56, right. The bridge symbols for the new surface Γ are shown in the figure. The base point x^ remains unchanged.*

As before, let $\gamma_1, \gamma_2, \gamma_3$ be elementary bypasses about $\sigma_1, \sigma_{2\#}, \sigma_3$ in the positive direction starting and ending at x^ .*

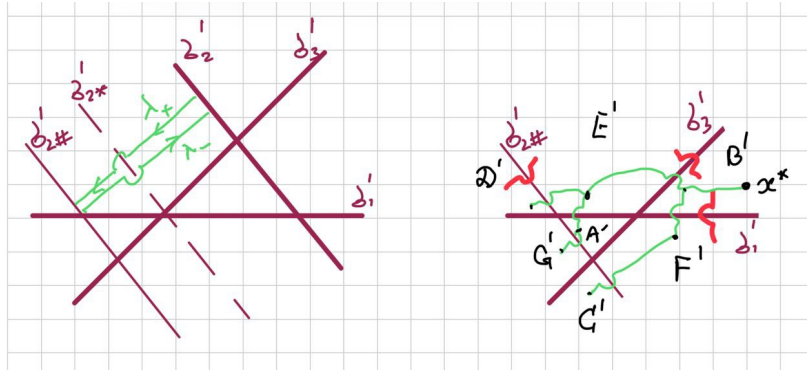


Fig. 56: A bypass λ_+

The bypass λ_+ transforms the relative homologies as follows:

$$A_e \xrightarrow{\lambda_+} A'_e, \quad (179)$$

$$B_e \xrightarrow{\lambda_+} B'_e - A'_e, \quad (180)$$

$$C_e \xrightarrow{\lambda_+} C'_e - A'_e, \quad (181)$$

$$D_e \xrightarrow{\lambda_+} D'_e - A'_e, \quad (182)$$

$$E_e \xrightarrow{\lambda_+} E'_e + A'_e, \quad (183)$$

$$F_e \xrightarrow{\lambda_+} F'_e + A'_e, \quad (184)$$

$$G_e \xrightarrow{\lambda_+} G'_e + A'_e, \quad (185)$$

We note that $\gamma_1, \gamma_2, \gamma_3$ in the right-hand side of (179)–(185) are elementary bypasses about $\sigma_1, \sigma_{2\#}, \sigma_3$, respectively.

Let us prove this lemma. First, note that the σ_2 does not intersect Γ in the course of the deformation λ_+ .

Second, it is easy to see that (179) is valid.

Third, consider the transformation of G . It is easy to see that (185) is valid.

Fourth, consider the transformation of B . Represent B_e as

$$B_e = (B_e + A_e) - A_e.$$

It is easy to see that

$$(B_e + A_e) \xrightarrow{\lambda_+} B'_e.$$

Together with (179) this yields (180).

Relations (181), (182), (183), (184) are considered in a similar way.

Note that the formulae (179)–(185) do not depend on the position of the x^* : it can be located at any polygon except the vanishing (the A).

Lemma 8.3. *Let λ' be some deformation of singularities. Define the fundamental group of $\mathbb{R}_\delta^2 \setminus \sigma$ before the deformation by π_1 , and after deformation by π'_1 . The deformation λ' induces a map*

$$\psi : \pi_1 \rightarrow \pi'_1.$$

Let some formula of transformation be valid for this λ' :

$$Q_\gamma \xrightarrow{\lambda'} \alpha_A A_{\gamma_A} + \cdots + \alpha_G G_{\gamma_G}, \quad (186)$$

where $\gamma \in \pi_1$, $\gamma_A, \dots, \gamma_G \in \pi'_1$.

Let $\gamma^\# \in \pi_1$ be an arbitrary element.

Then

$$Q_{\gamma^\#} \xrightarrow{\lambda'} \alpha_A A_{\psi(\gamma^\#)\gamma_A} + \cdots + \alpha_G G_{\psi(\gamma^\#)\gamma_G}, \quad (187)$$

The lemma is trivial. The map ψ in our case is quite simple: the generators of π_1 (elementary bypasses about the components of singularity) are mapped into the generators of π'_1 .

Finally, we can finish the proof of Theorem 5.1. Describe the change of the configuration when the deformation λ_- shown in Fig. 29, left, is performed. For this, use Lemma 8.2 after some geometrical changes. One can see that the lemma cannot be applied directly, since the mutual position of the base paths and the bypass λ_- is different from the conditions of the lemma. To change this, introduce the new base paths, apply Lemma 8.2, and then apply Lemma 4.1.

The new paths $\tilde{\gamma}'_A, \dots, \tilde{\gamma}'_G$ for the singularities $\sigma_1, \sigma_{2\#}, \sigma_3$ (Fig. 57, left) and $\tilde{\gamma}_A, \dots, \tilde{\gamma}_G$ for $\sigma_1, \sigma_2, \sigma_3$ (Fig. 57, right).

One can see by rotation of the graph that Lemma 8.2 describes the bypass λ_- if the basic contours $\tilde{\gamma}'_Q, \tilde{\gamma}_Q$ are chosen. Thus, for these contours,

$$A'_e \xrightarrow{\lambda_-} A_e,$$

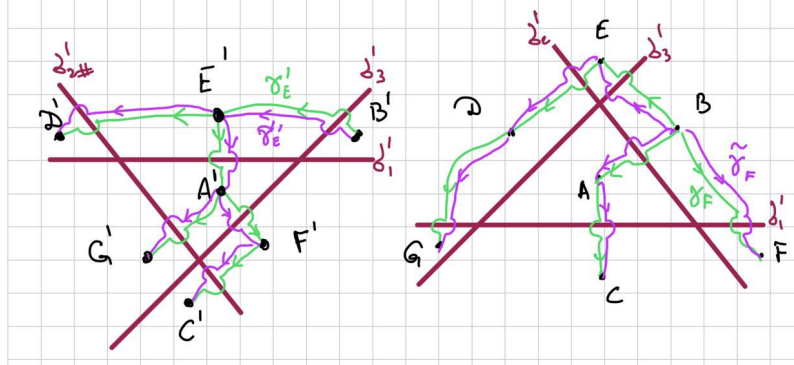


Fig. 57: “Old” and “new” base contours

$$B'_e \xrightarrow{\lambda_-} B_e + A_e,$$

$$C'_e \xrightarrow{\lambda_-} C_e + A_e,$$

$$D'_e \xrightarrow{\lambda_-} D_e + A_e,$$

$$E'_e \xrightarrow{\lambda_-} E_e - A_e,$$

$$F'_e \xrightarrow{\lambda_-} F_e - A_e,$$

$$G'_e \xrightarrow{\lambda_-} G_e - A_e.$$

Let us return to the initial base contours γ_Q and γ'_Q . For this, apply Lemma 4.1:

$$A'_{\tilde{\gamma}'_A(\gamma'_A)^{-1}} \xrightarrow{\lambda_-} A_{\tilde{\gamma}_A\gamma_A^{-1}}, \quad (188)$$

$$B'_{\tilde{\gamma}'_B(\gamma'_B)^{-1}} \xrightarrow{\lambda_-} B_{\tilde{\gamma}_B\gamma_B^{-1}} + A_{\tilde{\gamma}_A\gamma_A^{-1}}, \quad (189)$$

⋮

As one can see from Fig. 57,

$$\tilde{\gamma}'_A(\gamma'_A)^{-1} = \gamma_1^{-1}\gamma_3^{-1}, \quad \tilde{\gamma}_A\gamma_A^{-1} = \gamma_2, \quad \tilde{\gamma}_B\gamma_B^{-1} = e.$$

Thus,

$$A'_{\gamma_1^{-1}\gamma_3^{-1}} \xrightarrow{\lambda_-} A_{\gamma_2},$$

⋮

Taking into account Lemma 8.3, we can rewrite (188) and (189) as

$$A'_e \xrightarrow{\lambda_-} A_{\gamma_1\gamma_2\gamma_3}, \quad (190)$$

$$B'_e \xrightarrow{\lambda_-} B_e + A_{\gamma_2}, \quad (191)$$

Similarly, obtain the relations

$$C'_e \xrightarrow{\lambda_-} C_e + A_{\gamma_1}, \quad (192)$$

$$D'_e \xrightarrow{\lambda_-} D_e + A_{\gamma_3}, \quad (193)$$

$$E'_e \xrightarrow{\lambda_-} E_e - A_{\gamma_2\gamma_3}, \quad (194)$$

$$F'_e \xrightarrow{\lambda_-} F_e - A_{\gamma_1\gamma_2}, \quad (195)$$

$$G'_e \xrightarrow{\lambda_-} G_e - A_{\gamma_1\gamma_3}. \quad (196)$$

Applying these relations after (179)–(185), i.e. performing the composition of changes λ_+ and λ_- , obtain (172)–(178).

Indeed, it would be enough to prove the theorem only for the polygons A , B , and G , all other polygons can be obtained in a similar way.

Finally, let us pass from the formulae (172)–(178) to the matrix form (41). Consider, say, (173). In the vector form, it can be rewritten as

$$(0, e, 0, 0, 0, 0, 0) \xrightarrow{\lambda} (\gamma_2 - \gamma_1\gamma_2\gamma_3, e, 0, 0, 0, 0, 0).$$

Let us generalize this formula. Let us describe an evolution of B_γ , $\gamma \in \pi_1$ instead of that of B_e . Apply Lemma 8.3:

$$(0, \gamma, 0, 0, 0, 0, 0) \xrightarrow{\lambda} (\psi(\gamma)\gamma_2 - \psi(\gamma)\gamma_1\gamma_2\gamma_3, \psi(\gamma), 0, 0, 0, 0, 0).$$

Taking into account Lemma 5.1,

$$(0, \gamma, 0, 0, 0, 0, 0) \xrightarrow{\lambda} (\gamma\gamma_2 - \gamma\gamma_1\gamma_2\gamma_3, \gamma, 0, 0, 0, 0, 0) = \gamma(\gamma_2 - \gamma_1\gamma_2\gamma_3, e, 0, 0, 0, 0, 0).$$

A further generalization is possible. Let be $a_B \in \Omega$. Then

$$(0, a_B, 0, 0, 0, 0, 0) \xrightarrow{\lambda} a_B(\gamma_2 - \gamma_1\gamma_2\gamma_3, e, 0, 0, 0, 0, 0).$$

The same generalization can be applied to the rest of the formulae (172)–(178).

Proof of Theorem 5.2

Similarly to Theorem 5.1, we first prove the relations

$$A_e \xrightarrow{\lambda} -A_{\gamma_1\gamma_2}, \quad (197)$$

$$B_e \xrightarrow{\lambda} B_e + A_{\gamma_1} + A_{\gamma_1\gamma_2}, \quad (198)$$

$$C_e \xrightarrow{\lambda} C_e + A_{\gamma_2} + A_{\gamma_1\gamma_2}, \quad (199)$$

$$D_e \xrightarrow{\lambda} D_e - A_{\gamma_1\gamma_2}, \quad (200)$$

$$E_e \xrightarrow{\lambda} E_e - A_{\gamma_1\gamma_2}, \quad (201)$$

And then apply Lemma 8.3.

The biangle case can be reduced to the triangle case by the idea proposed in [4]. Namely, without the restriction of generality we can consider the singularities

$$\sigma_1 : z_1 = t, \quad \sigma_2 : z_2^2 - z_1 = 0$$

with t moving along the loop shown in Fig. 32.

Introduce the variable

$$\zeta_2 = z_2^2$$

and consider the configuration in the coordinates (z_1, ζ_2) . The singularities σ_1 and σ_2 become straight lines, and a singularity

$$\sigma_3 : \zeta_2 = 0$$

is added due to branching of z_2 over ζ_2 (see Fig. 58). Introduce also a bypass γ_3 about σ_3 .

The bypass about σ_3 has the property $\sigma_3^2 \cong e$.

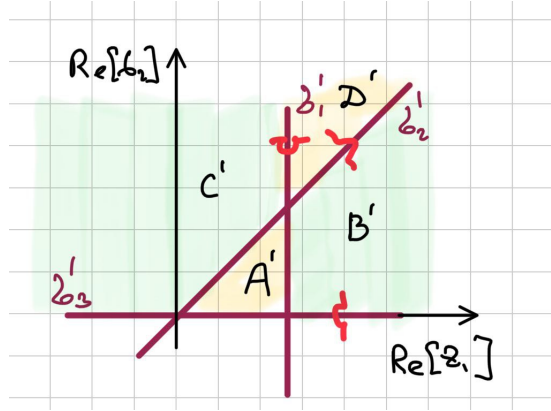


Fig. 58: Transformation to the coordinates (z_1, ζ_2)

The “old” homologies can be expressed through the “new” homologies as

$$\begin{aligned} D_e &= D'_e, & E_e &= E'_e, \\ A_e &= A'_e - A'_{\gamma_3}, & B_e &= B'_e - B'_{\gamma_3}, & C_e &= C'_e - C'_{\gamma_3}, \end{aligned}$$

One can see that the deformation of singularity σ_1 in the coordinates (z_1, z_2) corresponds to the conditions of Theorem 5.1. Thus,

$$\begin{aligned} A'_e &\rightarrow A'_{\gamma_1\gamma_2\gamma_3}, \\ B'_e &\rightarrow B'_e + A'_{\gamma_1} - A'_{\gamma_1\gamma_2\gamma_3}, \\ C'_e &\rightarrow C'_e + A'_{\gamma_2} - A'_{\gamma_1\gamma_2\gamma_3}, \\ D'_e &\rightarrow D'_e - A'_{\gamma_1\gamma_2} + A'_{\gamma_1\gamma_2\gamma_3}, \end{aligned}$$

Finally,

$$\begin{aligned} A_e = A'_e - A'_{\gamma_3} &\longrightarrow A'_{\gamma_1\gamma_2\gamma_3} - A'_{\gamma_1\gamma_2} = -A_{\gamma_1\gamma_2}, \\ B_e = B'_e - B'_{\gamma_3} &\longrightarrow \\ B'_e + A'_{\gamma_1} - A'_{\gamma_1\gamma_2\gamma_3} - (B'_{\gamma_3} + A'_{\gamma_1\gamma_3} - A'_{\gamma_1\gamma_2}) &= B_e + A_{\gamma_1} + A_{\gamma_1\gamma_2}, \\ D_e = D'_e &\longrightarrow D'_e - A'_{\gamma_1\gamma_2} + A'_{\gamma_1\gamma_2\gamma_3} = D_e - A_{\gamma_1\gamma_2}. \end{aligned}$$

The remaining identities (199) and (201) are proven in a similar way.

Proof of Theorem 5.3

As above, we prove the formulae

$$A_e \xrightarrow{\lambda} A_{\gamma_1}, \quad (202)$$

$$B_e \xrightarrow{\lambda} B_e, \quad (203)$$

and apply Lemma 8.3. The proof of (202), (202) is similar to the reasoning of Theorem 5.2. One should introduce the new variables (ζ_1, ζ_2) as

$$\zeta_1 = z_1^2, \quad \zeta_2 = z_2^2.$$

Appendix E

It can be done in three steps. The change λ_3 is represented as a composition of $\lambda_+\lambda_0\lambda_-$ (see Fig. 59, left). We move the singularity σ_a . In the course of the bypass λ_+ , the singularity σ_a passes one of the crossing points of σ_b and σ_c . We choose A as the vanishing triangle. As the result of the bypass λ_+ , we obtain a configuration shown in Fig. 59, right, with an intermediate position of σ_a denoted by $\sigma_{2\sharp}$. For this configuration, we introduce the basic contours by setting the bridge notations (shown in red). We assume that the basic contours are chosen on the indented real plane Γ corresponding to these bridges.

Elements of $H_2(\tilde{U}, \tilde{U}_1)$ corresponding to the diagram in Fig. 59 are described by vectors

$$w' = (a'_{A'}, \dots, a'_{M'}).$$

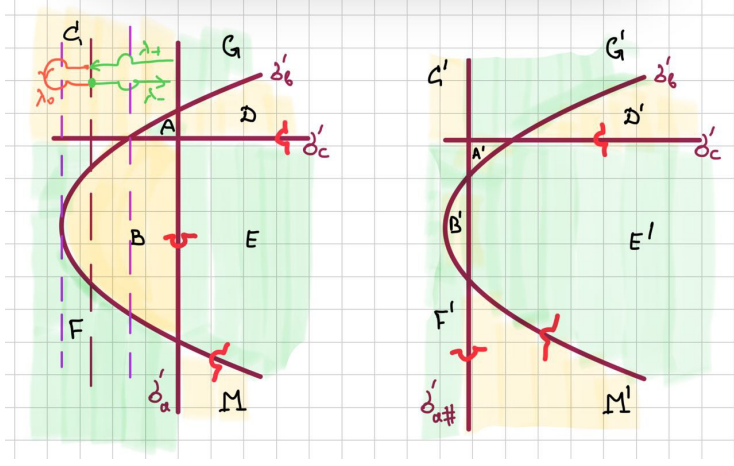


Fig. 59: Auxiliary step of building \mathbf{T}_3

The change

$$W \xrightarrow{\lambda_+} W', \quad w \rightarrow w',$$

is described by the following matrix relation:

$$w' = w \mathbf{T}_+, \quad \mathbf{T}_+ = \begin{pmatrix} e & 0 & 0 & 0 & 0 & 0 & 0 & 0 \\ -e & e & 0 & 0 & 0 & 0 & 0 & 0 \\ -e & 0 & e & 0 & 0 & 0 & 0 & 0 \\ -e & 0 & 0 & e & 0 & 0 & 0 & 0 \\ e & 0 & 0 & 0 & e & 0 & 0 & 0 \\ e & 0 & 0 & 0 & 0 & e & 0 & 0 \\ e & 0 & 0 & 0 & 0 & 0 & e & 0 \\ 0 & 0 & 0 & 0 & 0 & 0 & 0 & e \end{pmatrix} \quad (204)$$

One can see that matrix \mathbf{T}_+ is obtained from (179)–(185) by applying it to the vanishing triangle A and its neighbors.

Then the singularity σ_a travels along λ_0 about the line parallel to σ_a and tangent to σ_b . For this bypass, the biangle B' vanishes. Thus, the bypass can be described in a matrix form, and the matrix is built on the base of (43):

$$w'_{\lambda_0} = w' \mathbf{T}_0, \quad \mathbf{T}_0 = \begin{pmatrix} e & -ab & 0 & 0 & 0 & 0 & 0 & 0 \\ 0 & -ab & 0 & 0 & 0 & 0 & 0 & 0 \\ 0 & 0 & e & 0 & 0 & 0 & 0 & 0 \\ 0 & 0 & 0 & e & 0 & 0 & 0 & 0 \\ 0 & a+ab & 0 & 0 & e & 0 & 0 & 0 \\ 0 & b+ab & 0 & 0 & 0 & e & 0 & 0 \\ 0 & 0 & 0 & 0 & 0 & 0 & e & 0 \\ 0 & -ab & 0 & 0 & 0 & 0 & 0 & e \end{pmatrix} \quad (205)$$

Finally, we move σ_2 to its initial position along the path λ_- . This operation is described by

$$w'_{\lambda_0} \xrightarrow{\lambda_-} w_{\lambda_3},$$

$$w_{\lambda_3} = w'_{\lambda_0} \mathbf{T}_-, \quad \mathbf{T}_- = \begin{pmatrix} abc & 0 & 0 & 0 & 0 & 0 & 0 & 0 \\ c & e & 0 & 0 & 0 & 0 & 0 & 0 \\ b & 0 & e & 0 & 0 & 0 & 0 & 0 \\ a & 0 & 0 & e & 0 & 0 & 0 & 0 \\ -ac & 0 & 0 & 0 & e & 0 & 0 & 0 \\ -bc & 0 & 0 & 0 & 0 & e & 0 & 0 \\ -ab & 0 & 0 & 0 & 0 & 0 & e & 0 \\ 0 & 0 & 0 & 0 & 0 & 0 & 0 & e \end{pmatrix} \quad (206)$$

This formula is based on (190)–(196).

Finally,

$$\mathbf{T}_3 = \mathbf{T}_+ \mathbf{T}_0 \mathbf{T}_- = \begin{pmatrix} 0 & -ab & 0 & 0 & 0 & 0 & 0 & 0 \\ -abc & 0 & 0 & 0 & 0 & 0 & 0 & 0 \\ b & ab & e & 0 & 0 & 0 & 0 & 0 \\ a & ab & 0 & e & 0 & 0 & 0 & 0 \\ abc & a & 0 & 0 & e & 0 & 0 & 0 \\ abc & b & 0 & 0 & 0 & e & 0 & 0 \\ -ab & -ab & 0 & 0 & 0 & 0 & e & 0 \\ -abc & -ab & 0 & 0 & 0 & 0 & 0 & e \end{pmatrix} \quad (207)$$